UNIVERSIDADE FEDERAL DE CAMPINA GRANDE

CENTRO DE CIÊNCIAS E TECNOLOGIA

COORDENAÇÃO DE PÓS-GRADUAÇÃO EM ENGENHARIA QUÍMICA

SISTEMA DE CONTROLE INTELIGENTE BASEADO EM REDES NEURAIS ARTIFICIAIS APLICADO AO PROCESSO DE DESTILAÇÃO EXTRATIVA

Thiago Gonçalves das Neves

Campina Grande – PB

Novembro/2020

Thiago Gonçalves das Neves

SISTEMA DE CONTROLE INTELIGENTE BASEADO EM REDES NEURAIS ARTIFICIAIS APLICADO AO PROCESSO DE DESTILAÇÃO EXTRATIVA

Tese de doutorado apresentada ao Programa de Pós-graduação em Engenharia Química da Universidade Federal de Campina Grande como parte dos requisitos exigidos à obtenção do título de Doutor em Engenharia Química.

Orientador

Dr. Romildo Pereira Brito

Campina Grande – PB

Novembro/2020

N518s Neves, Thiago Gonçalves das.
Sistema de controle inteligente baseado em redes neurais artificiais aplicado ao processo de destilação extrativa / Thiago Gonçalves das Neves. - Campina Grande, 2020.
132 f. : il. color.

Tese (Doutorado em Engenharia Química) - Universidade Federal de Campina Grande, Centro de Ciências e Tecnologia, 2020.
"Orientação: Prof. Dr. Romildo Pereira Brito.
Referências.

1. Etanol Anidro. 2. Destilação Extrativa. 3. Redes Neurais Artificiais. 4. Misturas Não-Ideais. 5. Controle Inteligente. I. Brito, Romildo Pereira. II. Título.

CDU 662.754(043)

FICHA CATALOGRÁFICA ELABORADA PELO BIBLIOTECÁRIO GUSTAVO DINIZ DO NASCIMENTO CRB-15/515

SISTEMA DE CONTROLE INTELIGENTE BASEADO EM REDES NEURAIS ARTIFICIAIS APLICADO AO PROCESSOSDE DESTILAÇÃO EXTRATIVA

Thiago Gonçalves das Neves

Tese aprovada em: 27 / 11 / 2020

Banca Examinadora

ROMILDO PEREIRA BRITO:41912675404 Digitally signed by ROMILDO PEREIRA BRITO:41912675404 Date: 2020.12.06 10:54:04 -03'00'

Dr. Romildo Pereira Brito
Orientador

Dr. Arioston Araújo de Morais Júnior
Examinador

Dr. Luís Gonzaga Sales Vasconcelos
Examinador

Dr. Márcio Henrique dos Santos Andrade
Examinador

Dr. Wagner Brandão Ramos
Examinador

Campina Grande – Paraíba

Novembro/2020

Agradecimentos

Ao meu Deus pela minha existência e por ter me guiado até aqui.

À minha esposa Savana, pela compreensão, apoio, carinho, afeto e amor sincero. Por ter sido minha companheira de trabalho e contribuído de forma direta com o desenvolvimento desse trabalho.

Ao meu filho Heitor, por me fazer sentir seu super-herói, por me fazer encontrar todas as motivações para superar os desafios que apareceram.

Aos meus pais Maria Ofélia e Pedro Raimundo e meu irmão Wagner, por sempre terem torcido por mim e estarem ao meu lado.

Ao meu orientador Professor Romildo Pereira Brito, pelas orientações e contribuições. Seus incentivos desde o início da graduação me motivaram a ser cada dia melhor.

Aos funcionários e demais professores da Universidade Federal de Campina Grande, pela contribuição de cada um para tornar realidade esse sonho.

Aos colegas Ascendino Pereira de Araújo Neto e Fabricia Araújo Sales, e demais integrantes do LARCA pelas proveitosas discussões.

Aos colegas de trabalho do IFCE e do IFRN, pela ajuda nos momentos que mais precisei.

Ao apoio financeiro da CAPES nos primeiros anos do doutorado.

Aos amigos que me acompanharam até aqui, especialmente aqueles cuja amizade se fortaleceu com o tempo.

A todos que não citei aqui, mas que contribuíram de forma direta ou indireta para a consolidação desse trabalho.

Resumo

Os processos de destilação extrativa são amplamente utilizados nas indústrias químicas para a separação de misturas não ideais, por exemplo, na desidratação de etanol pelo seu grande interesse industrial por causa de suas diversas aplicações, exigindo que a produção se ajuste as diferentes demandas do mercado, principalmente no que diz respeito à composição. Além disso, rígidas especificações de qualidade do produto e rigorosas regulamentações ambientais exigem que o sistema de controle possua alto grau de desempenho. Devido à dificuldade da medição de composição de uma forma contínua, o controle em coluna de destilação ainda é um desafio, e uma alternativa muito utilizada é a instalação de sensores de temperatura para inferir a concentração. Porém para misturas multicomponentes não-ideais, com comportamento termodinâmico complexo, a temperatura é um fraco indicador da composição. O objetivo principal desse trabalho é desenvolver alternativas de controle inteligente, baseadas em Redes Neurais Artificiais, capazes de fazer com que a composição dos produtos em um processo de destilação extrativa siga em direção a novas especificações e que, independente dos distúrbios, mantenham a saída no *set-point* estabelecido. As malhas de controle incluem o controle convencional, o avançado e o baseado em modelos, evitando o uso de analisadores de composição caros e de alta manutenção. Os modelos foram baseados no uso de Redes Neurais Artificiais (RNA), desenvolvidas no software MATLAB®, sendo necessário usar tantos dados quantos possíveis a fim de construir modelos que cubram uma larga faixa de condições operacionais do processo, os quais foram obtidos com auxílio do *Aspen Plus*™. Uma análise feita no *Aspen Plus Dynamics*™ mostrou que o controle inteligente por meio da modificação de set-points de controladores presentes na instrumentação original é capaz de fazer com que os distúrbios na alimentação não afetem a qualidade do produto final ou através de um simples comando do operador, o sistema de controle é capaz de utilizar uma lógica matemática para modificar a composição do produto a fim de alcançar a especificação desejada dependendo do planejamento da produção. Diante dessas características, o controle inteligente, com relação ao controle convencional, apresentou melhor desempenho e flexibilidade para o problema proposto, com baixa oscilação e respostas rápidas.

Palavras-chave: etanol anidro, destilação extrativa, redes neurais artificiais, misturas não-ideais, controle inteligente.

Abstract

Extractive distillation processes are widely used in chemical industries for the separation of non-ideal mixtures, for example, in the dehydration of ethanol due to its great industrial interest because of its diverse applications, requiring that production adjust to different market demands, mainly about composition. In addition, strict product quality specifications and strict environmental regulations require that the control system has a high degree of performance. In addition, strict product quality specifications and strict environmental regulations require that the control system has high performance. Due to the difficulty of measuring composition continuously, the control in a distillation column is still a challenge, and a widely used alternative is the installation of temperature sensors to infer the concentration. However, for non-ideal multicomponent mixtures, with complex thermodynamic behavior, temperature is a weak indicator of composition. The main objective of this work is to develop alternatives for intelligent control, based on Artificial Neural Networks, capable of making the composition of the products in an extractive distillation process move towards new specifications and that, regardless of the disturbances, keep the output in the set point established. Control loops include conventional, advanced and model-based control, without the use of expensive, high-maintenance composition analyzers. The models were based on the use of Artificial Neural Networks (ANN), developed in the MATLAB® software, being necessary to use as much data as possible in order to build models that cover a wide range of operational conditions of the process, which were obtained with the help of Aspen Plus ™. An analysis in Aspen Plus Dynamics ™ showed that the intelligent control through the set points modification gifts controllers in the original instrumentation is able to cause disturbances in power do not affect the quality of the final product or through a simple command operator, the control system is able to use mathematical logic to modify the composition of the product to achieve the desired specification depending on production planning. In view of these characteristics, intelligent control, in relation to conventional control, presented better performance and flexibility for the proposed problem, with low oscillation and fast responses.

Keywords: anhydrous ethanol, extractive distillation, artificial neural networks, non-ideal mixtures, intelligent control.

Lista de Figuras

CAPÍTULO 2

CAPÍTULO 3

CAPÍTULO 4

CAPÍTULO 5

Lista de Tabelas

CAPÍTULO 2

CAPÍTULO 3

CAPÍTULO 4

CAPÍTULO 5

Sumário

CAPÍTULO 1

INTRODUÇÃO

CAPÍTULO 1 – INTRODUÇÃO

1. 1 Contextualização

A separação de misturas nas quais os componentes formam azeótropos ou têm pontos de ebulição muito semelhantes ainda é um problema comum nas indústrias químicas e petroquímicas. Apesar da existência de muitas técnicas de separação, a destilação permanece como umas das principais alternativas para separação de misturas em larga escala. Obter os componentes praticamente puros de uma mistura não ideal, quando a volatilidade relativa é muito perto de um, torna-se inviável em uma destilação convencional. A destilação extrativa, destilação com variação de pressão e destilação azeotrópica são algumas das alternativas que devem ser consideradas.

A destilação extrativa precisa introduzir solventes que causam uma alteração suficiente nas volatilidades relativas entre componentes, que é aplicável à separação da maioria dos sistemas azeotrópicos (Dong et al., 2018; Hu et al., 2019; Yang et al., 2019).

A destilação extrativa com variação de pressão aproveita o fato de que a mudança de pressão causa o deslocamento da composição do azeótropo, sendo uma boa opção para a separação de misturas azeotrópicas sensíveis à pressão, porque não há componentes adicionais introduzidos (Tripodi et al., 2017; Wang et al., 2019).

A destilação azeotrópica requer o uso de um solvente que forma uma mistura heterogênea. Para alguns sistemas que apresentam um desvio muito intenso da lei de Raoult, pode ocorrer que, em certa faixa de composição, os líquidos formados do azeótropo tornam-se imiscíveis e acontece uma separação de fases. Por exemplo, quando o benzeno é adicionado à mistura etanol/água, o solvente forma um azeótropo ternário de mínimo ponto de ebulição, que por ser mais volátil é retirado no topo da coluna azeotrópica e o etanol anidro pode ser obtido na base (Guang et al., 2019; Pla-Franco et al., 2019).

1. 2 Definição do problema

A destilação extrativa é menos complexa e mais amplamente usada que a destilação azeotrópica por causa da ausência de azeótropos e pelo fato do solvente poder ser recuperado por destilação simples. Uma das maiores aplicações do processo de destilação extrativa é a

produção de etanol anidro. Esse álcool pode ser produzido a partir de qualquer material que contém açúcar, amido ou celulose (Gnansounou, 2005).

O etanol anidro pode ter várias aplicações e consequentemente é comercializado em diferentes composições. É utilizado em aplicações industriais como reativo, solvente, tintas, na fabricação de aerossóis (inseticidas, repelentes de insetos, desodorantes de ambientes, fungicidas, etc.). Uma das maiores aplicações do etanol anidro é como combustível automotivo, podendo ser misturado com a gasolina. A legislação para o etanol anidro utilizado como combustível segue a Resolução ANP Nº 764, DE 20.12.2018 (Brasil, 2018).

Outra aplicação do etanol é na produção de biodiesel. Segundo Leung et al. (2010), a reação de síntese do biodiesel, via transesterificação, deve acontecer na ausência de água, pois ela é precursora de reações paralelas de saponificação, as quais comprometem o seu rendimento e a qualidade do biodiesel formado. Portanto, quanto mais próxima a graduação alcoólica de 100% melhor para a eficiência do processo. Segundo Schwab (1987) e Tabatabaei et al. (2019), a produção de biodiesel com metanol é tecnicamente mais viável do que com etanol, particularmente se esse corresponde ao etanol hidratado, cujo teor em água (4-6%) retarda a reação. O uso de etanol anidro na reação efetivamente minimiza este inconveniente.

Diante do exposto fica clara a necessidade da produção de etanol anidro se ajustar as diferentes demandas do mercado, principalmente no que diz respeito a sua composição. Na prática, para levar o processo para um novo regime estacionário no intuito de modificar a composição do produto, o operador lança mão de sua experiência baseando-se na vivência com o processo e nas respostas já geradas a partir do sistema real investigado. De forma tradicional, mede-se a composição do produto, sendo necessárias análises laboratoriais que são realizadas com frequência relativamente baixa, ou utilização de analisadores em linha, que ainda são muito caros, para comparar o seu valor com a especificação desejada. Essa diferença é alimentada no controlador que mudará a variável manipulada de modo a levar a composição do produto (variável controlada) ao valor desejado. No caso de plantas altamente integradas, a lógica necessária para uma mudança de especificação, embora possa ser deduzida e escrita com antecedência, pode ser muito detalhada e complexa para ser facilmente absorvida pelos operadores. Além disso, os tempos de reação exigidos em determinadas circunstâncias podem ser muito curtos para a fisiologia humana típica (Araújo Neto et al., 2019).

Além das dificuldades de modificar a composição do etanol no produto, manter a especificação estabelecida ainda é um desafio pelo fato de que os processos químicos estão

altamente integrados e no caso da destilação, informações precisas sobre a composição do produto, variável de difícil medição, é de extrema importância. O controle aprimorado da destilação extrativa pode ter um impacto significativo na redução do consumo de energia, melhorando a qualidade do produto e proteção dos recursos ambientais. Mas, tanto a modelagem quanto o controle desse tipo de processo são tarefas difíceis porque geralmente são processos multivariáveis, não estacionários e sujeitos a restrições e perturbações, apresentando um dos maiores desafios para os engenheiros (Skogestad, 2007), daí o crescente interesse no uso de esquemas avançados de controle.

É sabido que geralmente o uso de controle avançado de processo aumenta sistematicamente o desempenho e a flexibilidade de fábricas de produtos químicos, garantindo a satisfação do cliente e restrições de segurança. O comportamento não linear da maioria dos processos industriais é aproximado apenas por modelos lineares, mas sabe-se que informações adicionais devem ser fornecidas para projetar controladores confiáveis e de bom desempenho. O uso de redes neurais artificiais é uma alternativa pois são sistemas adaptativos que mudam sua estrutura com base nos dados de entrada/saída aplicados durante a fase de aprendizagem e podem prever o comportamento não linear de um processo. Redes neurais são ferramentas de dados estatísticos que podem ser usadas para modelar relações complexas entre sinais de entradas e saídas com base em dados de desempenho (Haykin, 2009). Esses sistemas adaptativos têm sido amplamente utilizados em diversas aplicações de processos industriais, como análise de dados de sensores, detecção de falhas e identificação não linear de plantas e controle de colunas de destilação, entre outras (Hussain, 1999; Xiong e Jutan, 2002).

1. 3 Objetivos

O objetivo principal desse trabalho é desenvolver alternativas de controle inteligente, baseadas em Redes Neurais Artificiais, capazes de fazer com que a composição dos produtos em um processo de destilação extrativa siga em direção a novas especificações e que, independente dos distúrbios, mantenham a saída no *set-point* estabelecido.

O trabalho tem como objetivos específicos:

- Modelagem em regime estacionário do processo de produção de etanol anidro;
- Modelagem em regime transiente do processo de produção de etanol anidro com um sistema de controle;

- Aplicação de Redes Neurais Artificiais, com o uso da ferramenta *Neural Network Toolbox* do MATLAB® para a construção do controle inteligente;
- Desenvolvimento da comunicação entre o MATLAB® e *Aspen Plus Dyanamics*™ para simular a atuação do sistema de controle inteligente;
- Analisar o comportamento do processo frente a mudanças de especificações no produto;
- Analisar o comportamento do processo frente a distúrbios;
- Comparar o sistema de controle inteligente com o controle convencional.

1. 4 Contribuições

Definida a problematização e a partir da solução para os objetivos traçados para este trabalho, as principais contribuições são:

- Desenvolvimento de um modelo matemático de inferência que descreva bem as relações entre as variáveis controladas, distúrbios e especificações do produto em um processo de destilação extrativa;
- Desenvolvimento de uma comunicação entre diferentes dispositivos com a finalidade de controlar o processo e modificar a composição dos produtos, dependendo das condições do mercado, com comandos mínimos do operador;
- Desenvolvimento de um sistema de controle inteligente, baseado no uso de redes neurais artificiais, que ajuste os set-points dos controladores do processo prevendo uma condição de baixo consumo de energia nos refervedores;
- Dois artigos foram gerados diretamente a partir deste trabalho. O primeiro foi publicado na revista *Korean Journal of Chemical Engineering* em 2018 (Capítulo 3) e outro publicado na revista *Neural Computing and Applications* em 2019 (Capítulo 4).

1. 5 Estrutura do Trabalho

O Capítulo 2 aborda uma revisão bibliográfica a qual se discute conceitos basilares, apresentando fundamentos termodinâmicos do equilíbrio de fases e a utilização de redes neurais artificiais em processos de destilação extrativa como uma nova estratégia frente aos desafios do controle em processos de destilação extrativa apresentados no Capítulo 1.

O capítulo 3 apresenta um artigo publicado na revista *Korean Journal of Chemical Engineering*. Esse trabalho destaca a possibilidade de controle utilizando três redes neurais, sendo que a composição do etanol na alimentação do azeótropo é inferida por uma primeira rede neural (RNA_1) e este resultado é utilizado como entrada em uma segunda rede neural (RNA_2), a qual atualiza os set-points dos controladores do processo para manter o produto dentro da especificação. Como podem existir regiões em que a RNA_2 não está suficientemente treinada, uma terceira rede (RNA_3) a substitui, atuando somente na região deficitária.

O capítulo 4 reporta um artigo publicado na revista *Neural Computing and Applications*. O controle desenvolvido se adapta às novas situações para levar o processo a um novo estado estacionário com o consumo mínimo de energia. As mudanças nas condições operacionais são possíveis através de modelos baseados em várias redes neurais simulados em MATLAB®/Simulink que atuam de forma independente.

O capítulo 5 apresenta um artigo que foi publicado na revista *Separation and Purification Technology*. Esse capítulo mostra que é possível utilizar um controle inteligente, baseado em apenas uma rede neural artificial, com possibilidade de levar o processo para um novo regime estacionário, minimizando simultaneamente oscilações diante distúrbio na alimentação e sempre prevendo um consumo mínimo de energia. Tanto no capítulo 3 quanto no capítulo 5, é feita uma comparação entre o controle convencional e a nova proposta.

O capítulo 6 apresenta as conclusões diante os resultados obtidos, destaca a solução para o problema abordado e sugestões para trabalhos futuros.

CAPÍTULO 2

REVISÃO BIBLIOGRÁFICA

CAPÍTULO 2 – REVISÃO BIBLIOGRÁFICA

Neste capítulo, é apresentada uma revisão bibliográfica referente à mistura azeotrópica etanol/água, destilação e os fundamentos termodinâmicos de equilíbrio de fases líquido-vapor, destilação extrativa e controle em colunas de destilação utilizando também comunicação entre diferentes dispositivos. Outras revisões bibliográficas são realizadas na introdução dos capítulos 3, 4 e 5, sendo esse capítulo 2 uma complementação para ampliar conceitos teóricos sobre o problema apresentado.

2. 1 Mistura azeotrópica etanol/água

Os investimentos em biocombustíveis na matriz energética mundial estão acontecendo de forma expressiva. Nesse cenário, o etanol tornou-se uma substância estratégica para a economia brasileira, pois o país tem tradição e conhecimento na sua produção, apostando nesse biocombustível como uma alternativa viável diante da perspectiva de esgotamento de fontes energéticas de origem fóssil, como o petróleo (Junqueira et al., 2010).

No Brasil, ele é fabricado principalmente através da cana-de-açúcar, mas pode ser obtido também através de outros vegetais, como milho e beterraba, ou em processos químicos controlados em laboratório. A cana-de-açúcar, por exemplo, dispõe de grandes quantidades de sacarose. A fermentação desse carboidrato é realizada utilizando leveduras comerciais como *Saccharomyces cerevisiae*. A reação química é composta pela hidrólise enzimática da sacarose seguida de fermentação de açúcares simples (Ahmed et al., 2020).

Primeiro, a invertase (uma enzima presente na levedura) catalisa a hidrólise da sacarose para convertê-la em glicose e frutose.

$$\underset{\text{Sucrose}}{C_{12}H_{22}O_{11}} + H_2O \xrightarrow{Invertase} \underset{\text{Glicose}}{C_6H_{12}O_6} + \underset{\text{Frutose}}{C_6H_{12}O_6} \tag{2.1}$$

Em seguida outra enzima (*zymase*), também presente na levedura, converte glicose e frutose em etanol e dióxido de carbono.

$$\underset{\text{Glicose ou frutose}}{C_6H_{12}O_6} + H_2O \xrightarrow{Zymase} \underset{\text{etanol}}{C_2H_5OH} + CO_2 \tag{2.2}$$

O produto da fermentação, também chamado de vinho, contém além de álcool, outros componentes de natureza líquida, sólida e gasosa. O álcool presente neste vinho é recuperado por destilação, processo que se utiliza dos diferentes pontos de ebulição das diversas substâncias voláteis. O álcool hidratado, produto dos processos de destilação é uma mistura binária álcool/água que atinge um teor de no máximo 89,52 mol% (95,62 massa%) de etanol (Confalonieri, 2019). Esses resultados podem ser confirmados com dados de equilíbrio líquido (x)/vapor (y) disponibilizado pelo módulo do Instituto Nacional de Padrões e Tecnologia Americano (NIST - Nacional Institute of Standards and Thecnology) que são encontrados no simulador *Aspen Plus*™, o qual também tem um recurso de busca de azeótropos em uma mistura. A partir do banco de dados do modelo escolhido, o simulador compara os dados binários entre os componentes de um sistema específico e disponibiliza um relatório com dados de propriedades como temperatura de ebulição e composição de azeotrópica.

De acordo com a Figura 2.1, o modelo que representa bem o equilíbrio de fases etanol/água é o *non-random two liquids* (NRTL), o qual é recomendado para descrever soluções fortemente não lineares e equilíbrio líquido-líquido (Kiss e Suszwalak, 2012).

Figura 2.1. Equilíbrio Líquido/Vapor para etanol e água e Etanol a pressão de 1 atm simulado no *Aspen Plus*™

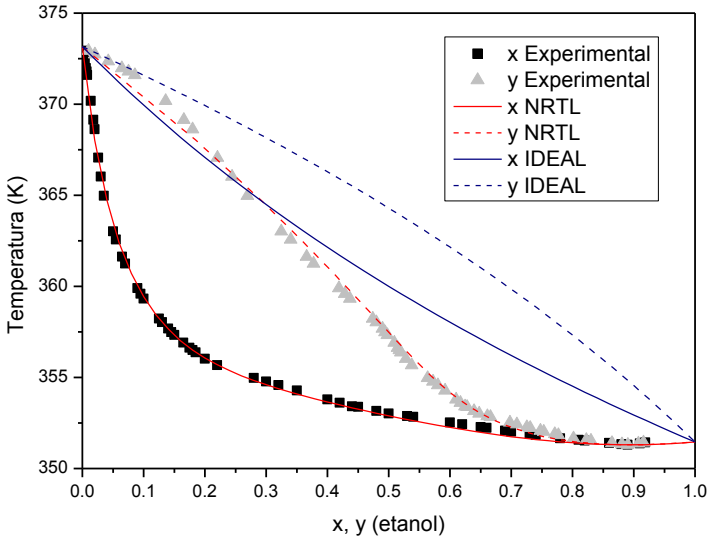

A mistura etanol/água é considerada não ideal e seu comportamento não pode ser descrito pela Lei de Raoult, pois são substâncias não similares que apresentam atrações moleculares quando misturadas. Na temperatura de 78,15 °C (351,3 K) o vapor e o líquido adquirem a mesma composição (mistura azeotrópica), e o ponto de ebulição deste azeótropo é menor em comparação com os pontos de ebulição de seus componentes puros. Sendo a

destilação baseada na diferença de volatilidade, esse fenômeno físico impede que os componentes sejam completamente separados pelo processo de destilação convencional já que na temperatura azeotrópica, os componentes adquirem a mesma volatilidade.

2. 2 Destilação e os Fundamentos termodinâmicos do equilíbrio de fases

Uma das formas de separar os componentes de uma mistura homogênea é por vaporizações e condensações sucessivas, aproveitando as diferentes volatilidades dos componentes. Dessa forma, a parte vaporizada fica mais rica no componente mais volátil, enquanto a parte condensada fica mais rica com o componente menos volátil. Esse processo que é feito em colunas ou torres de destilação tem a termodinâmica como base, a qual possibilita a descrição e compreensão da estabilidade e transformações das fases.

Para uma maior eficiência no processo, é necessário que as fases entrem em equilíbrio, ou seja, o número de moléculas que abandona a fase líquida para a fase vapor é igual ao número de moléculas que voltam da fase vapor para a fase líquida. Nesse caso, as fases devem entrar em contato por tempo suficiente, o qual depende dos detalhes construtivos da coluna e consequentemente dos conhecimentos termodinâmicos sobre equilíbrio de fases (Seader e Henley, 1998).

De acordo com Van Ness (2005) e Atkins (2014), os principais critérios utilizados para considerar um sistema em equilíbrio, em termos de quantidades intensivas são: temperatura (T), pressão (P) e potencial químico (μ), conforme mostra as Equações 2.3, 2.4 e 2.5.

$$T^{\alpha} = T^{\beta} = ...T^{\pi} \tag{2.3}$$

$$P_i^{\alpha} = P_i^{\beta} = ...P_i^{\pi} \tag{2.4}$$

$$\mu_i^{\alpha} = \mu_i^{\beta} = ...\mu_i^{\pi} \tag{2.5}$$

onde i representa os componentes e $\alpha, \beta, ..., \pi$ representam as fases em equilíbrio.

Por definição o potencial químico pode-se relacionar com a energia livre de Gibbs (G). A energia livre de Gibbs parcial molar ($\overline{G}$) está de acordo Equação 2.6 quando se considera gás ideal (*gi*).

$$\mu_i^{gi} \equiv \overline{G_i^{gi}} = C_i + RT \ln P_i \tag{2.6}$$

onde C_i é uma constante de integração a temperatura constante que depende da espécie i, P_i é a pressão parcial da espécie i e R é a constante universal dos gases. Porém, a expressão do potencial químico para um gás real pode ser parecida com a mostrada na Equação 2.6. Nesse caso, substitui-se a pressão parcial por uma pressão efetiva, chamada de fugacidade do componente i na mistura ($\hat{f}_i$).

$$\mu_i = C + RT \ln \hat{f}_i \tag{2.7}$$

A fugacidade é uma função da pressão e da temperatura, e sendo potenciais químicos variáveis não mensuráveis nem fáceis de manipular, é preferível expressar o equilíbrio termodinâmico em função das fugacidades,

$$f^{\alpha} = f^{\beta} = \ldots f^{\pi} \tag{2.8}$$

Para líquido-vapor:

$$f^{v} = f^{l} \tag{2.9}$$

As fugacidades podem ser expressas através de coeficientes de fugacidade (ϕ), preferentemente para a fase vapor, ou de coeficientes de atividade (γ), mais usados para a fase líquida. Então, numa abordagem gamma-phi, a equação de isofugacidade pode ser escrita como:

$$y_i \hat{\phi}_i P = x_i \gamma_i \phi_i^{sat} P^{sat} e^{\left[\frac{V_i^l (P - P_i^{sat})}{RT}\right]} \tag{2.10}$$

onde y_i é a fração molar do componente i na fase vapor, $\widehat{\emptyset}_i^v$ é o coeficiente de fugacidade na fase vapor do componente i, x_i é a fração molar do componente i na fase líquida, P_i^{sat} é a pressão de vapor do componente i puro, $\emptyset_i^{sat}$ é o coeficiente de fugacidade do vapor do componente i puro, V_i^l é o volume molar do líquido saturado do componente i puro, e R é a constante universal dos gases. O termo exponencial é conhecido como correção de *Poynting*, e expressa os desvios da fase líquida devidas ao efeito da pressão. Se a pressão de trabalho é baixa ou próxima da pressão de vapor, este termo é usualmente desprezado.

Existem na literatura vários tipos de correlação para cálculo de pressão de saturação em função da temperatura, como pode ser visto em Reid et al. (1988). Algumas correlações são a DIPPR (*Design Institute for Physical Properties*), Antoine e Antoine estendido. A equação DIPPR permite representar faixas de temperatura maiores, bem como permite extrapolações mais seguras e é usada pelo *Aspen Plus*™ nas simulações deste trabalho.

$$\ln P^{sat} = A + \frac{B}{T} + C\ln T + DT^{E} \tag{2.11}$$

sendo A, B e C, D e E as constantes ajustadas a dados experimentais de pressão de vapor.

Para que os resultados dos cálculos de equilíbrio líquido-vapor sejam precisos, principalmente quando se trata de misturas com fortes desvios da idealidade, é fundamental que se disponha de boas correlações para o cálculo dos coeficientes de atividade, com parâmetros ajustáveis a partir de dados experimentais confiáveis.

Em sistemas multicomponentes, a escolha de um modelo de equilíbrio líquido-vapor torna-se limitada. As correlações de Margules e Van Laar são estritamente válidas para sistemas binários, não podendo ser modificadas para sistemas multicomponentes. Então, outros modelos são usados para misturas multicomponentes, tais como: Wilson, *non-random two liquids* (NRTL) e *Universal Quasi Chemical* (UNIQUAC). O grande conveniente destes modelos é que os parâmetros requeridos são conjuntos de interações binárias. Deste modo, uma vez que os dados de equilíbrio líquido-vapor tenham sido medidos experimentalmente para cada binário no sistema multicomponente, todos os parâmetros são disponíveis para predizer o comportamento multicomponente.

No presente trabalho, o modelo termodinâmico escolhido para a representação da fase líquida é o NRTL, por corresponder aos resultados experimentais obtidos por Meirelles et al. (1992) e por corresponder aos dados experimentais de equilíbrio líquido/vapor disponibilizado pelo NIST conforme mostrado na Figura 2.1.

Uma das principais vantagens do NRTL é que os parâmetros requeridos são conjuntos de interações binárias, as quais para o sistema etanol/água podem ser tomadas a partir do banco de dados do *Aspen Plus*™. Deste modo, uma vez que os dados de equilíbrio líquido-vapor tenham sido medidos experimentalmente para cada binário no sistema multicomponente, todos os parâmetros são disponíveis para predizer o comportamento multicomponente.

No modelo NRTL para os coeficientes de atividade em uma mistura multicomponente é descrito de acordo com a Equação 2.11.

$$\ln \gamma_i = \frac{\sum_j \tau_{ij} G_{ij} x}{\sum_k G_{ki} x_k} + \sum_j \frac{x_j G_{ij}}{\sum_k G_{ki} x_k} \left[\tau_{ij} - \frac{\sum_k x_k \tau_{kj} G_{ki}}{\sum_k G_{ki} x_k} \right] \tag{2.12}$$

onde,

$$\tau_{ij} = \frac{\Delta g_{ij}}{RT}, \qquad \tau_{ij} \neq \tau_{ji} \tag{2.13}$$

$$\Delta g_{ij} = A_{ij}T + B_{ij} \tag{2.14}$$

$$\tau_{ij} = A_{ij} + \frac{B_{ij}}{T} \tag{2.15}$$

$$G_{ij} = \exp(-\alpha_{ij}\tau_{ij}), \quad \alpha_{ij} = \alpha_{ji} \tag{2.16}$$

Os parâmetros A_{ij} e B_{ij} não dependem da temperatura, estão relacionados à energia característica da interação entre as moléculas (cal/gmol) i e j, e podem ser determinados por uma regressão de dados de equilíbrio líquido–vapor. O α_{ij} é o parâmetro não randômico para interação binária (Alvarez et al., 2009 e Zhang et al., 2009).

2. 3 Destilação extrativa

Os processos de destilação extrativa são amplamente utilizados nas indústrias químicas para a separação de misturas não ideais. Geralmente se utiliza um solvente de alto ponto de ebulição, causando um aumento na volatilidade relativa dos principais componentes. Além disso, o solvente é completamente miscível na mistura, como pode ser visto em Seader e Henley (1998).

Luyben (2015), Doherty e Malone (2001) também estudaram solventes com ponto de ebulição intermediário com relação aos componentes envolvidos na mistura azeotrópica. Nesse caso existem duas configurações possíveis. Na sequência de separação direta, o componente chave leve é removido no destilado na primeira coluna extrativa. O solvente e o componente chave pesado saem na base e são alimentados na segunda coluna em que o componente chave pesado sai na parte inferior e o solvente no destilado, que é reciclado de volta à primeira coluna. Na sequência de separação indireta, o componente chave pesado é removido como produto de fundo da primeira coluna extrativa. O solvente e o componente chave leve saem no destilado e são alimentados a uma segunda coluna na qual o componente chave leve sai no destilado e o fundo é o solvente, que é reciclado de volta à primeira coluna.

Uma destilação extrativa típica é a desidratação de etanol pelo seu grande interesse industrial, principalmente devido ao potencial do etanol como fonte renovável de energia. Etanol é um combustível de queima relativamente limpa, e quanto comparado outros

combustíveis de origem fóssil, pode reduzir a poluição emitida para a atmosfera (Vorayos et al., 2006). Nesse sentido, Shealy et al. (1987) estudaram esse processo de desidratação utilizando a dimetilformamida, com o objetivo de verificar a possibilidade de utilizar esse solvente em substituição ao etilenoglicol. Embora apresente a vantagem de possuir uma temperatura normal de ebulição mais baixa do que a do etilenoglicol, a dimetilfomamida tem tendência a sofrer hidrólise, impedindo a sua utilização como solvente na destilação extrativa.

Reis (2002) utilizou os mapas de curvas residuais em seu trabalho para verificar o melhor solvente para separar a mistura etanol/água. Com auxílio de simulação computacional, concluiu que o etilenoglicol é um bom solvente para obter etanol puro, pois como não forma novos azeótropos no sistema, pode-se obter os três produtos puros ao final do processo. O solvente deve ser escolhido de modo que minimize os custos de produção, tenha baixa pressão de vapor, maior afinidade com a água, de modo a arrastá-la em maior quantidade e menor quantidade de etanol possível para fornecer a separação desejada com o mínimo de solvente.

Ravagnani (2010) estudou um processo de destilação extrativa para obter etanol puro usando etilenoglicol e tetraetilenoglicol como solventes. Mapas de curva residuais também são usados para analisar os comportamentos de mistura e viabilidade de colunas de destilação. O autor conclui que o processo de separação da mistura etanol-água utilizando tetraetilenoglicol é possível e interessante uma vez que essa substância é menos tóxica do que o etileno glicol. Entretanto, quando o solvente é o tetraetilenoglicol, a coluna extrativa deve ser maior, consumindo mais energia.

Alternativamente a destilação extrativa, o sistema de peneiras moleculares pode ser usado para desidratação, como ocorre mais amplamente nos Estados Unidos com o etanol de milho (Manochio et al., 2017). Bastidas et al. (2010) realizaram um estudo de simulação comparando as principais vantagens e desvantagens dessas tecnologias e observaram que nas mesmas condições de alimentação, a quantidade de etanol obtida através da técnica de peneiras moleculares era inferior com relação a produção via colunas de destilação. Dessa forma, a destilação extrativa com etilenoglicol teve uma melhor eficiência com relação ao consumo total de energia por quilograma de etanol produzido.

Os líquidos iônicos têm atraído muito atenção como uma alternativa na obtenção de etanol anidro, devido ao baixo ponto de fusão, baixa volatilidade, fácil recuperação e seletividade (Jelinski e Cysewski, 2017). Porém, o custo dos líquidos iônicos e o complexo processo de síntese são fatores limitantes para realizar, na atualidade, a implementação deste

processo em escala industrial. Além disso, apresentam baixa biodegradabilidade e potencial de toxidade, fugindo do consenso cada vez mais geral sobre o uso de solventes verdes, ou seja, aqueles que reduzem o impacto ambiental (Dong et al., 2017, Mondal e Saha, 2018; Kerton e Marriott, 2013).

Ultimamente vem crescendo a quantidade de estudos relacionados ao uso de acoplamento térmico em sistemas de destilação extrativa, mostrando redução do consumo energético em relação aos sistemas convencionais (Anokhina e Timoshenko, 2015; Brito et al. 2016; Wu et al., 2013). Embora os estudos mostrem que os métodos são eficientes em termos energéticos, ainda não foram amplamente utilizados na indústria devido às complexidades do projeto e do controle (An et al., 2015).

Neste trabalho utilizar-se-á a destilação extrativa como técnica de separação da mistura azeotrópica etanol/água utilizando etilenoglicol como solvente. Vários trabalhos disponíveis na literatura reforçam a técnica da destilação extrativa como uma alternativa viável, amplamente utilizada, baixo consumo energético e com flexibilidade para seleção de possíveis solventes (Brito, 1997; Dias, 2008; Figueroa, 2011; Figueirêdo et al., 2015; Ramos et al., 2016; Lei, 2014).

A simulação computacional é uma ferramenta poderosa e muito presente na resolução de problemas da engenharia química, permitindo predizer o comportamento de processos usando relações de balanços de massa, energia e equilíbrio termodinâmico (Aspentech, 2001). Nesse sentido, avaliou-se o etilenoglicol utilizando diagramas pseudo-binários, onde a razão molar de um dos componentes é mantida constante com relação aos outros dois componentes. Neste caso as composições da água e do etanol foram variadas, mantendo constante a composição do solvente. Então, é possível representar o efeito do solvente no equilíbrio binário. Considerando o sistema ternário água/etanol/solvente, o diagrama em base livre de solvente pode ser construído de acordo com as equações a seguir:

$$x_1' = \frac{x_1}{x_1 + x_2} \tag{2.17}$$

A soma das composições de todos os componentes na fase líquida é sempre igual a 1:

$$x_1 + x_2 + x_3 = 1 \tag{2.18}$$

$$x_2 = 1 - x_1 - x_3 \tag{2.19}$$

Substituindo a Equação 2.19 na Equação 217:

$$x_1' = \frac{x_1}{x_1 + x_2} = \frac{x_1}{1 - x_3} \tag{2.20}$$

onde $x_1, x_2\ e\ x_3$ são a fração molar da fase líquida de etanol, água e solvente, respectivamente. E o apostrofo indica a fração molar da fase líquida livre de solvente.

Analogamente,

$$y_1' = \frac{y_1}{y_1 + y_2} = \frac{y_1}{1 - y_3} \tag{2.21}$$

Onde $y_1, y_2\ e\ y_3$ são a fração molar da fase vapor de etanol, água e solvente, respectivamente. E o apostrofo indica a fração molar da fase vapor livre de solvente.

Logo, com a utilização do *Aspen Plus*™, o diagrama y_1' em função de x_1' pode ser construído para diferentes concentrações de solvente.

Figura 2.2. Diagrama pseudo-binário para o sistema etanol/água/etilenoglicol à pressão constante de 1 atm

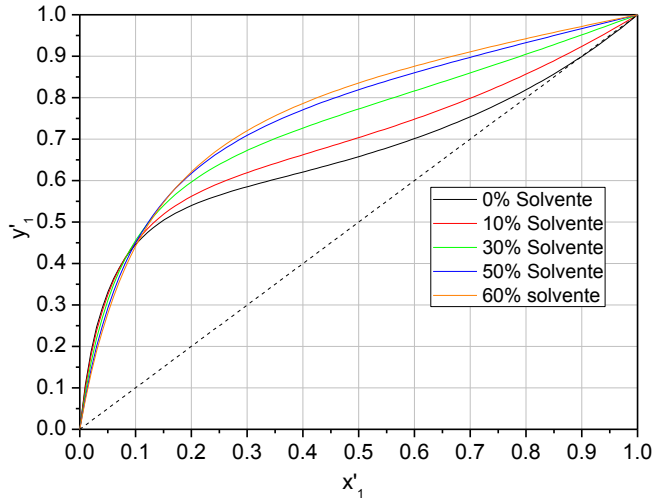

O diagrama pseudo-binário mostra como a volatilidade relativa é afetada pela razão de alimentação entre o solvente e azeótropo. Com 0% de solvente, a mistura apresenta um ponto azeotrópico, ou seja, um ponto em que as composições da fase líquida e da fase vapor são iguais. Á medida que uma maior quantidade de etilenoglicol é introduzida, o comportamento da mistura assemelha-se a uma mistura binária ideal

2. 4 Controle em colunas de destilação

O grande problema nos processos de destilação é a necessidade de controle da composição, por ser ainda uma variável de difícil medição. Esse problema vendo sendo estudado a mais de 40 anos por autores como Brosilow et al. (1978), Dahlqvist, (1980), Meyer et al. (1977) Tolliver e McCune (1980).

Atualmente existe uma forte tendência em utilizar tecnologias modernas com informações em tempo real sobre os processos químicos, permitindo otimizar eficiências dos sistemas de controle (Bakhtadze, 2004).

A inteligência artificial usada como método para a construção do modelo de um sistema de controle avançado tende a solidificar-se com o aumento da velocidade dos processadores eletrônicos. Dentre os métodos de inteligência computacional existentes destacam-se as redes neurais artificiais, a lógica fuzzy, os algoritmos genéticos, etc.

A destilação extrativa consome a maior parte da energia usada em um processo típico de produção de etanol anidro, mostrando a alta necessidade de controlar e otimizar esse processo para minimizar o consumo energético (Lee e Pahl, 1985; Sholl e Lively, 2016).

Ramos et al. (2016) utilizaram uma corrente de *by-pass* no trocador de calor, que faz uma integração térmica das correntes de alimentação de uma coluna extrativa. Essa estratégia de dividir a corrente de reciclo, fazendo com que uma parte não passe pelo trocador, se mostrou eficaz para controlar a temperatura de alimentação do solvente, uma vez que uma válvula foi introduzida nessa corrente para funcionar como elemento final de controle. Sistemas de controle alternativos para controle de pressão em coluna já foram estudados também utilizando correntes de *by-pass* (Kister e Hanson, 2015; Luyben, 2006; Sloley, 2001). A estratégia de desvio de vapor de topo sem passar pelo condensador da coluna de destilação se mostrou como uma boa alternativa capaz de eliminar a necessidade de manipular dinamicamente o fluido de resfriamento do trocador de calor (Ciannella et al., 2018). Nesses trabalhos, se percebe que um bom controle na temperatura de alimentação e de pressão de topo da coluna de destilação consequentemente melhora o controle da composição do produto.

Tututi-Ávila et al. (2014) exploraram o desempenho do controle dinâmico de uma coluna extrativa de parede dividida para processo de desidratação de etanol. A estratégia geral de controle do processo com a coluna de parede dividida foi comparada com uma configuração

convencional e em ambos os casos, a composição de etanol no destilado apresentou pequenos offsets quando distúrbios na composição da alimentação foram testados, sendo a configuração com parede dividida com o menor desempenho.

Para modelar e identificar a dinâmica de sistemas reais, é necessário o conhecimento detalhado do processo, algo que demanda muito tempo e que acarreta custo para o projeto do sistema de controle e monitoramento. Em processos de destilação os modelos são complexos do ponto de vista matemático, pois envolvem sistemas de equações não lineares (Ramaswamy et al., 2005; Nagy, 2007).

Então, é de grande interesse industrial o desenvolvimento de teorias de controle que levem em consideração as não linearidades e as mudanças das condições operacionais. Muitos desses modelos, envolvem equações diferenciais, apresentando relativa complexidade, tanto para serem criados, como para serem utilizados em tempo real para controladores avançados. O elevado número de equações presentes na modelação das colunas de destilação aumenta o número de parâmetros, que são muitas vezes difíceis de estimar. Assim, mesmo quando se utiliza um modelo de controle preditivo (MPC) tradicional, isto poderia conduzir a dificuldades de convergência, ou produzir resultados com precisão insuficiente. Por questões práticas, muitos são inviáveis financeiramente ou acabam tendo respostas não aceitáveis dentro de um intervalo de tempo reduzido, pois o grande número de parâmetros envolvidos demanda muito esforço computacional (Luyben, 1990, Osuolane e Zhang, 2016).

O uso das técnicas de identificação de sistemas caixa-preta é a mais indicada quando a elaboração do modelo fenomenológico é inviável (Aguirre, 2015). Para empregá-las definem-se: o conjunto de dados de entrada-saída dentro da faixa de interesse para que o modelo possa ser construído. Redes Neurais Artificiais (RNA) se apresentam como uma boa alternativa por apresentar características em captar não linearidades, considerando-se a relação entre o estímulo de entrada e a resposta de saída, com esforço computacional relativamente baixo, tornando-se possível para otimização e controle em tempo real (Osuolane e Zhang, 2016).

2. 5 Redes Neurais Artificiais

As RNAs tiveram início em 1943, quando Wax Ten McCulloch e Walter Pitts modelaram o funcionamento do neurônio biológico (Haykin, 2009). Mas, só em 1988 as RNA tiveram seu início na Engenharia Química, com a publicação do primeiro artigo por Hoskins e

Himmelblau (1988), que aplicaram uma RNA para o diagnóstico de erros em um sistema de reatores químicos.

O neurônio artificial mais utilizado é baseado no modelo proposto por McCulloch e Pitts (1943). A Figura 2.3 ilustra uma representação esquemática de uma RNA, onde o neurônio da camada *j* está à direita dos neurônios da camada *i*.

Figura 2.3. Esquema de um neurônio artificial

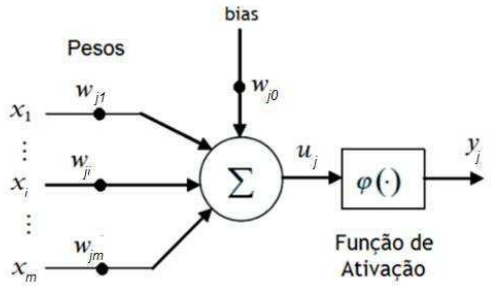

Uma rede neural artificial é composta basicamente por um conjunto de sinapses, funções de transferências e bias:

- Conjunto de Sinapses: cada uma com um peso sináptico (w_{ji}). Os pesos, na maioria das arquiteturas de rede hoje propostas, são ajustáveis e representam a memória e o conhecimento usado na solução do problema.
- Função de ativação (φ): A função de ativação é aplicada sobre os sinais de entrada, a partir de uma saída intermediária (u_i). Sem a função de ativação, a RNA seria simplesmente um modelo de regressão linear, estando sujeita as mesmas restrições de modelos lineares. Logo a função de ativação é essencial para dar características não lineares, gerando o sinal de saída do neurônio (y_i), o qual é propagado para os neurônios seguintes da rede (Goodfellow et al., 2016).
- Bias: um termo opcional (b_j) que provê um valor fictício de entrada igual a 1, dando um grau de liberdade maior para a função de saída do neurônio. Como o bias pode ser encarado como sendo o peso w_{j0}, para um neurônio cuja entrada é sempre 1, percebe-se que a mesma regra para atualização dos pesos é válida também para a atualização do bias, tornando assim mais fácil a tarefa.

A proposta da utilização das técnicas de Redes Neurais Artificiais baseia-se no fato de que em problemas de grande porte pode não ser viável utilizar um modelo fenomenológico.

Comuns são os problemas de inicializar todas as variáveis desejadas, pois pode não haver disponibilidade destes valores e o tempo de resolução do modelo pode ser elevado devido ao grande conjunto de equações algébrico-diferenciais. A rede neural, uma vez bem treinada, é capaz de fornecer os resultados sem os problemas citados anteriormente. Com isto, torna-se possível testar várias alternativas de modelagem sem que seja necessário reconstruir totalmente o modelo.

De acordo com a Figura 2.3, as Equações 2.22 e 2.23 descrevem de forma simplificada um neurônio artificial.

$$u_j = x_1.w_{j1} + x_2.w_{j2} + x_3.w_{j3} + ... + x_m.w_{jm} + w_{j0} \tag{2.22}$$

$$y_j = \varphi(u_j) \tag{2.23}$$

A função de ativação funciona como um limitante à amplitude de saída do neurônio, normalizando dentro de um intervalo fechado, geralmente [0, 1] ou [-1, +1].

O software MATLAB® tem diversas funções de ativação já embutidas. A Tabela 2.1 apresenta as principais funções de ativação utilizadas no MATLAB®.

Tabela 2.1. Funções de ativação disponíveis no MATLAB®

Função	**Descrição**
hardlim	Função degrau
harlims	Função degrau simétrica
satlin	Função linear com saturação
satlins	Função linear simétrica com saturação
logsig	Função logística sigmoidal
tansig	Função tangente sigmoidal
poslin	Função linear positiva
purelin	Função Linear

As funções de ativação tipo degrau permitem que os neurônios escolham uma dentre duas saídas (largamente empregada em problemas de classificação). Enquanto as funções lineares com ou sem saturação apresentam um espectro de saída maior para o neurônio (bastante utilizadas em problemas que exigem aproximadores lineares). As funções de ativação sigmoidais são contínuas em todo o intervalo e são as mais utilizadas em redes neurais artificiais, pois apresentam um balanço entre o comportamento linear e não linear (Beale et al., 2010).

Uma vez que a rede tenha minimizado o erro de predição, de acordo com a Figura 2.6, através de algum algoritmo de treinamento, seus parâmetros são fixados, e a rede estará pronta para ser usada com dados da situação corrente.

Figura 2.4. Esquema simplificado aprendizado de uma rede neural artificial

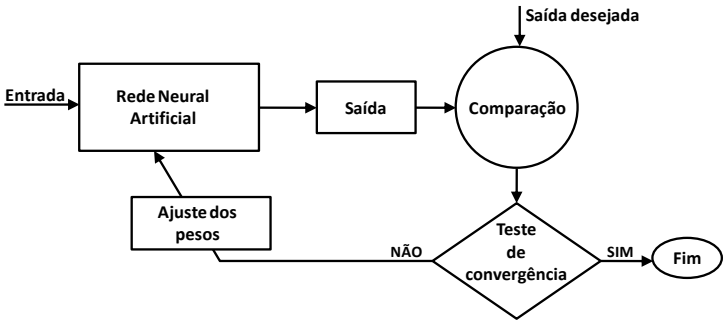

Vários algoritmos de treinamento foram desenvolvidos, e o software MATLAB® já dispõe de vários deles prontos para serem usados (Tabela 2.2).

Tabela 2.2. Algoritmos de treinamentos disponíveis no MATLAB®

Função	Descrição
Traingd	Gradiente descendente básica. Apresenta resposta lenta.
traingdm	Gradiente descendente com momentum. Geralmente é mais rápido do que o traingd.
Traingdx	Taxa de aprendizado adaptativa. Convergência mais rápida do que traingd, porém só pode ser utilizado em treinamento por batelada.
Trainrp	Resilent backpropagation. Batelada com rápida convergência e pouca memória requisitada.
traincgf	Gradiente conjugado de Fletcher-Reeves. Possui os menores requisitos de memória dentre os algoritmos de gradiente conjugado.
traincgp	Gradiente conjugado de Polak-Ribiére. Requer um pouco mais de memória do que o traincgf, mas apresenta convergência rápida para determinados tipos de problemas.
traingb	Gradiente conjugado de Powell-Beale. Requer um pouco mais de memória do que o traincgp, mas apresenta convergência rápida.
trainscg	Gradiente conjugado em escala. O único algoritmo de gradiente conjugado que não necessita da função line seach. Adapta-se com facilidade a uma grande variedade de problemas.
trainbfg	Método quase-Newton BFGS. Necessita o armazenamento da aproximação da matriz Hessiana e requer mais recurso computacional a cada interação do que os algoritmos de gradiente conjugado, porém geralmente converge em poucas interações.
trainoss	One Step Secant Mhetod. Meio termo entre métodos de gradiente conjugado e quase-Newton.
Trainlm	Algoritmo de Levenberg-Marquardt. É o algoritmo de treinamento mais rápido para redes de tamanho moderado. Possui a função de redução de memória para ser utilizada quando possuir muitos dados para treinamento.
trainbr	Regularização de Bayesian. É uma modificação do algoritmo de treinamento de Levenberg-Maquardt para gerar redes com melhor generalização. Reduz a dificuldade de se determinar a arquitetura de rede otimizada.

Dentre as várias classes de redes neurais, pode-se destacar as redes feedforward de múltiplas camadas (*Feedforward Multi layer perceptron - MLP)* e a rede recorrente de Elman. Na primeira classe existe a presença de uma ou mais camadas ocultas. A informação nesse tipo

de arquitetura é distribuída em um só sentido. É capaz de aproximar qualquer função desde que possua número suficiente de neurônios nas camadas ocultas (Haykin, 2009).

Figura 2.5. Esquema de uma rede feedforward de múltiplas camadas

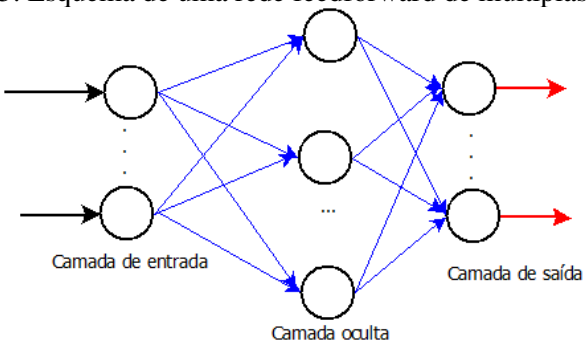

Já as redes recorrentes de Elman tem pelo menos um laço de realimentação onde são criadas unidade de contexto ou operadores de atraso unitário (Z^{-1}). Inicialmente a camada de entrada recebe o primeiro padrão. Tanto a camada de entrada como as unidades de contexto ativam a camada oculta que, por sua vez, ativa a camada de saída. No início do treinamento, as ativações das unidades intermediárias são desconhecidas e, geralmente, são inicializadas para a metade do valor máximo que as unidades intermediárias podem ter. É uma rede parcialmente recorrente, em que as conexões são principalmente feedforward, mas também incluem um conjunto de conexões de backward, que permitem que a rede lembre-se de sugestões recentes (Huang et al. 2005).

Figura 2.6. Esquema de uma rede recorrente de Elman

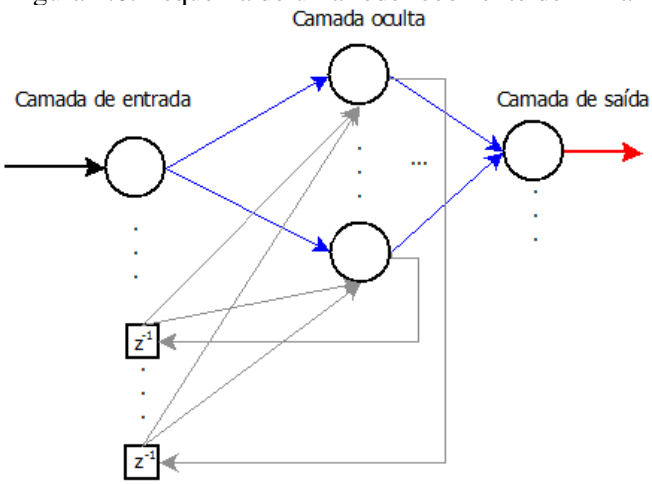

As redes neurais já foram aplicadas com sucesso na identificação e controle de sistemas dinâmicos. As capacidades de aproximação universal de redes multicamadas faz delas uma

escolha popular para modelar sistemas não lineares e para implementar controladores não lineares de uso geral (Hagan e Demuth, 1999; Beale et al., 2010).

Quanto ao modo de treinamento, geralmente utiliza-se o modo sequencial padrão devido ao menor armazenamento de dados, além de ser menos suscetível ao problema de mínimos locais, devido à pesquisa de natureza estocástica que realiza. No treinamento sequencial padrão, os pesos são atualizados após a apresentação de cada exemplo de treinamento.

Seja o sinal de erro na saída do neurônio *j* da camada de saída na iteração *n* (isto é, na apresentação do *n*-ésimo vetor de treinamento) definido por

$$e_j(n) = d_j(n) - y_j(n) \tag{2.24}$$

sendo d_j a saída desejada para o neurônio *j*.

Define-se o valor instantâneo do erro quadrático para o neurônio *j* de acordo com $e_j^2(n)/2$. O valor instantâneo da soma dos erros quadráticos $\varepsilon(n)$ é obtida somando $e_j^2(n)/2$ sobre todos os neurônios da camada de saída. A soma instantânea dos erros quadráticos na camada de saída é então escrita de acordo com a Equação 2.25.

$$\varepsilon(n) = \sum_{j \in C} \frac{e_j^{\,2}(n)}{2} \tag{2.25}$$

sendo *C* o conjunto que inclui todos os neurônios na camada de saída

O algoritmo *backpropagation* aplica a correção $\Delta w_{ji}(n)$ ao peso sináptico, tendo como base a direção contrária do gradiente local $\Delta\varepsilon(n) / \Delta w_{ji}(n)$ da superfície do erro $\varepsilon(w)$ relativo ao peso sináptico.

A correção $\Delta w_{ji}(n)$ aplicada a $w_{ji}(n)$, ditada pela Regra Delta Generalizada, definida por

$$\Delta w_{ji}(n) = w_{ji}(n+1) + w_{ji}(n) = -\eta \frac{\partial \varepsilon(n)}{\partial w_{ji}(n)} \tag{2.26}$$

onde η é a constante que determina a razão de aprendizado do algoritmo *backpropagation*. O uso do sinal negativo impõe a movimentação contrária à direção apontada pelo gradiente na superfície de erro definida no espaço de pesos sinápticos

De acordo com a regra da cadeia do cálculo diferencial, o gradiente local pode ser expresso pela Equação 2.27.

$$\frac{\partial \varepsilon(n)}{\partial w_{ji}(n)} = \frac{\partial \varepsilon(n)}{\partial e_j(n)} \frac{\partial e_j(n)}{\partial y_j(n)} \frac{\partial y_j(n)}{\partial u_j(n)} \frac{\partial u_j(n)}{\partial w_{jj}(n)} \tag{2.27}$$

Expandindo o somatório Equação 2.25, pode-se chegar na Equação 2.28.

$$\varepsilon(n) = \sum_{j=1}^{m} \frac{e_j{}^2(n)}{2} = \frac{1}{2}\left\{e_1^2(n) + e_2^2(n) + ... + e_j^2(n) + ... + e_M^2(n)\right\} \tag{2.28}$$

onde *M* é o número de neurônios da camada de saída.

Derivando a Equação 2.28 em relação à $e_j(n)$ obtém-se a Equação 2.29.

$$\frac{\partial \varepsilon(n)}{\partial e_j(n)} = e_j(n) \tag{2.29}$$

Derivando a equação 2.24 com relação à $y_j(n)$,

$$\frac{\partial e_j(n)}{\partial y_j(n)} = -1 \tag{2.30}$$

Derivando a equação 2.23 da variável de saída $y_j = \varphi(u_j)$ com relação à $u_j(n)$, tem-se:

$$\frac{\partial y_j(n)}{\partial u_j(n)} = \varphi'(u_j) \tag{2.31}$$

onde $\varphi'(u_j)$ é a derivada da função de ativação.

Derivando a Equação 2.22 em relação à $w_{ji}(n)$ resulta em

$$\frac{\partial u_j}{\partial w_{ji}} = \frac{\partial}{\partial w_{ji}}\begin{bmatrix}(x_1(n)w_{j1}(n) + w_{j0}) + (x_2(n)w_{j2}(n) + w_{j0}) + (x_3(n)w_{j3}(n) + w_{j0}) + \\ ... + (x_i(n)w_{ji}(n) + w_{j0}) + ... + (x_m(n)w_{jm}(n) + w_{j0})\end{bmatrix} = x_i \tag{2.32}$$

Substituindo as Equação 2.29, 2.30, 2.31 e 2.32 na Equação 2.27:

$$\frac{\partial \varepsilon(n)}{\partial w_{ji}(n)} = \frac{\partial \varepsilon(n)}{\partial e_j(n)} \frac{\partial e_j(n)}{\partial y_j(n)} \frac{\partial y_j(n)}{\partial u_j(n)} \frac{\partial u_j(n)}{\partial w_{jj}(n)} = e_j(n)(-1)\varphi'(u_j)x_i(n) \tag{2.33}$$

Substituindo a Equação 2.33 na Equação 2.26:

$$\Delta w_{ji}(n) = \eta \frac{\partial \varepsilon(n)}{\partial w_{ji}(n)} = \eta e_j(n)(-1)\varphi'(u_j)x_i(n) \tag{2.34}$$

Assim, a correção dos erros (w_{ij}) depende dos erros associados ao neurônio da camada *j*, da derivada da função de ativação a ele associada, da constante de aprendizado e da saída dos neurônios da camada *i* imediatamente anterior (entrada no neurônio *j*).

A popularidade do algoritmo *backpropagation* resulta de sua relativa simplicidade de implementação e do fato de ser um poderoso dispositivo para armazenar o conteúdo de informação (adquirido pela rede MLP a partir do conjunto de dados) nos pesos sinápticos da rede.

A utilização do algoritmo backpropagation na prática tende a convergir muito lentamente, exigindo-se alto esforço computacional. Para contornar este inconveniente, várias técnicas de otimização têm sido incorporadas ao algoritmo backpropagation a fim de reduzir o seu tempo de convergência e diminuir o esforço computacional requerido.

O algoritmo de treinamento utilizado neste trabalho foi o Levenberg-Marquardt (LM), pois é uma variação do backpropagation padrão que utiliza a derivada segunda como forma de otimização do mesmo. Este algoritmo é capaz de conduzir o treinamento de redes neurais artificiais de forma mais rápida que algoritmos tradicionais, pois a performance da rede é avaliada pelo erro médio quadrático, e o objetivo é minimizar funções que são a soma dos quadrados de outras funções não lineares. Singh et al. (2007) utilizam um algoritmo LM para treinamento da rede. Os autores comparam os resultados com outro algoritmo de treinamento e observaram que os resultados com a utilização de LM foram muito mais precisos.

Considerando a função erro usada na MLP, a equação usada no método de Gauss-Newton para a atualização dos pesos da RNA e consequente minimização da função erro é:

$$\mathbf{w}(n+1) = \mathbf{w}(n) - \mathbf{H}^{-1}\nabla f(\mathbf{w}) \tag{2.35}$$

onde **w** é o vetor dos pesos. O gradiente $\nabla f(\mathbf{w})$ pode ser representado pela Equação 2.36.

$$\nabla f(\mathbf{w}) = \mathbf{J}^T\mathbf{e} \tag{2.36}$$

onde **e** é um vetor que armazena o erro relativo a todos os padrões de entrada da RNA. A matriz hessiana pode ser calculada pela Equação 2.37.

$$\mathbf{H} = \mathbf{J}^T\mathbf{J} + \mathbf{S} \tag{2.37}$$

onde **J** é a matriz Jacobiana.

$$\mathbf{J} = \begin{bmatrix} \frac{\partial e_1}{\partial w_{j1}} & \frac{\partial e_1}{\partial w_{j2}} & \cdots & \frac{\partial e_1}{\partial w_{jm}} \\ \frac{\partial e_2}{\partial w_{j1}} & \frac{\partial e_2}{\partial w_{j2}} & \cdots & \frac{\partial e_2}{\partial w_{jm}} \\ \vdots & \vdots & \ddots & \vdots \\ \frac{\partial e_n}{\partial w_{j1}} & \frac{\partial e_n}{\partial w_{j2}} & \cdots & \frac{\partial e_M}{\partial w_{jm}} \end{bmatrix} \tag{2.38}$$

A Jacobiana **J** é a transposta da matriz de gradiente $\nabla \mathbf{e}$ com *m* linhas e *M* colunas e

$$\mathbf{S} = \sum_{j=1}^{M} e_j \nabla^2 e_j \tag{2.39}$$

Pode-se supor que **S** é um valor pequeno, se comparado ao produto da matriz Jacobiana, logo, a matriz Hessiana pode ser representada por:

$$\mathbf{H} \approx \mathbf{J}^T \mathbf{J} \tag{2.40}$$

A atualização dos pesos apresentado na Equação 2.35 pode ser expressa pela Equação 2.41.

$$\mathbf{w}(n+1) = \mathbf{w}(n) - \left(\mathbf{J}^T \mathbf{J}\right)^{-1} \mathbf{J}^T \mathbf{e} \tag{2.41}$$

Para superfícies genéricas nada garantirá que a Hessiana é positiva definida e em uma determinada iteração o valor da função poderá aumentar. Nesse ponto, o algoritmo de Levenberg-Marquardt apresenta uma modificação e, portanto, a atualização dos pesos é realizada de acordo com a Equação 2.42.

$$\mathbf{w}(n+1) = \mathbf{w}(n) - \left(\mathbf{J}^T \mathbf{J} + \mu \mathbf{I}\right)^{-1} \mathbf{J}^T \mathbf{e} \tag{2.42}$$

Sendo que **I** é a matriz identidade e μ, um parâmetro que torna a matriz Hessiana definida positiva. Quando o μ é zero, este é apenas o método de Newton, usando a matriz Hessian aproximada. Quando μ é grande, o método aproxima-se do gradiente descendente. O método de Newton é mais rápido e preciso perto de um mínimo de erro, de modo que o objetivo é o de mudar para o método de Newton tão rapidamente quanto possível. Assim, μ diminuiu após cada etapa de sucesso (redução na função do desempenho) e é aumentado apenas quando um passo preliminar seria aumentar a função de desempenho. Desta forma, o desempenho da função vai ser sempre reduzida em cada iteração do algoritmo (Lu et al., 2010).

Ressalta-se que os pesos somente são ajustados na fase de treinamento da rede, ou seja, são realizadas correções sinápticas necessárias. Já na fase de operação, nenhum tipo de ajuste é efetuado nos parâmetros internos da rede para gerar as saídas da rede.

2. 6 Comunicação entre diferentes dispositivos

Atualmente é possível monitorar e controlar um processo de forma remota e a tendência é que os controladores de campo sejam reunidos em um único ambiente que pode centralizar os elementos de controle. Diante desse cenário, os sistemas supervisórios vêm ganhando notoriedade por serem capazes de fazer esse tipo de gerenciamento. Segundo Boyer (2010), o termo SCADA é um acrônimo para *Supervisory Control and Data Acquisition*, ou seja, é um Sistema de Controle Supervisório e Aquisição de Dados.

O software nos sistemas SCADA usa banco de dados em tempo real e dentre as várias funcionalidades, permite a um usuário coletar dados de uma ou mais dispositivos distantes, monitorar alarmes e enviar ações de controle para estes locais (Daneels e Salter, 1999). Essa integração só é possível através de protocolos de comunicação eficientes e padronizados (Fruhwirth e tal., 2015; Hernandez et al., 2012). As variáveis importadas ou exportadas são associadas a objetos do sistema chamados *tags* que podem ser exibidas na interface do software, seja em forma numérica, gráfica ou sinótipo animado (representação gráfica geral da planta) que são atualizados conforme os valores provindos do processo.

Apesar do MATLAB®/SIMULINK ter a capacidade de se comunicar com o *Aspen Plus Dynamics*™, utilizando a tecnologia *Component Object Model* (COM), conforme é mostrado no capítulo 4, essa comunicação para controle de processos pode ser feita através do protocolo OPC, que significa OLE for Process Control, onde OLE significa Object Linking Embedding, sendo um padrão industrial desenvolvido para possibilitar a interconectividade entre dispositivos para comunicação de dados (Rohjans et al., 2013). Essa estrutura é utilizada nos capítulos 3 e 5. Em uma planta real, a comunicação OPC permite que o modelo de RNA desenvolvido no MATLAB® envie e receba dados para um controlador lógico programável (CLP), o qual é capaz de acionar os dispositivos físicos do processo. O controlador PID pode ser implementado no CLP e utiliza uma saída analógica para manipular as válvulas de controle.

Chinprasit e Panjapornpon (2019) estudam um processo de produção de monômero de cloreto de vinila simulado no *Aspen Plus Dynamics*™, com ação de controle baseada em um modelo de controle preditivo (MPC) que é calculada no MATLAB®/Simulink. Ambos os

softwares estão vinculados usando o padrão de comunicação COM, mais especificamente a tecnologia ActiveX.

Kummer (2019) faz uma análise de situações relacionadas à segurança de um processo de concentração de hidróxido de cumeno em uma coluna de destilação a vácuo simulada no *Aspen HYSYS*. Essa análise é feita no MATLAB® utilizando a estrutura OPC para conectar os softwares.

Guan et al. (2011) apresenta uma coluna de destilação em escala laboratorial e estuda como o SCADA pode ser explorado para fazer uma avaliação de impacto de risco e diagnóstico de falhas.

Neves et al. (2018) utiliza o sistema SCADA com protocolo de comunicação OPC para controlar uma coluna de destilação extrativa de produção de etanol anidro.

Outros trabalhos avaliam o SCADA para gerenciar plantas químicas através de protocolos de comunicação OPC (Morsi e El-Din, 2014; Fonseca et al., 2017; Golob e Bratina, 2013; Luo et al., 2015; De Lima et al., 2019).

CAPÍTULO 3

INTELLIGENT CONTROL SYSTEM FOR EXTRACTIVE DISTILLATION COLUMNS[i]

[i] Paper published in Korean Journal of Chemical Engineering. DOI:10.1007/s11814-017-0346-0

CAPÍTULO 3 – INTELLIGENT CONTROL SYSTEM FOR EXTRACTIVE DISTILLATION COLUMNS

Thiago Gonçalves das Neves, Wagner Brandão Ramos[i], Gilvan Wanderley de Farias Neto, and Romildo Pereira Brito

Chemical Engineering Department, Federal University of Campina Grande, Av. Aprígio Veloso, 882, Campina Grande - PB, 58429-900, Brazil (*Received 25 September 2017 • accepted 12 December 2017*)

Abstract - This work aims to develop and implement an intelligent control system to be used in an extractive distillation column that produces anhydrous ethanol using ethylene glycol as solvent. The concept of Artificial Neural Networks (ANN) was used to predict new set-points after disturbances, and proved to be a fast and feasible solution. The developed control system receives data from temperature, flowrate and composition measurements of the azeotrope feed, and the ANN estimates the new set-points of the controllers to maintain 99.5 mol% of ethanol at the top and less than 0.1 mol% at the bottom; feed composition was also estimated using an ANN. All ANN were trained to provide output data corresponding to an optimized operating condition. The results showed that the intelligent control system can predict a new operating condition for any disturbances in column feed and presented superior performance when compared with the control system without ANN.

Keywords: Ethanol, Extractive Distillation, Artificial Neural Networks, Control, Set-points

3. 1 Introduction

Control of distillation columns is a complex task because it is interactive, non-linear, often not stationary, and it is subject to restrictions. One of the major restrictions in the distillation process is related to the mode from which values of the product compositions are obtained, since the composition is generally not directly measurable and hence difficult to control (Mansour et al., 2015).

[i]To whom correspondence should be addressed.
E-mail: wagner.ramos@eq.ufcg.edu.br

Mejdell and Skogestad (1991) report in their work that one of the greatest difficulties in distillation column control is measuring the composition of the products, with gas chromatography being one of the most used techniques among the alternatives of physical analyzers. However, this technique presents long delays in obtaining measurements and presents high operational costs while used on-line.

Several studies present indirect methods that measure the composition in real time, from a mathematical model built to infer the composition of products (top and bottom) through variables such as temperature, which mainly present low-cost measurers, good accuracy and fast response (Zhongzhou et al., 2010; Udugama et al., 2015; Kano et al., 2003, Kalbani and Zhang, 2015).

Model predictive control (MPC) is a widely-studied technique in recent decades and refers to a class of control algorithms that consider the future response of the process from its mathematical model, aiming to keep the process output in well-defined set-points. However, most MPC algorithms are based on a linear process model, and this is their main disadvantage because they may provide low control performance throughout the operating range and large disturbances.

Non-linear controllers based on phenomenological modeling can be developed; however, for practical reasons, they must offer an acceptable response within a short time interval, where it is often not possible. In fact, one of the main difficulties for the widespread use of non-linear models in advanced control techniques in chemical/petrochemical industries is the high computational effort. Furthermore, the high number of equations of a distillation column model increases the number of parameters which are hard to estimate, and could lead to convergence difficulties or produce results with low accuracy (Maciejowski, 2002; Qin and Badgwell, 2003; Sharma and Singh, 2012; Luyben, 1990).

Using Artificial Neural Networks (ANN) it is possible to quickly infer important parameters of a system from real data. In this way, the use of ANN presents an option which may result in many control strategies (Kittisupakorn et al, 2014; Niamsuwan et al., 2014; Konakom et al., 2012; Lu et al., 2010). ANN utilizes a type of empirical modeling: it describes the process by mapping the input and output data. Thus, the ANN associates a given input pattern to an output signal, where the size of the input pattern may be different from the output pattern. However, it is necessary to train an ANN, and a data set must be presented containing a representative behavior of the full expected amplitude in which the plant will operate.

This study aims to develop an intelligent control system based on ANN, capable of maintaining the specifications of the distillate and bottom streams of an extractive distillation column for anhydrous ethanol production using ethylene glycol as solvent. In this work, the developed ANN receives data from process disturbances: temperature, flowrate and composition of the azeotropic feed; then the ANN estimates the new set-points of the controllers present in the plant. The intelligent controller was developed to maintain 99.5 mol% of ethanol at the top, and less than 0.1 mol% at the bottom. The ANN was trained with data obtained from a model implemented in Aspen Plus™ to provide output data corresponding to an optimized operating condition.

3. 2 Problem Statement

The case-study of this work is the extractive distillation process, normally used to promote the separation of mixtures that form azeotrope, where a third component named the solvent is used to alter the relative volatility of the initial azeotropic mixture, making separation possible.

Gil and Rodríguez (2012) studied the conventional extractive distillation process where a control configuration was developed using temperature to control the composition. According to the authors, larger off-sets are observed for disturbances in the azeotrope composition because it implies in a different temperature profile, including the temperature of the sensitive stage, in order to maintain the desired products' specifications. To minimize the off-set, Ramos et al. (2016) used dual control for temperature, although this is not recommended by many researchers.

To use temperature, it is necessary to determine the best stage to have this variable controlled, which consists in selecting the tray where considerable temperature variations from tray-to-tray exist. There are several methods to select a sensitivity tray, however, all types of disturbances should be considered because the choice is theoretically definitive.

Figure 3.1 shows the required temperature value of the sensitive tray to keep product specification for feed disturbances constant (flowrate, temperature and composition) for an extractive distillation column with 24 stages in order to produce high purity anhydrous ethanol using ethylene glycol as solvent. According to Figure 3.1, it is possible to infer difficulties to keep the product specification when the option is to control the sensitive stage temperature because of the ongoing need to change the set-point of the controller.

Temperature and flow meters are cheap and accurate; however, some problems arise to measure feed composition. For this case, the ideal tool would be an online analyzer with acceptable response time, reasonable accuracy and low cost; which is hardly found in industrial practice (Fortuna et al., 2005; Zamprogna et al., 2005). Alternative techniques based on the analysis of refractive index, density and dielectric constant can also be used, but they do not ensure good precision to determine it. Therefore, in this work, a soft sensor based on ANN was developed as an option to estimate the feed composition.

Figure 3.1. Stage 22 temperature of an extractive column to maintain product compositions within specifications.

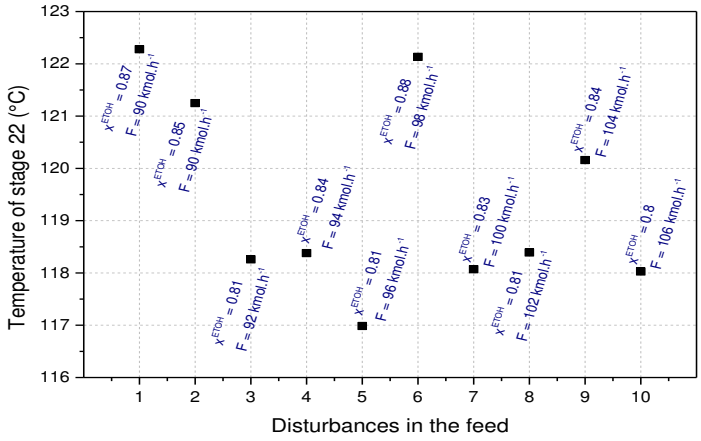

A soft sensor could be developed to infer the composition of products, and this way the estimate value would be used in a feedback controller. However, the advantage of inferring the composition in the feed is that it can be used as input information to another model based on ANN, and this can be used to predict the best operating condition of the plant to keep the product compositions constant. In other words, it suppresses deficiency in the feedback control, which implies in the necessity of the existence of an error so that the controller takes some action.

In summary, feeding disturbances (temperature, flowrate and composition of azeotropic) are introduced into the model using the ANN, so that the intelligent controller provides a feedforward response. No article was found with this type of control system in the consulted literature.

3. 3 Steady-State and Dynamic Simulations

The performance of the developed intelligent controller was tested using a model implemented in Aspen Plus™, and playing the role of an industrial plant, as shown in Figure

3.2. Condensers and reflux vessels were decoupled from the column to obtain a more rigorous and realistic model. The RadFrac™ routine was used for modeling the column, with a fixed Murphree efficiency of 100%. The condenser and reflux vessel was simulated with Heater and Flash2 routines, respectively; moreover, total condensation was assumed in the condenser by setting null vapor fraction, leading to no vapor production in the reflux vessel.

Phase equilibrium (VLE) was represented through a γ−φ procedure with the nonrandom two-liquid (NRTL) model for activity coefficient calculations (γ), and Redlich−Kwong equation of state (EOS) for calculating fugacity values (Dias et al., 2009; Meirelles and Weiss, 1992).

According to Figure 3.2, the azeotropic mixture of ethanol/water (AZEOTROP) is fed into the middle region of the extractive column (COL1), while pure ethylene glycol (EG) is fed close to the top. The distillate product from the extractive column is practically pure ethyl alcohol (ETOH), and the bottom product is essentially a water/ethylene glycol binary mixture (EG+H2O). The vapor from the top of the column is condensed in a heat exchanger (EXCH1), and then flows to a reflux vessel (DRUM1). After pumping (PUMP1), the condensed overhead product is sent to a splitter (SPLIT1), with one fraction being used for reflux and the other is withdrawn as top product (ETOH).

Figure 3.2. Flowsheet used for steady-state simulations.

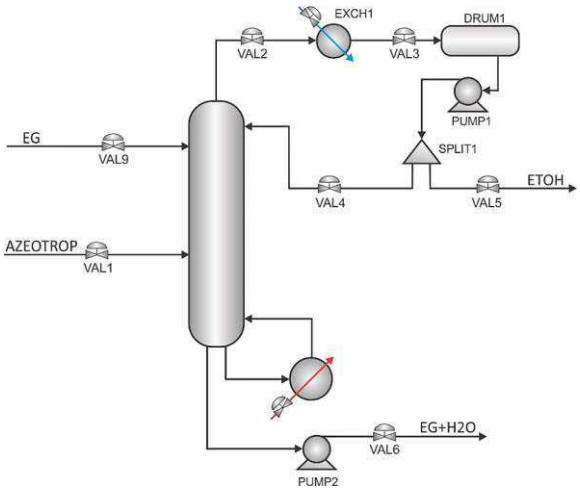

Design and process data to reach the desired specifications are shown in Table 3.1, and were based on literature reports (Gil et al., 2012; Dias et al., 2009, Meirelles and Weiss, 1992; Figueirêdo et al., 2015; Junqueira et al., 2010). The data not referenced are results of this work.

The top pressure value was chosen to permit using cooling water as utility and medium pressure steam was used in the column reboiler.

Table 3.1. Extractive column and stream data.

Variable	Stream		
	Azeotrope	Solvent	Distillate
Temperature (°C)	40[i]	80[i]	75.3
Mole flowrate (kmol.h-1)	100[ii]	76.94	85.4
Mole composition of ethanol	0.85[iii]	-	0.995
Mole composition of ethylene glycol	-	1.0[i]	113 ppm
	Column		
Number of stages	24[i]		
Reflux ratio	0.377		
Top pressure (atm)	1.0[iv]		
Bottom pressure (atm)	1.2[v]		
Solvent feed stage	4[v]		
Azeotrope feed stage	12[i]		
Column diameter (m)	0.8		

The column diameter was calculated using the Tray Sizing tool from Aspen Plus™, while length and diameter of reflux vessels and sump column height were calculated using the methodology proposed by Luyben (2013) for a 5 min hold-up when the vessel or column base is 50% full, as based on the entering or exiting volumetric flowrates.

We decided to use a single temperature control in this work, and the sensitive tray was selected based on the following methods (Gil et al., 2012; Luyben, 2013): successive stages, sensitivity symmetry, maximum sensitivity and singular value decomposition (SVD). The sensitivity analysis was done in an open loop with disturbances of ±5% in the reboiler heat duty. The two most sensitive stages were determined in each analysis, and according to Table 3.2, stage 22 showed the best results, thus being chosen as the sensitive stage.

Table 3.2. Comparison of methods for determining the optimal stage for temperature measurement.

Method	**Chosen stage**
Successive stages	22 or 23
Sensitivity symmetry	Inconclusive
SVD from the sensitivity matrix	22 or 21
Maximum sensitivity	22 or 23

[i] Meirelles and Weiss (1992)
[ii] Gil et al. (2012)
[iii] Dias et al. (2009)
[iv] Junqueira et al. (2010)
[v] Figueirêdo et al. (2015)

The steady state simulations performed in Aspen Plus™ were exported to Aspen Plus Dynamics™, and a basic control scheme was implemented, including:

- Feed flowrate control;
- Top pressure of the column by manipulating the condenser duty;
- Reflux vessel level by manipulating the distillate flowrate;
- Sump column level by manipulating the bottom product flowrate.

Furthermore, the following controllers were also added:

- Reflux ratio by manipulating the reflux flowrate (Arifin and Chien, 2008);
- Stage 22 temperature by manipulating the reboiler heat duty;
- Ratio between the solvent and azeotropic feed flowrates (S/F) by manipulating the solvent flowrate (Gil et al., 2012).

The process flow diagram (PFD) in Aspen Plus Dynamics™ environment, including all controllers, is presented in Figure 3.3. Level controllers are only proportional with $K_c = 2$ for reflux vessels, and $K_c = 10$ for sump level (Gil et al., 2012; Luyben, 2002); pressure controllers are proportional-integral with $K_c = 20$ and $\tau_I = 12$ min (Gil et al., 2012). Flowrate controllers are proportional-integral with $K_c = 0.5$ and $\tau_I = 0.3$ min (Luyben, 2002). To tune the temperature control, an analysis was conducted with disturbances in the reboiler heat duty within the range of ± 5% of its nominal value. Next, the parameters were calculated using the Tyreus-Luyben method (Luyben, 2002; Tyreus and Luyben, 1993) for a Proportional-Integral (PI) type controller, with $K_c = 3.59$ and $\tau_I = 10.56$ min.

3. 4 Soft-Sensor and Intelligent Controller

The general idea is that the developed ANN receives information about process disturbances and calculates new controller's set-points, for the new operating condition. The objective of this type of control is to adapt itself to the new situations in order to take the process to a new steady-state with the minimum energy consumption, while keeping the product specifications. To reach this objective, the ANN was developed with the help of Neural Networks Toolbox (NNT) from MATLAB® and trained using steady-state data from Aspen Plus™. The software Aspen Plus Dynamics™ was used to reproduce a real plant operation,

which environment enables the integration with MATLAB® and allows the control system using ANN to be tested in transient regime.

The link between Aspen™ and MATLAB® was done using the Elipse Supervisory Control and Data Acquisition (SCADA) software. In this specific application, Aspen Plus Dynamics™ and MATLAB® work as the client and Elipse SCADA works as the server. Figure 3.4 shows a scheme of the communication between the software and works.

Figure 3.3. Flowsheet used in dynamics simulations.

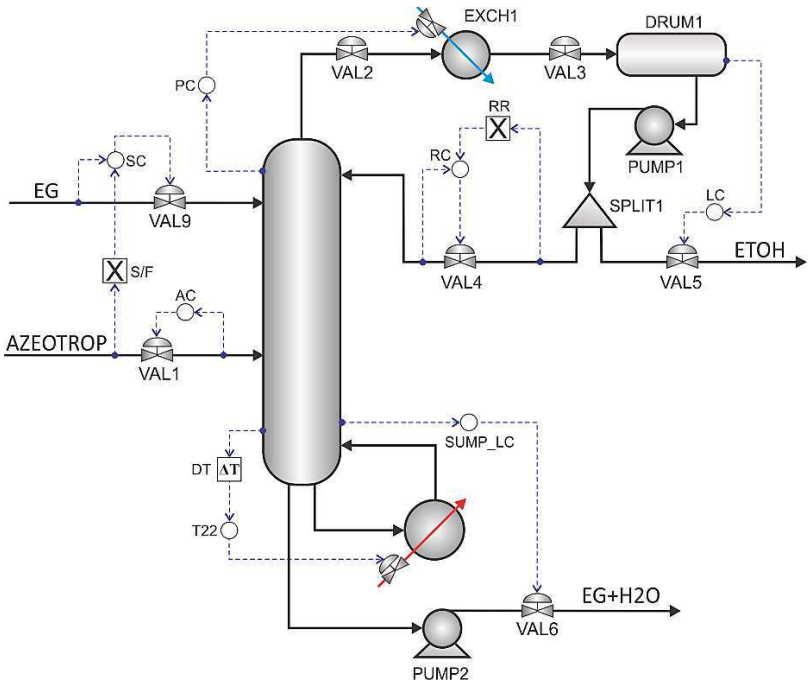

Figure 3.4. Communication between used software programs.

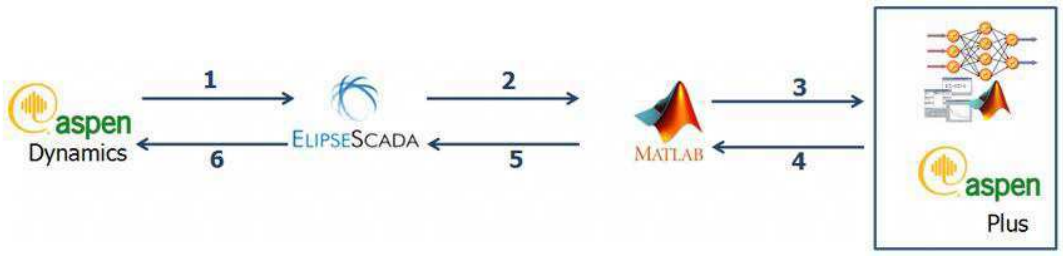

1) Aspen Plus Dynamics™ provides data for Elipse SCADA.
2) Elipse SCADA sends data to MATLAB®.
3) MATLAB® accesses the ANN (trained using simulations data obtained by Aspen Plus™) from its Neural Networks Toolbox tool (NNT).
4) ANN returns a response (new set-point values) to MATLAB®.

5) The value of the ANN output is available on Ellipse SCADA.
6) Aspen Plus Dynamics™ receives new set-point values of the controllers.

As cited before, online analyzers are hardly found in the industry, and an alternative is to use soft sensors which are commonly developed to infer the composition of products to estimate the value to be used in a feedback controller. However, in this work, a soft sensor based on ANN was developed as an option to estimate the feed composition (Haykin, 2009; Fausset, 1994; Morsi and El-Din, 2014; Nerrand et al., 1993).

To obtain the models based on ANN, the first step is to analyze the behavior of the column outside its nominal state. In this way, it is possible to raise historical data of the plant in an operating range at which it is likely to operate. The obtained data to train, validate and test the ANN were obtained from the steady-state simulations using Aspen Plus™ for two different moments: to infer the composition of ethanol in the feed stream, and to predict the set-points of the controllers to keep the product specifications for the process operating at optimum condition.

The first Artificial Neural Network (ANN_1) was created to estimate the composition of ethanol in azeotrope feed stream. For this, disturbances in reboiler heat duty, reflux ratio, distillate flowrate, solvent flowrate and azeotrope feed (flowrate, temperature and composition) were carried out. Disturbances ensure that the historical data is significant and cover the major problem domain. Several and important easy-to-measure variables will be used as ANN_1 input data to relate them to the variable to be inferred (ANN_1 output):

- ANN_1 input – azeotrope feed flowrate (F); Azeotrope feed temperature (T); reboiler heat duty (Q_R) reflux ratio (RR); solvent flowrate (S); Distillate flowrate (D); Temperatures of stages 4 ($T4$), 8 ($T8$) and 22 ($T22$) of the extractive column;
- ANN_1 output: Ethanol composition in the azeotrope feed (x^{ETOH}).

Regarding the choice of variables used as inputs to ANN_1, it is important to emphasize that the cited disturbances change the temperature profile of the column, so it is necessary to modify other variables to define a new temperature profile that maintains product specifications with minimum energy consumption for a new operating condition, and for which their choices as inputs to the network are justified. These variables can be classified into two different types: directly manipulated (solvent flowrate, distillate flowrate, temperature and azeotrope feed

flowrate) and indirectly manipulated (reboiler heat duty, reflux ratio and column temperature profile).

Temperatures of all stages of the column were not used because the training set would be very large, resulting in greater computational effort and slow inference by the ANN. The temperatures of stages 4, 8 and 22 were chosen because they present significant variations with disturbances, according to sensitivity analysis performed in the previous item.

The second Artificial Neural Network (ANN_2) was used for the development of an intelligent controller system. The temperature, flowrate and composition of the azeotrope feed were changed in *Aspen Plus*™.

Optimal values of the variables to be controlled for operating at minimum energy consumption were observed for different disturbance combinations, thereby maintaining the product specifications. This procedure was possible using the Model Analysis Tool/Optimization from *Aspen Plus*™, which uses the Sequential Quadratic Programming (SQP) method for optimization.

Energy consumption of the distillation column reboiler (Q_R) was defined as the objective function (F_{obj}) to be minimized, Equation 3.1, manipulating the following decision variables: reflux ratio, solvent flowrate and distillate flowrate. The Model Analysis Tools/Constraint used to consider the process constraints: mole fraction of ethanol (x^{ETOH}) and recovered mole fraction (FR^{ETOH}) in distillate; according to Equations 3.2 and 3.3, respectively.

$$F_{obj} = Q_R \tag{3.1}$$

Subject to

$$x^{ETOH} \geq 0.995 \tag{3.2}$$

$$FR^{ETOH} \geq 0.999 \tag{3.3}$$

The two developed ANN work together; the ethanol composition in the azeotrope feed is estimated by ANN_1 and this result is used as input to ANN_2, as shown in Figure 3.5.

Using *Aspen Plus*™, a collection of 8000 input patterns with their desired responses was used to estimate the composition of ethanol in the azeotrope feed; 70% was used for training, 25% for validation and 5% for testing. In order to develop an intelligent controller, a collection of 5300 input patterns from *Aspen Plus*™ was used: 50% were used for training, 10% for validation and 40% for testing.

As shown in Figure 3.6, it is possible to predict the values of the set-points (output) needed to maintain product specifications from disturbances in azeotrope feed (input) at minimal reboiler heat duty:

- ANN_2 input – ethanol molar composition (x^{ETOH}) estimated by ANN_1, temperature (T) and feed flowrate (F) of azeotrope;
- ANN_2 output – temperature of stage 22 ($T22$), reflux ratio (RR) and feed ratio between solvent and azeotrope streams (S/F).

Figure 3.5. Two ANN in cascades to predict the best set-points of the controllers.

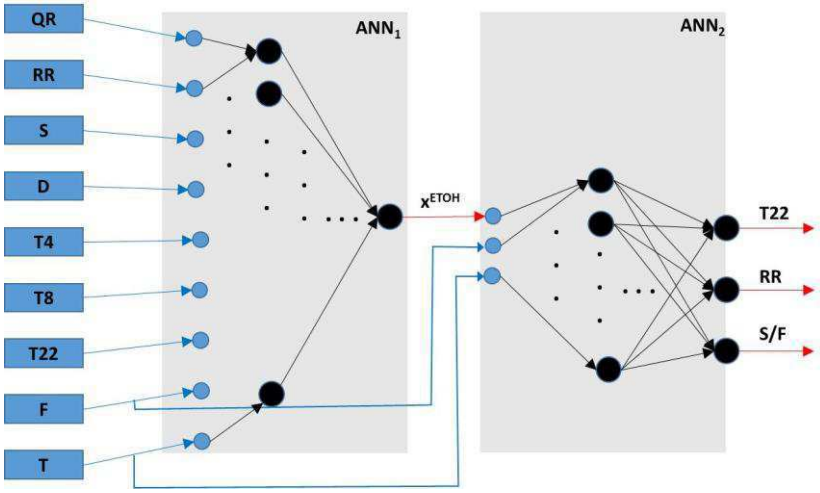

Figure 3.6. Diagram of the intelligent control system using ANN.

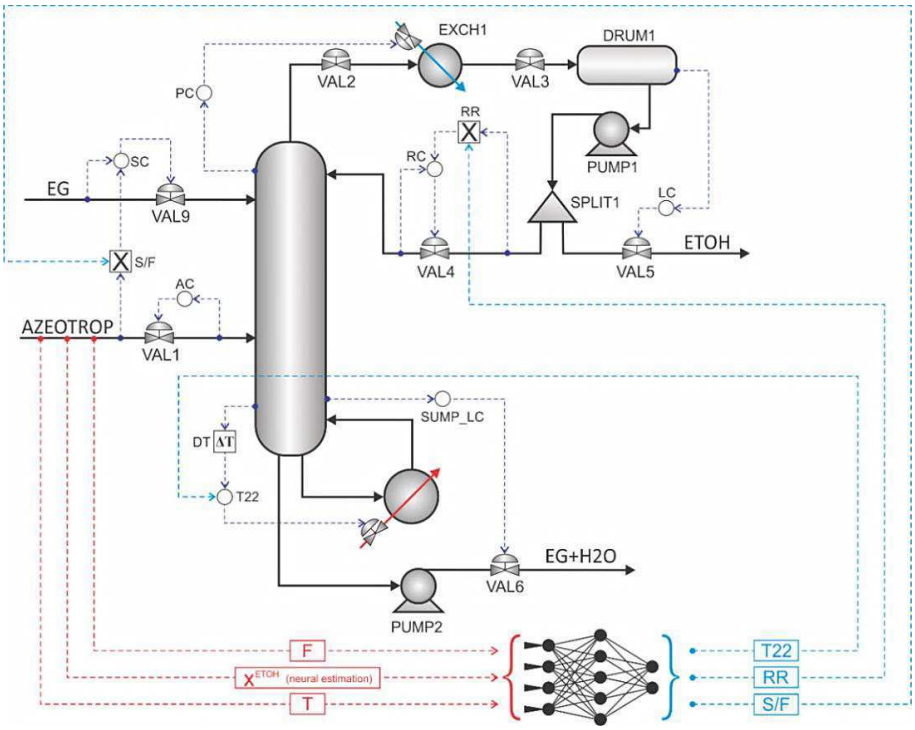

3. 5 Choosing the ANN

The choice of the ANN architecture includes decisions about: number of layers, number of units in each one, type of activation function and the training algorithm. It was decided to select two different types of architectures and evaluate them according to their performance related to the problem data. The selected ANNs were:

- Feedforward backpropagation: this is an ANN without feedback, where information is distributed in only one direction (Haykin, 2009).
- Elman recurrent: this ANN has an added feedback in its feed layer of the outputs of this layer to the input thereof; this makes it capable to store passed information (Elman, 1990).

Tangent sigmoid activation function was used for all layers, since it showed good results with respect to the other one tested. The number of hidden neuron layers was set empirically and takes into account the trade-off between success and computational effort; however, the number of neurons in the input and output layers is determined in accordance with the problem. The ANN training method used in this work was the Levenberg-Marquart algorithm (Marquardt, 1963).

Tables 3.3 and 4.4 give the best results of some types of feedforward and recurrent Elman ANN (Elman, 1990). The number of hidden layers and neurons per layer is presented as the name that identifies the neural network. For example, the network "2 3" indicates that the ANN has two neurons in the first hidden layer, and three neurons in the second hidden layer.

Table 3.3. Summary of ANN results for soft sensor development.

Number of hidden layers	Number of neurons per layer	Feedforward networks			Recurrent Elman Networks		
		MSE ($x10^{-8}$)		Maximum Error ($x10^{-3}$)	MSE ($x10^{-8}$)		Maximum Error ($x10^{-3}$)
		Training	Validation		Training	Validation	
1	“10”	500.66	508.51	20.30	98.85	98.97	20.31
2	“5 5”	20.66	21.1	20.54	20.31	20.88	18.32
2	“10 10”	1.99	1.99	3.64	0.51	1.02	3.25
3	“5 5 5”	1.58	2.10	5.23	0.06	0.07	5.14
3	“10 10 10”	0.88	0.97	1.66	0.11 [a]	0.12 [a]	0.60 [a]
3	“20 20 20”	1.78	2.01	2.48	0.18	2.15	0.14
4	“5 5 5 5”	2.11	2.13	3.55	0.12	0.19	2.36
4	“10 10 10 10”	3.22	3.23	2.39	0.18	0.18	2.36
4	“20 20 20 20”	1.09	1.54	1.71	1.25	1.29	1.22

[a] Best results

Table 3.4. Summary of ANN results used to develop intelligent controllers.

Number of hidden layers	Number of neurons per layer	Feedforward networks			Recurrent Elman Networks		
		MSE (x10^{-6})		Maximum Error	MSE (x10^{-6})		Maximum Error
		Training	Validation		Training	Validation	
2	"2 3"	3.21	3.24	0.0298	3.05	3.20	0.0277
2	"5 6"	3.13	3.30	0.0193	2.85	2.94	0.0193
2	"10 10"	3.03	3.10	0.0194	2.97	3.21	0.0208
3	"10 5 6"	2.94	2.98	0.0223	3.55	3.78	0.0221
3	"10 6 9"	2.97	3.08	0.0204	2.84	2.99	0.0197
3	"9 8 8"	2.76	2.91	0.0199	2.51	2.70	0.0183
4	"10 4 8 10"	2.44	2.46	0.0185	2.01 [a]	2.13 [a]	0.0171[a]
4	"5 6 7 2"	2.64	2.55	0.0187	2.5	2.58	0.0190
4	"8 9 10 6"	3.10	3.11	0.0189	3.14	2.19	0.0192

[a] Best results.

According to Table 3.3, the network chosen as the best option to estimate the ethanol composition in the azeotrope feed was the Elman network "10 10 10" with 3 hidden layers.

According to Table 3.4, the network chosen as the best option to predict the best set-points was Elman network "10 4 8 10" with 4 hidden layers.

In fact, the best ANNs have the lowest mean squared error (MSE), which indicates that the networks led to good results and the largest error obtained in the test set is small compared to the others. Recurrent neural networks can reuse the transformed information, producing dynamic mappings. The presence of feedback information allows for creating internal connections and memory devices capable of processing and storing temporal information and sequential signals (Morsi and El-Din, 2014). Other networks which are not in the tables presented larger errors, indicating that they converged to local minimums.

A different data set from those used in the training and validation phase was used during the testing phase of the highest ranked neural network. The absolute error (E) for each sample (j) was obtained according to Equation 3.4:

$$E = \frac{|d_j - y_j|}{d_j} \tag{3.4}$$

Figure 3.7 presents the errors and the comparison between predicted results (ANN_1 estimation) and expected results (Aspen output) of the ethanol composition in the feed stream of the azeotrope.

It can be concluded from Figure 3.7 that the RNA training chosen for the development of the soft sensor presented good convergence, since the difference between the simulator result and the result estimated by the soft sensor is minimal. Consequently, the errors present uniform values, showing that the network has an excellent estimation capacity.

Figure 3.7. Comparison between the a) values generated by *Aspen Plus*™ and the values estimated by ANN; and b) the respective absolute errors.

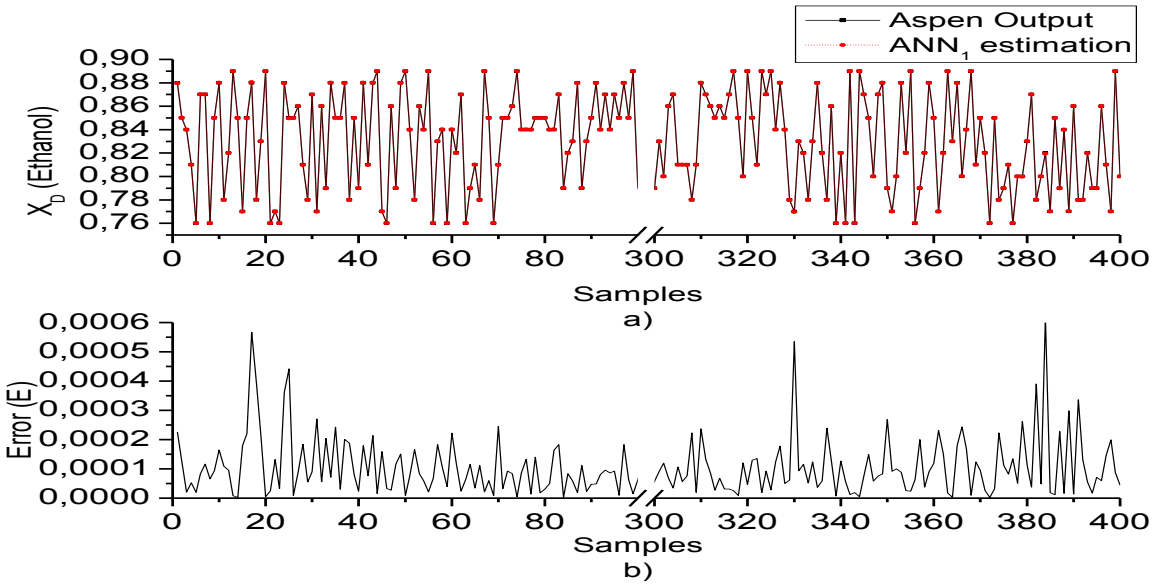

In the tests to predict the new set-points after the disturbances, it was noticed that for a given set of points, the errors found were quite higher compared to the others; therefore, the network in this region was not sufficiently trained. Thus, a new ANN training was performed with an increase of 500 points around the deficit region to solve this problem. When analyzing the results, it could be noted that the increase in the number of training data reduced the error in the deficit region, but there was considerable loss in the estimation quality of other points, indicating that the condition obtained in the initial training was lost. An alternative was to create and train a new neural network (ANN_3) with the same features of the best network already chosen, acting exclusively in the deficit region and with the addition of new points around this region (Figure 3.8).

Figure 3.8. Absolute errors for the variables (a) reflux ratio, (b) stage 22 temperature and (c) S/F ratio with two ANN in the retraining.

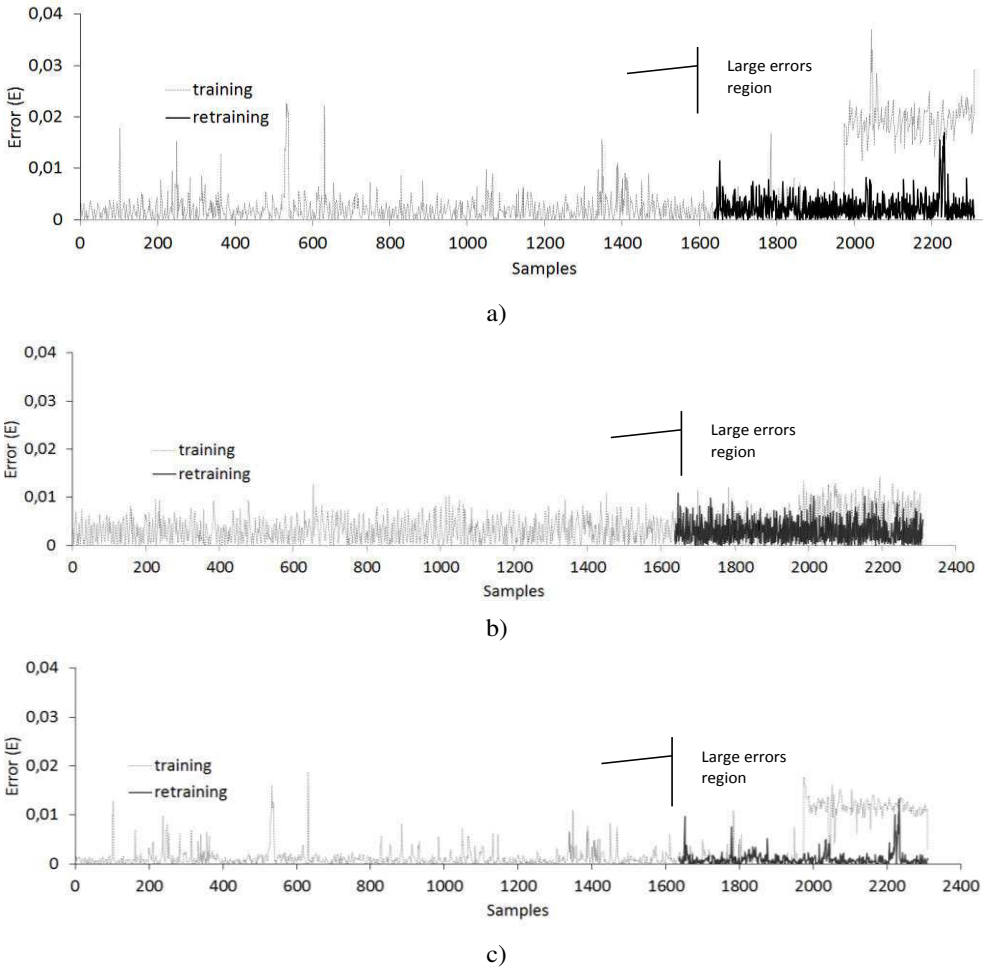

Figure 3.8 shows that the retraining using two neural networks can improve the large errors region without damaging the other, and this reflects in better control of product composition (as shown next). To predict the set-points in on-line use, the two ANNs (ANN_2 and ANN_3) never act simultaneously, since each one is programmed to operate in distinct and specific regions where the smallest errors are observed.

3. 6 Control System Performance

The intelligent controller developed was tested with the aim to maintain the ethanol composition at the top at 99.5 mol%, and with a loss lower than 0.1 mol% at the bottom stream of the column for disturbances in the azeotropic feed stream.

Figure 3.9 shows the ethanol composition behavior at the top product from disturbances in the feed stream by comparing the control system performance with and without the use of the developed intelligent controller.

Figure 3.9. Dynamic response for disturbance of -10% (a) and + 4.7% (b) in the azeotrope feed composition, and simultaneous disturbances in composition, flowrate and temperature of the azeotrope feed (c) and (d).

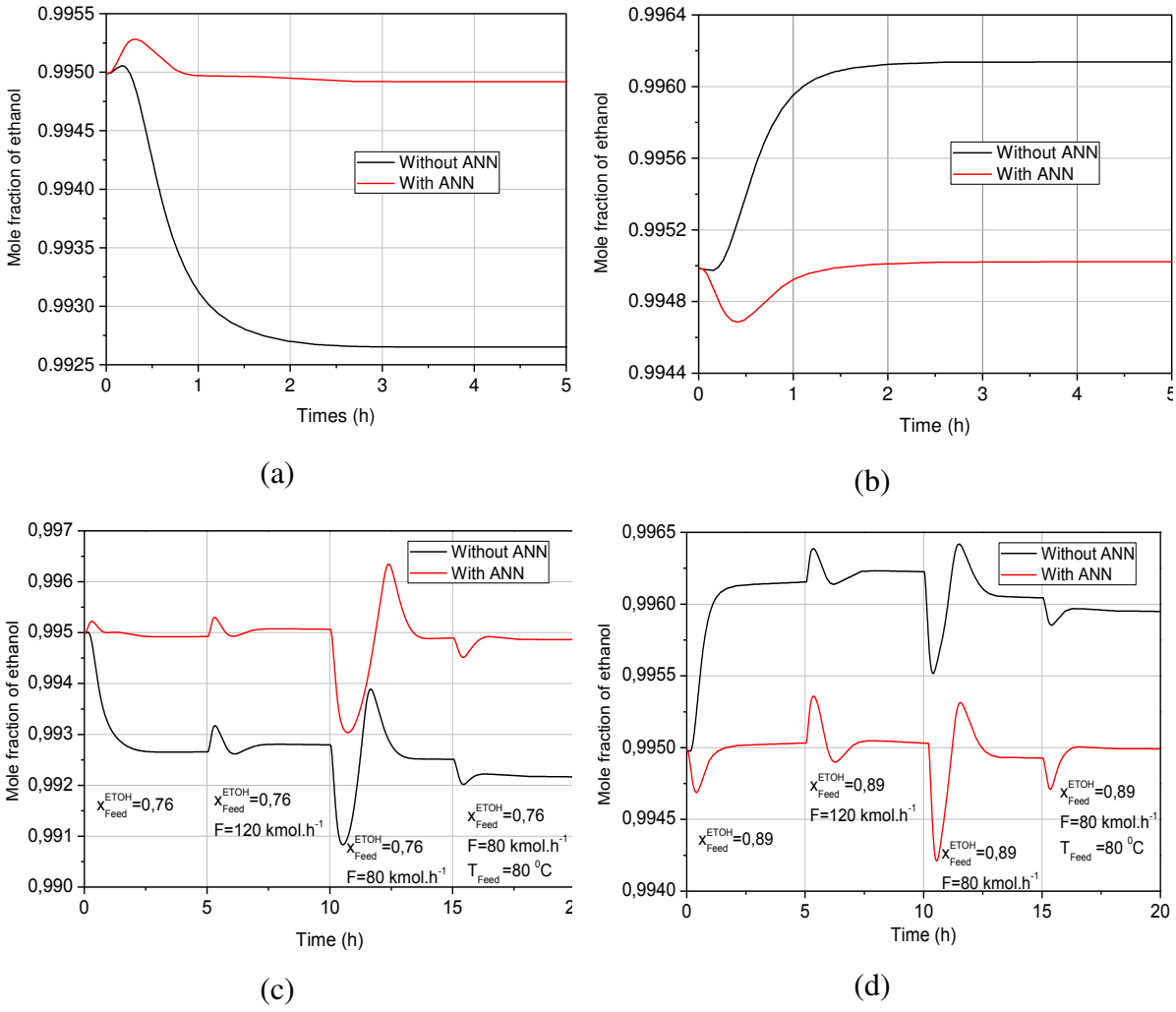

The control system without ANN only works for feed flowrate disturbance. The ethanol composition behavior had no significant changes to a disturbance of ±20% in the azeotrope feed flowrate and the results were omitted.

On the other hand, the control system with ANN rejected all disturbances well. However, it is important to highlight that the control becomes more difficult when the disturbances are simultaneous, so that product specifications are more difficult to reach.

The computational time was approximately 2 min to simulate 20 h of processing. This computational time is relatively short since the use of ANN reduces calculation requirements. The detector is fed in online mode, and may be extremely fast in processing the results since most calculations are performed in the ANN training phase.

It must be emphasized that this type of control not only presented satisfactory performance, but also presented energy efficiency, meaning that it guarantees the quality of the products with minimum heat duty and optimizes the operational conditions during ANN training. For example, the control without ANN can maintain quality of the product within specifications only for disturbances in the feed flowrate, but with greater energy consumption when compared to the intelligent control system, as shown in Figure 3.10. Therefore, the control using ANN is the most interesting alternative because the energy consumption in the reboiler presented savings of 0.90% e 0.94% for disturbances of -20% and +20% in the azeotrope feed flowrate, respectively.

Figure 3.10. Dynamic response of reboiler heat duty for disturbances of -20% (a) and +20% (b) in the azeotrope feed flowrate.

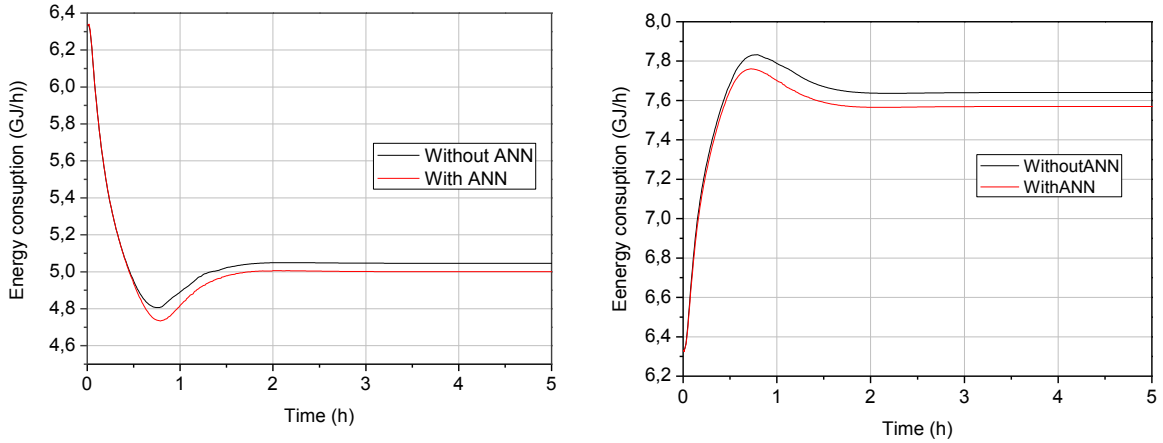

(a) (b)

Figure 3.11 shows that the performance of the intelligent control using two networks (ANN_2 and ANN_3) is better compared to the use of only one network (ANN_2) to predict the best set-points. A performance error stems from the fact that any adjustment promoted by a control system takes a while to complete, and accumulates control errors during that time (desired value - set-point - less measured value). It is important to emphasize that Figure 3.11 was constructed using two different intelligent controllers, i.e., a control system with one ANN and a control system with two ANN. The computational effort is almost the same because in

the final product (control system using two ANN) each ANN will only act depending on the disturbance in the feed composition.

Figure 3.11. Comparison of control with set-point change using one ANN and two ANN for different disturbances in the azeotropic feed composition.

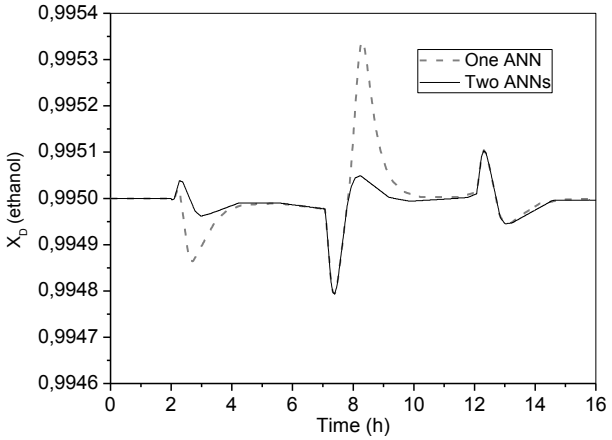

For the transient adjustment, the value of the instantaneous error (ISE), represented by Equation 3.5, can also be obtained, resulting in a cumulative overall error, which depends on the values of the controller action constants.

$$ISE = \int_0^\infty [e(t)]^2 dt \tag{3.5}$$

The value of ISE for the simulation depicted in Figure 3.10 using one and two neural networks was 9.02×10^{-8} and 2.4×10^{-8}, respectively. The bottom product composition had no significant changes for all the simulations, with the ethanol composition remaining below 0.1 mol%.

3. 7 Concluding Remarks

The intelligent controller using ANN could predict the new condition from disturbances in the azeotropic feed, making changes in the set-points of the controllers to keep specifications of the product at the top and bottom of the column.

The success of an intelligent controller using ANN depends on a consistent analysis of the system to define which topology best meets the needs of the proposed problem and in choosing which data are relevant for processing. The technique used in this study shows that it

is possible to obtain good accuracy in estimating the values of new set-points using two ANN without increasing the computational effort.

A third network can be used without increasing the computational effort. This can be explained because the networks used to predict the set-points (ANN_2 and ANN_3) do not act simultaneously, providing good results when one of the input variables is the ethanol composition in the azeotrope feed. Such a variable is inferred by ANN_1 which has proven to be an interesting solution to replace expensive measurers of composition.

This new control approach is conceptually simple and can be easily implemented in the chemical industry as it improves the performance of the conventional controller when it acquires feedforward characteristics. Furthermore, it is possible to eliminate additional energy costs and additional costs associated with product specifications.

CAPÍTULO 4

CHANGING PRODUCT SPECIFICATION IN EXTRACTIVE DISTILLATION PROCESS USING INTELLIGENT CONTROL SYSTEM[i]

[i] Paper published in Neural Computing and Applications. DOI:10.1007/s00521-019-04664-1

CAPÍTULO 4 –CHANGING PRODUCT SPECIFICATION IN EXTRACTIVE DISTILLATION PROCESS USING INTELLIGENT CONTROL SYSTEM

A. P. Araújo Neto[i] • G. W. Farias Neto1 • T. G. Neves1 • W. B. Ramos1 • K. D. Brito1 • R. P. Brito1

Received: 11 September 2019 / Accepted: 3 December 2019

Abstract - Obtaining anhydrous ethanol by extractive distillation has already been the object of several studies in the control literature. However, despite the presence of varying degrees of purity of anhydrous ethanol owing to its applications in industrial and commercial sectors, little attention has been given to dynamic and control for changing the operating conditions to provide anhydrous ethanol with different specifications. Using a soft sensor based on artificial neural network, this work aimed to develop an intelligent control system to contemplate the changes in the specification of anhydrous ethanol, considering the whole process (extractive and recovery columns), and keeping the process operating at an optimal point. Using the developed intelligent control system, the only necessary modification is the new specification and all new set-points values for controllers (temperature and solvent to azeotropic feed ratio) are updated automatically, without human interference, while with a conventional control system, all the new set-points values must be modified manually. The results showed that for the studied anhydrous ethanol specification range (99.1-99.9% mole), the new optimum operating conditions (new steady-state) was reached in a short time (between 1-2 h), with no evidence of overflow or emptying of sumps and reflux vessels of the columns. In addition to the easy implementation of the intelligent control system, the existing control structure remains unchanged, not requiring the investment for new instrumentation.

Keywords: Extractive distillation process Intelligent control system Soft sensor Artificial neural networks

✉ R. P. Brito
romildo.brito@eq.ufcg.edu.br

[i] Department of Chemical Engineering, Federal University of Campina Grande, Campina Grande, PB 58109-970, Brazil

4. 1 Introduction and problem definition

Unconventional distillation techniques, such as extractive distillation, azeotropic distillation, pressure swing distillation, pervaporation, and other hybrid method, are used for mixtures that have azeotrope or are formed by species with near boiling point to perform separation. However, extractive distillation is still the most attractive method owing to its applicability in industrial scale and in terms of energy consumption (Lei et al., 2003; Seader and Henley, 2011). This separation method is based on the addition of a solvent that is responsible for modifying the relative volatility of the original components.

The implementation of a suitable control structure is as important as process optimization, directly impacting the performance of the extractive distillation process and, consequently, the associated economic costs (Ramos et al., 2016). However, the control of distillation columns is considered a complex task because it is generally non-stationary, interactive, non-linear, and subject to restrictions and disturbances.

Maintaining the composition of the products is quite challenging because generally, it cannot be directly measured and therefore, difficult to control (Neves, 2016). Furthermore, it is known that the specification of the product may vary according to market demand. For example, ethanol is used in various degrees of purity owing to its applications in industrial and commercial sectors such as food industry, cosmetics and, mainly, as fuel. The international standards imposed by the European Union (EN 15376) and American Society for Testing Materials for fuel states that the quantity of ethanol must be between 99 and 99.8 wt%. (ASTM D 4806) (Kiss and Suszwalak, 2012; Ramírez-Márques et al., 2013).

In most situations, the relationships between the manipulated variables (reflux flowrate and steam flowrate to the reboiler) and controlled variables (temperature) are not available to the operators, thereby causing difficulties to take the process to the new steady-state of interest. Thus, the adjustment of the manipulated variables usually occurs using a trial and error process and each operator uses their own experience. However, in the case of integrated plants or equipment, the logic required for a specification change can be detailed and complex, thereby making it difficult for operators to make decisions.

To assist the operator in making decisions, a mathematical model that can relate process inputs and outputs is a real necessity because the analysis of product composition is performed with relatively low frequency, except in the cases where online analyzers are used, which are still very expensive and require a high maintenance rate. An alternative would be the use of

model-based predictive control (MPC). However, most of the algorithms are based on a linear model, while distillation is a strongly non-linear process with a high degree of coupling between the variables.

Furthermore, if MPC is used for changing the product specification, for each specification change, a new model must be identified. In this way, the number of parameters increases, which are often difficult to estimate. Thus, normally, most of the time, an MPC project is used in the identification work (Rivera, 2003).

An alternative would be the use of virtual analyzers (soft-sensor) based on computing approaches because they can predict the desired variable value through mathematical models, using secondary variables as input parameters, besides being a faster solution that does not generate a model with state variables but an external model with input and output variables (Zanata, 2005; Neves, 2018).

The concept of artificial neural networks (ANN) is commonly used to develop soft-sensor because they are computationally simple models and have an enormous processing power, speed, and generality. Artificial neural networks are artificial intelligence systems inspired by the human brain itself, based on the information processing characteristics found in biological neurons. Control systems that uses artificial intelligence like artificial neural networks, fuzzy logic and, machine learning, is called intelligent control system (ICS), and works as a feedforward controller.

Neves et al. (2018) developed an intelligent control system based on ANN capable of maintaining the specifications of the distillate (99.5% mole) and bottom (0.01% mole) streams of an extractive distillation column to produce anhydrous ethanol using ethylene glycol as solvent (the recovery column was not considered in this study). The general idea is that the developed control system receives information about the feed disturbances (composition, temperature, and flowrate) and, using a soft-sensor based on ANN, leads the process to the new operating conditions (new steady-state) by modifying automatically all set-points values of the controllers.

Using an ANN-based soft-sensor, the objective of this work was to develop an intelligent control system to contemplate the changes in the specification of anhydrous ethanol product, ranging from 99.1 to 99.9% mole, considering the dynamic behavior of the whole plant (extractive and recovery columns), and keeping the process operating at an optimal point. Using the developed intelligent control system, the only necessary modification is the new

specification and all new set-points values are updated automatically, without human interference, while with a conventional control system, all the new set-points values for controllers must be modified manually.

The soft-sensor was created using MATLAB's neural network tool (MathWorks, 2018) and *Aspen Plus*™ (Aspen Technology Inc., 2017), and blocks were generated in the Simulink platform (MathWorks, 2018) for later communication with Aspen Plus Dynamics (Aspen Technology Inc., 2017). *Aspen Plus*™ and *Aspen Plus Dynamics*™ were used to simulate the extractive distillation process (extractive and recovery columns).

4. 2 Steady-state simulation and optimization procedure: generating the artificial neural network database

The extractive distillation plant used by Ramos et al. (2016) was used as a case study. The process flow diagram was implemented using the *Aspen Plus*™ simulator, as shown in Figure 4.1.

The RadFrac routine was used to simulate the extractive (C1) and recovery (C2) columns, with Murphree efficiency equal to 100%, while the thermal integration was simulated using the HeatX routine. The thermodynamic model, NRTL (non-random two-liquid model), was used, which can accurately predict the non-ideality of the liquid phase of the azeotropic mixture of ethanol-water (Gil et al., 2012; Tututi-Avila et al., 2014, Ramos et al., 2016).

Figure 4.1. Process flow diagram of the extractive distillation process used as case study.

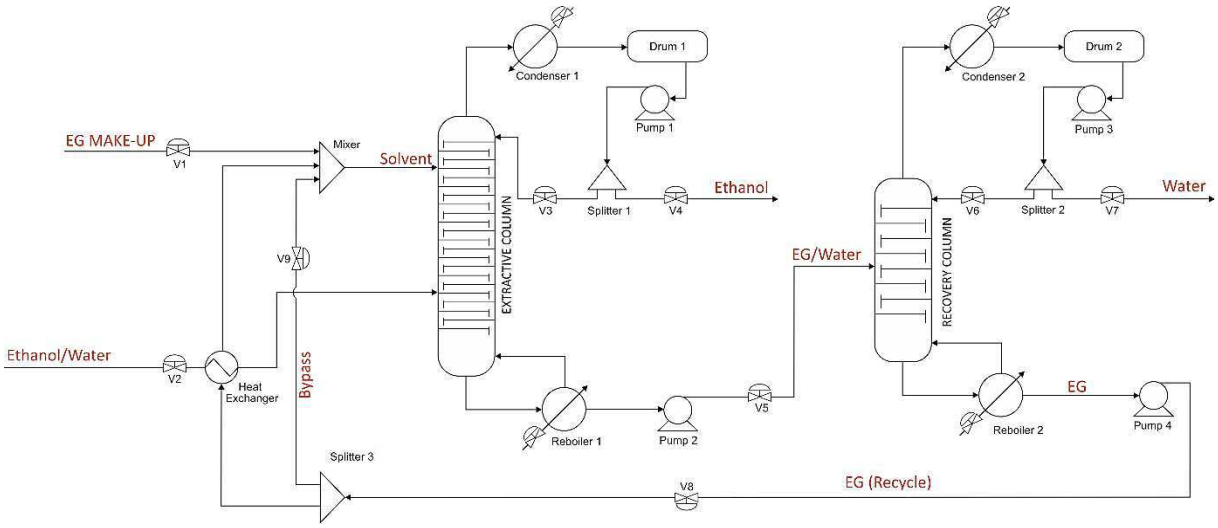

According to Figure 4.1, the azeotropic mixture (ethanol-water) is fed into the extractive column at stage #19. The solvent (EG) is fed close to the top of C1 on tray #4. Almost pure ethanol is recovered at the top product stream of C1 (ethanol), with a nominal molar fraction equal to 99.5% mole, while the base of C1 (EG-Water) is composed essentially of ethylene glycol and water (0.01% mole of ethanol). The *Aspen Plus*™ Design Spec tool, which manipulates the reflux ratio and distillate flowrate, was used to keep both specifications (two constraints for C1).

At the top product stream of C2 (Water), water is obtained with 99.3% mole, while the base of C2 is composed of ethylene glycol of 99.99% mole (EG-Recycle). The *Aspen Plus*™ Design Spec tool, which manipulates the reflux ratio and distillate flowrate, was again used to keep both specifications (two constraints for C2).

The EG-Recycle stream is divided to ensure that one part is used to preheat the ethanol-water stream through a heat exchanger and the other (By-pass) is used for solvent feed temperature control purposes.

Table 4.1 presents the operating and design conditions of the columns C1 and C2, based on the work of Ramos et al. (2016). The diameters of the columns were calculated using the *Aspen Plus*™ Column Internals tool and the reflux vessels were sized using the methodology proposed by Luyben (2013) for a 5 min hold-up when the vessel is 50% full.

A double temperature control was used, as proposed by Ramos et al. (2016), and the trays used to compose this control strategy are: #10 (C1), #20 (C1), #3 (C2), and #6 (C2).

The ethanol specification in the ethanol stream was defined as a variable parameter in the *Aspen Plus*™ Sensitivity Analysis tool. Thus, both tools (Design Spec and Sensitivity Analysis) work simultaneously to determine the conditions that result in all ethanol specification values within the given range. The variables of interest were defined as follows.

Column C1: Temperatures of trays #10 (C_1T_{10}), #20 (C_1T_{20}), and solvent to azeotropic feed ratio (S/F).

Column C2: Temperatures of trays #3 (C_2T_3) and #6 (C_2T_6).

Then, the behaviors of these variables for each new ethanol mole fraction in the distillate of column C1 were used as a database. The values of temperature and S/F ratio obtained by the sensitivity analysis were used as the outputs of the ANN, while the ethanol molar fractions at the top product stream of C1 was used as the inputs.

Tabela 4.1. Data used to simulate columns C1 and C2 and streams specifications.

Variable	Columns	
	Extractive Column	Recovery Column
Number of stages	24	10
Solvent feed stage	4	-
Azeotropic mixture feed stage	19	-
C2 feed stage	-	5
Solvent content (tray #4)	0.7	-
Top pressure (bar)	1.0	0.6
Reflux flowrate (kmol·h^{-1})	38.40	30.43
Reflux ratio	0.45	2.07
Reboiler duty (GJ/h)	5.03	2.16
Diameter of column (m)	0.84	0.62
Diameter of the reflux vessel (m)	0.90	0.50
Reflux vessel length (m)	1.80	1.00
Height of column base (m)	2.84	5.25

	Streams			
	Azeot	Solvent	Ethanol	Water
Temperature (K)	355.0	353.1	351.7	359.6
Molar flowrate (kmol·h^{-1})	100	88.7	85.4	14.6
Molar fraction of ethanol	0.85	-	0.995	-
Molar fraction of water	0.15	-	0.005	0.993
Molar fraction of EG	-	1.0	-	0.007

The mathematical model of distillations columns consists of mass balance equations (M), equilibrium-phase relations (E), mole fractions summations (S) and energy balance equation (H); referred to as MESH equations. The RadFrac routine of *Aspen Plus*™ uses the inside-out method to solve the MESH equations and convergence uses a combination of the bounded Wegstein method and the Broyden quasi-Newton method (Aspen Technology Inc., 2017).

The Optimization tool of *Aspen Plus*™, using Sequential Quadratic Programming (SQP), was used to simultaneously minimize the reboilers duties, Q_{r1} and Q_{r2}, of the columns C1 and C2, respectively, thereby manipulating the solvent flowrate. The objective function (F_{obj}) to be minimized is described in Equation 4.1.

$$F_{obj} = Q_{r1} + Q_{r2} \tag{4.1}$$

The SQP method is a quasi-Newton nonlinear programming algorithm and usually converges in only a few iterations but requires numerical derivatives for all decision and tear variables at each iteration (Aspen Technology Inc., 2017).

Each equipment of Figure 4.1 is solved individually, in a sequential form. For minimization of energy consumption, each equipment model is solved, and value of the objective function is calculated; reboiler heat duty of each column are the results used to calculate the value of the objective function. The optimization step does not present constraints, because these were included in Design Spec tool for each column, as mentioned before. The optimization decision variable is the solvent feed flowrate to the extractive distillation column.

The use of this optimization procedure generated a data for ANN training to ensure that the process will always operate optimally, i.e., with low energy consumption. One thousand and five hundred cases were generated, among which the ethanol molar fraction ranged from 99.1 to 99.9%, and the mixing of the obtained data was ensured to increase the generalization capacity of the soft-sensor. Figure 4.2 shows the procedure developed in this work and used to generate the database.

4. 3 Development of soft-sensor: architecture of used artificial neural network

To develop the soft-sensor, five artificial neural networks of the type single-input single-output (SISO) were used, whose architectures are characterized by non-feedback models and their neurons being grouped in layers (feedforward neural networks). The ANNs used uses the sigmoidal tangent activation function and an output layer whose activation function is linear.

Figure 4.2. Procedure used to generate artificial neural network database.

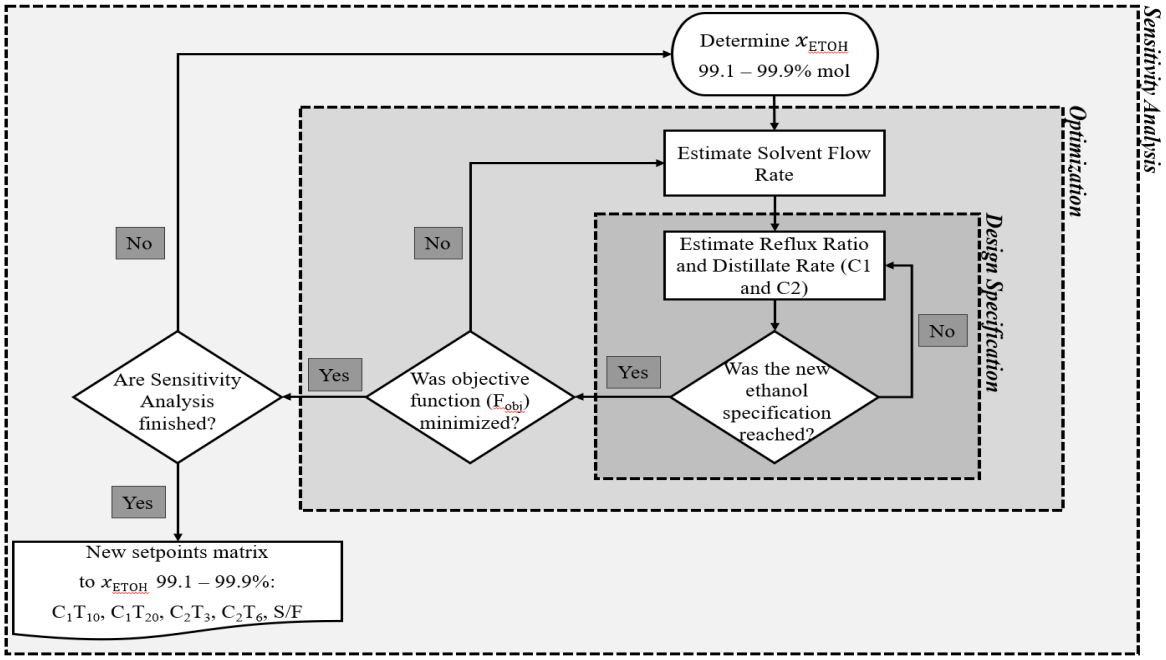

One difficulty observed in the topology of ANNs is the structuring of its architecture, which is characterized by the number of hidden layers, number of neurons in the input, intermediate and output layers, activation function, and training algorithm. It is not unusual to decide about these parameters by trial and error; despite the availability of techniques for automatic design of ANN to find the best artificial neural network, such as automated artificial neural network search (AANNS) (Sossa et al., 2012; Vijayaraghavan et al., 2019).

Hecth-Nielsen (1989), using neural-computing, proved that any continuous function can be represented by a three-layer scheme: the input layer with *n* inputs, the hidden layer with (2*n* + 1) processing elements (neurons) and the output layer with *m* outputs. In this work the performance of artificial neural networks was tested through trial and error, and results presented small differences when the number of neurons and hidden layers were increased, as depicted in Table 4.2. Therefore, minimum value of neurons and hidden layers were chosen to avoid unnecessary increase in the computational effort (highlighted row of Table 4.2).

Because there is only one neuron in the input layer (new specification of anhydrous ethanol), three neurons were used in the hidden layer and one neuron in the output layer because an ANN was developed for each temperature and S/F ratio, totaling the five SISO ANNs, as previously mentioned. Figure 4.3 shows the ANN structure used.

From the set of 1,500 data used, 70% were used for training, 25% for validation, and 5% for testing. The Levenberg-Marquardt algorithm was chosen as the training method, which has the advantage of coupling the Newton and Descending Gradient methods for optimization and convergence of the optimum point (Rao, 2009).

Tabela 4.2. MSE results for ANNs tested.

Hidden Layer	Neurons Hidden Layer	C_1T_{11}		C_1T_{20}		C_2T_3		C_2T_6		S/F	
		Validation	Training	Validation	Training	Validation	Training	Validation	Training	Validation	Training
1	3	1.0×10^{-6}	1.0×10^{-6}	9.8×10^{-7}	1.0×10^{-6}	1.8×10^{-8}	1.8×10^{-8}	2.0×10^{-8}	1.9×10^{-8}	1.3×10^{-4}	1.4×10^{-4}
2	3	8.5×10^{-7}	8.6×10^{-7}	9.3×10^{-7}	9.1×10^{-7}	1.9×10^{-8}	1.8×10^{-8}	4.0×10^{-8}	4.2×10^{-8}	1.1×10^{-4}	1.2×10^{-4}
3	3	8.6×10^{-7}	8.7×10^{-7}	9.3×10^{-7}	8.6×10^{-7}	8.7×10^{-8}	8.5×10^{-8}	4.5×10^{-8}	4.3×10^{-8}	1.1×10^{-4}	1.1×10^{-4}
1	5	8.6×10^{-7}	8.3×10^{-7}	8.8×10^{-7}	8.9×10^{-7}	1.8×10^{-8}	1.8×10^{-8}	2.0×10^{-8}	2.0×10^{-8}	1.0×10^{-4}	1.0×10^{-4}
2	5	8.1×10^{-7}	7.9×10^{-7}	8.3×10^{-7}	8.0×10^{-7}	1.4×10^{-8}	1.4×10^{-8}	1.4×10^{-8}	1.3×10^{-8}	1.0×10^{-4}	1.0×10^{-4}
3	5	7.1×10^{-7}	7.3×10^{-7}	7.4×10^{-7}	7.7×10^{-7}	1.4×10^{-8}	1.3×10^{-8}	1.2×10^{-8}	1.3×10^{-8}	9.5×10^{-5}	9.6×10^{-5}
1	7	7.2×10^{-7}	7.9×10^{-7}	7.9×10^{-7}	7.9×10^{-7}	1.9×10^{-8}	1.8×10^{-8}	1.6×10^{-8}	1.6×10^{-8}	1.0×10^{-4}	1.0×10^{-4}
2	7	7.3×10^{-7}	7.0×10^{-7}	7.8×10^{-7}	7.3×10^{-7}	1.4×10^{-8}	1.5×10^{-8}	1.3×10^{-8}	1.2×10^{-8}	9.7×10^{-5}	9.9×10^{-5}
3	7	7.1×10^{-7}	7.0×10^{-7}	7.2×10^{-7}	7.3×10^{-7}	1.6×10^{-8}	1.5×10^{-8}	1.1×10^{-8}	1.1×10^{-8}	9.9×10^{-5}	9.5×10^{-5}

Figure 4.3. Schematic of the artificial neural network used.

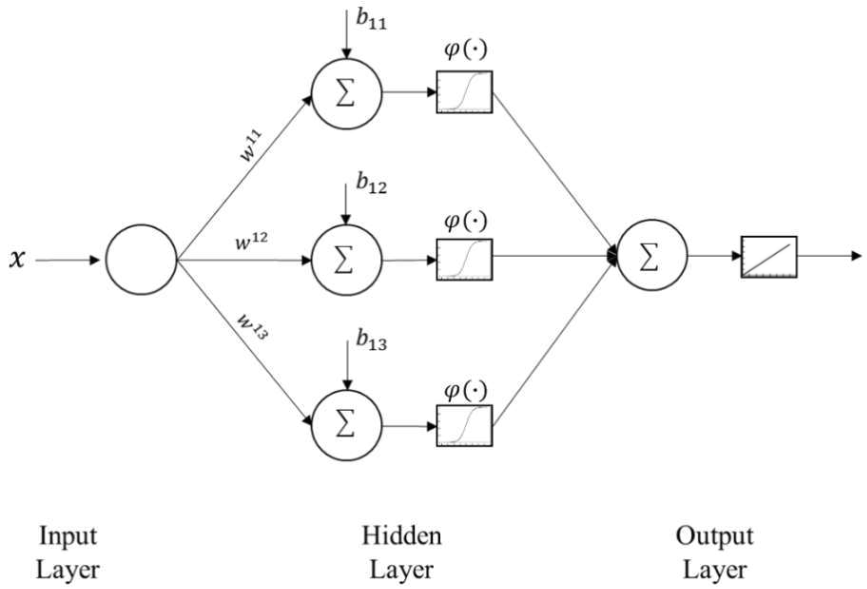

The analysis parameter of each artificial neural network performance was the mean squared error (MSE). The values used for training and validation are presented in Table 4.2. C_1T_{11}, C_1T_{20}, C_2T_3, C_2T_6 and, S/F represent the controllers whose set-points will be automatically updated for each new ethanol specification value. According to the numbers of Table 4.2, the highest MSE value was around 10^{-4}, for S/F ratio, which was considered acceptable given the goals of the work.

The pre-processing of the data was performed by normalizing the inputs and outputs for the interval [0, 1]. The normalization was performed using Equation 4.2, where P_i represents the data obtained by the sensitivity analysis and P_{max} is the maximum value in the dataset of each variable.

$$P_{i,norm} = \frac{P_i}{P_{max}} \tag{4.2}$$

Figure 4.4 shows the comparison between the values of the simulated plant in *Aspen Plus*™ and the values predicted by the soft-sensor, where a good prediction was observed for the values of temperature and S/F ratio for all cases.

Figure 4.4. Comparison between the values predicted by the soft-sensor and the simulated plant values obtained using *Aspen Plus*™.

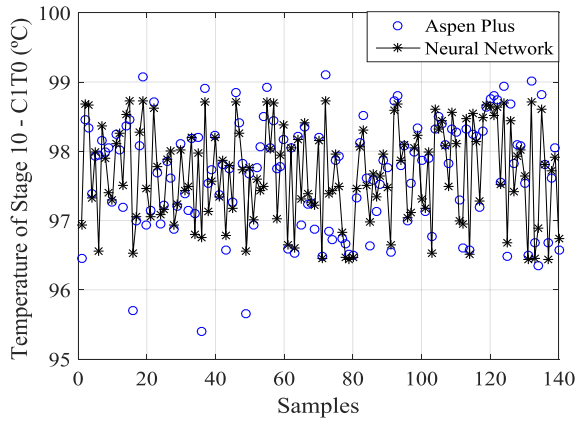

(a) Tray #10 temperature of C1.

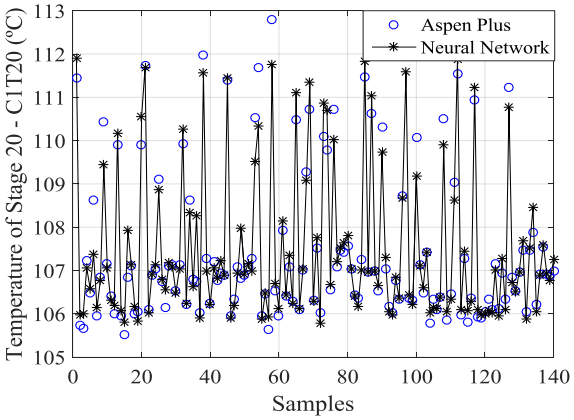

(b) Tray #20 temperature of C1.

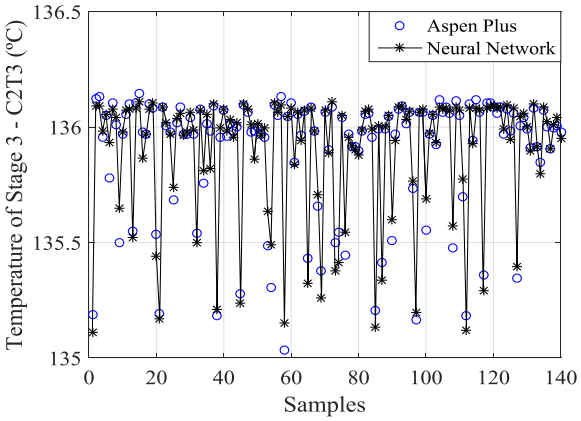

(c) Tray #3 temperature of C2.

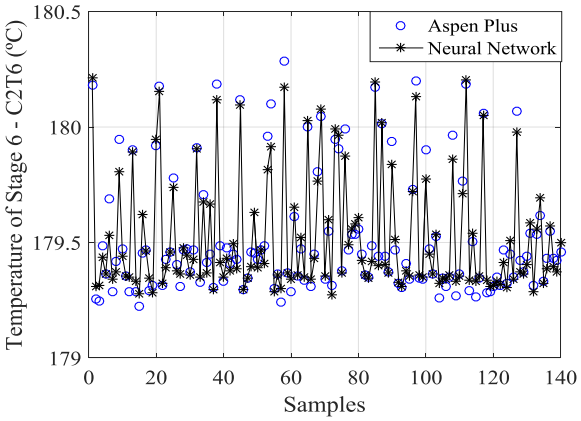

(d) Tray #6 temperature of C2.

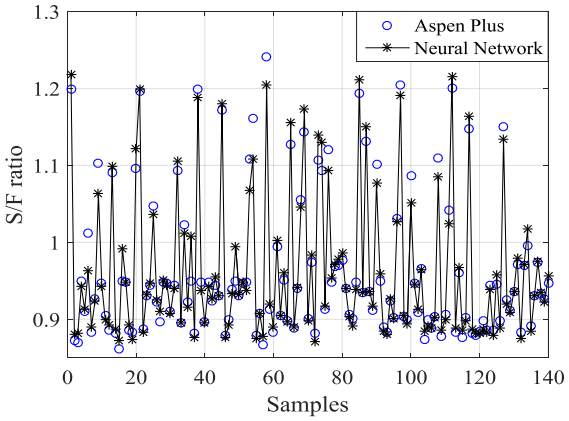

(e) S/F ratio.

4. 4 Dynamic simulations and developed intelligent control system

The steady-state simulation of the extractive distillation plant developed in *Aspen Plus*™ was exported to *Aspen Plus Dynamics*™ platform to investigate the dynamic behavior of the process. For the dynamic simulations, the reflux vessels and condensers of the columns C1 and C2 were decoupled and simulated using the Flash2 and Heater routines, respectively.

Aspen Plus Dynamics™ uses implicit Euler method with variable step to integrate the MESH equations in its differential form (Aspen Technology Inc., 2015).

The main variables that were analyzed were the levels of the reflux vessels and sumps of columns, to ensure that there is no overflow or emptying, and the time required to reach the new specification, thereby evaluating the performance of the proposed strategy.

Figure 4.5 shows the process flow diagram (PFD) with the implementation of the conventional control system, composed of regulatory control loops and temperature control. Each control loop is described below:

- Azeotropic mixture feed flowrate control (AZ_FC).
- Reflux flowrate control to keep the reflux ratio constant (RR1C and RR2C). Both controllers operate in cascade.
- Solvent feed flowrate control solvent to keep the S/F ratio constant (S/F_C).
- Temperature control of tray #10 of column C1 (10_TC) manipulating the reflux ratio.
- Temperature control of tray #20 of column C1 (20_TC) manipulating the steam flowrate to the reboiler.
- Temperature control of tray #3 of column C2 (3_TC) manipulating the reflux ratio.
- Temperature control of tray #6 of column C2 (6_TC) manipulating the ratio between the vapor flowrate to the reboiler and the column feed flowrate.
- Solvent feed temperature control of column C1 manipulating the by-pass stream flowrate (S_TC).
- Reflux vessels level control of C1 and C2 manipulating their respective distillate flowrates (DRUM1_LC and DRUM2_LC).
- Top pressure of each column is controlled by manipulating the heat duties of the condensers (DRUM1_PC and DRUM2_PC).
- Sump level control of C1 manipulating the bottom stream flowrate (SUMP1_LC).
- Sump level control of C2 manipulating the make-up stream flowrate (SUMP2_LC).

Temperature, pressure and flow controllers are proportional-integral (PI); reflux vessel and sump level controllers are proportional (P) only. The parameters were tuned using the

Tyreus-Luyben methodology (Tyreus and Luyben, 1992). Additional information about the controllers can be found in the works by Gil et al. (2012) and Ramos et al. (2016).

Considering a new specification value of the ethanol product, the new set-point values of the temperature of the sensitive trays and S/F ratio will be changed using the developed soft-sensor in *Aspen Plus Dynamics*™ via MATLAB®/Simulink.

As previously mentioned, the soft-sensor was created using MATLAB's neural network toolbox and blocks were generated in the Simulink platform for later communication with *Aspen Plus Dynamics*™ through the AMSimulation block present in the *Aspen Plus Dynamics*™ directory. Through the AMSimulation block, the SS outputs are used as the simulation inputs to *Aspen Plus Dynamics*™. The AMSimulation outputs represent the real plant data, i.e., the new ethanol specification, water molar fraction, and the new solvent content. It is important to note that the temperature controllers must be operating in cascade mode because their values will be supplied by the soft-sensor in Simulink. Figure 4.6 shows the schematic for product specification change.

Figure 4.5. Control system used in this study (Ramos et al., 2016).

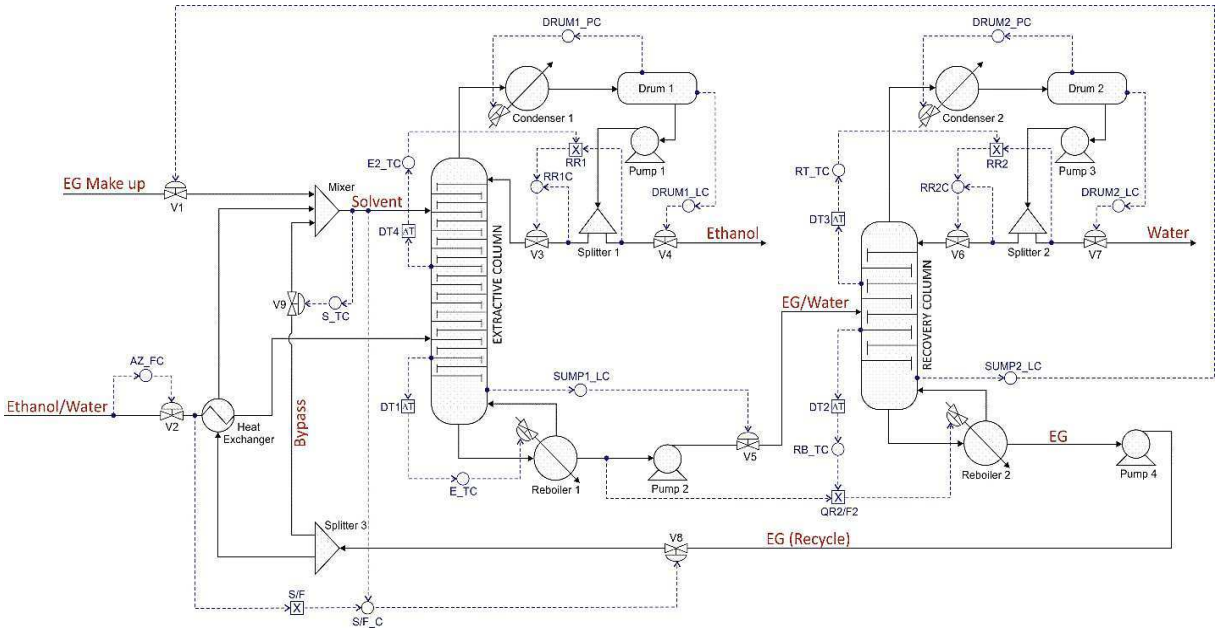

Figure 4.6. Intelligent control system for product specification change using soft-sensor.

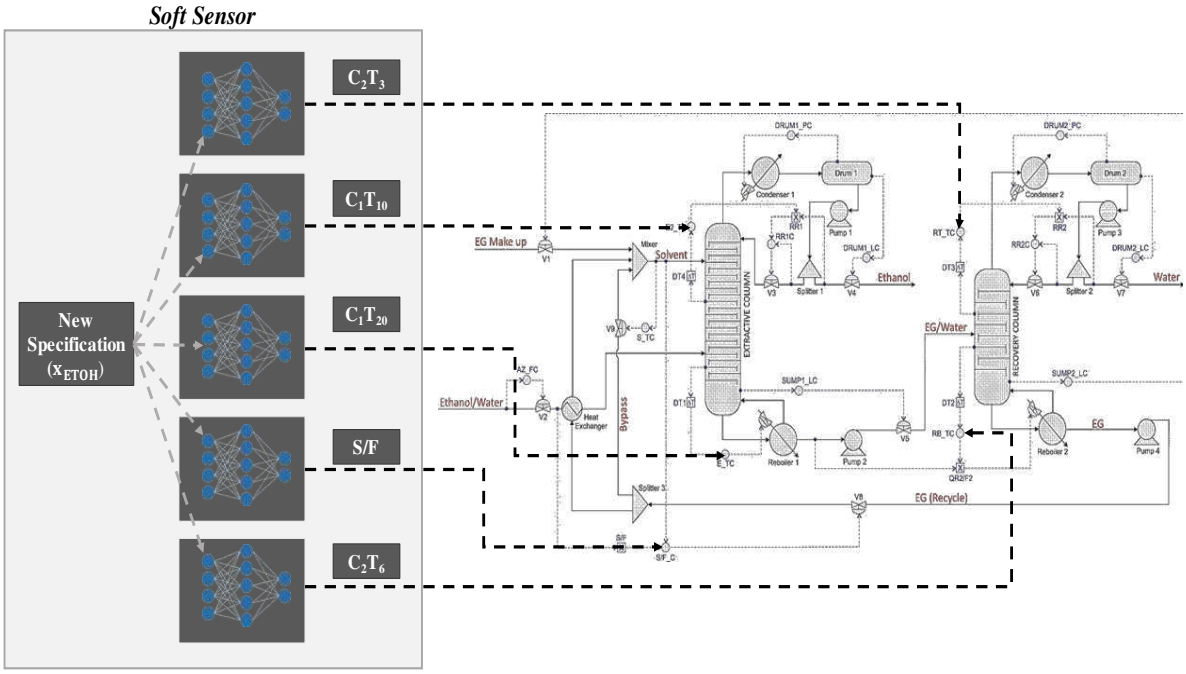

4. 5 Intelligent control system performance

Figure 4.7 shows the communication scheme between Simulink and *Aspen Plus Dynamics*™ (extractive distillation plant) and Figure 4.8 shows the dynamic responses of the product molar fractions in the distillate streams and the ethylene glycol content at the feed stage of C1 after the changes in ethanol specification from 99.1 to 99.9% mole.

Figure 4.7. Communication between *Aspen Plus Dynamics*™ and Simulink via AMSimulation.

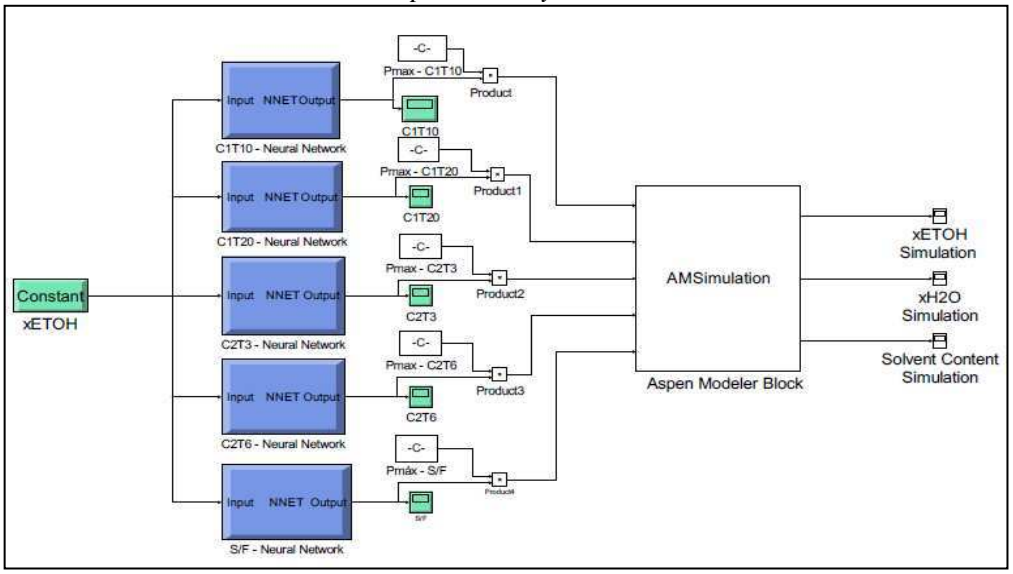

The intelligent control system demonstrated a good performance, which resulted in reaching the new desired specification of ethanol purity in a short period of time. Figure 4.8a shows that the process took approximately 1 h to reach the new steady-state for the ethanol specifications higher than the nominal value. For ethanol specifications lower than the nominal value, it took approximately 2 h. Figure 4.8b shows that the water molar fraction remains in the range of ±0.01% desired specification of 99.3% mole.

Figure 4.8c shows the mole fraction of ethanol at the bottom stream of C1 and an increase in its value is observed. However, it remains in the range of ±0.01%, i.e., there is no significant loss of ethanol through the bottom stream. It is important to emphasize that the solvent content responses shown in Figure 4.8d correspond to those used in the optimization step to minimize the energy consumption of the reboilers of columns C1 and C2. It should also be noted that each solvent content is specific to each desired new specification, i.e., to ensure the minimization of energy consumption in the columns, there must be a degree of freedom with respect to the solvent content.

Figure 4.9 shows the dynamic responses of the reboiler heat duty when the specification changes are performed. It is evident that for molar fractions higher than the nominal value (99.5% mole), there was a maximum increase of 3.7% in *Qr1* and 15% in *Qr2*. When changes are made to obtain molar fractions below the nominal value, the differences presented in *Qr1* and *Qr2* are not significant. The change in the heat duty of the reboilers occurs because more energy or less energy is required to reach the new specification value.

Figure 4.8. Dynamic behavior of the main variables.

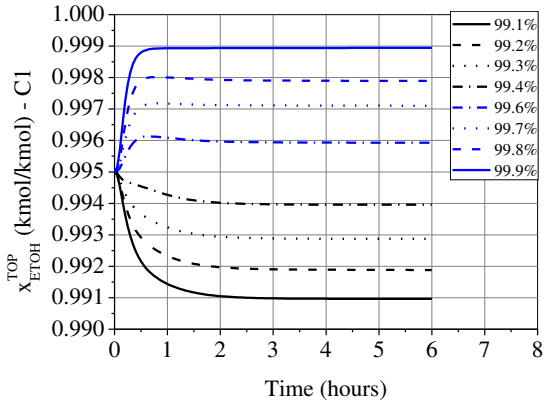

(a) Ethanol top molar fraction (C1)

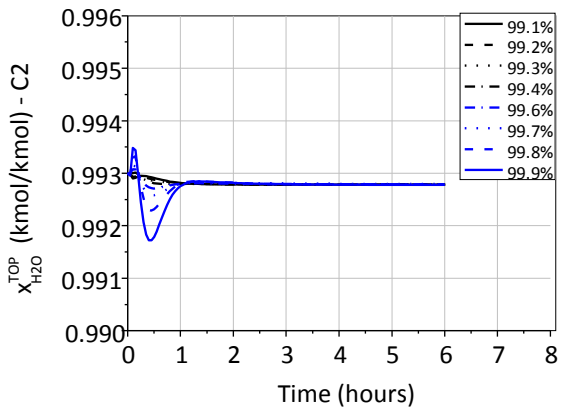

(b) Water top molar fraction (C2)

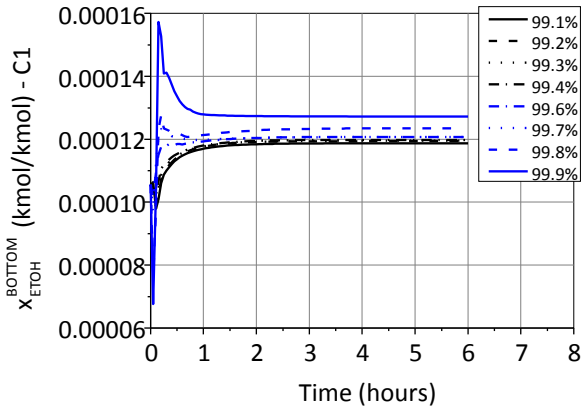

(c) Ethanol bottom molar fraction (C1)

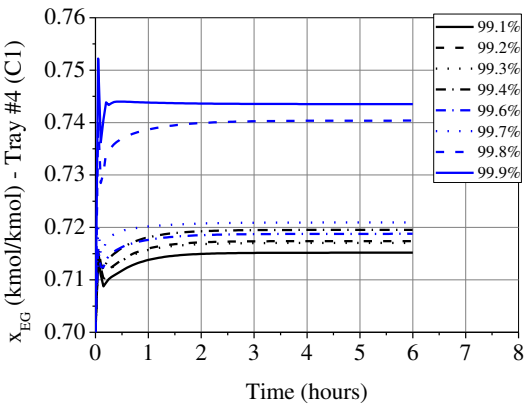

(d) Solvent content – Tray #4 (C1)

Figure 4.9. Heat duties for the new specifications.

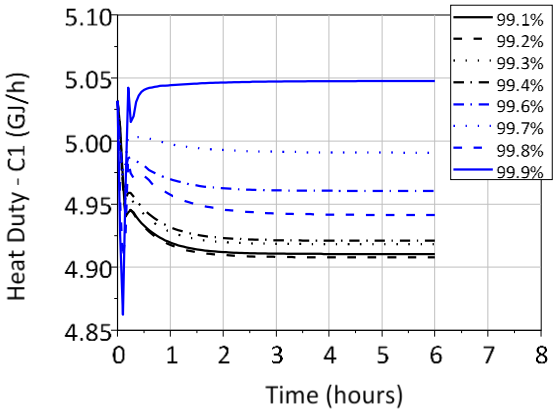

(a) Heat Duty (C1)

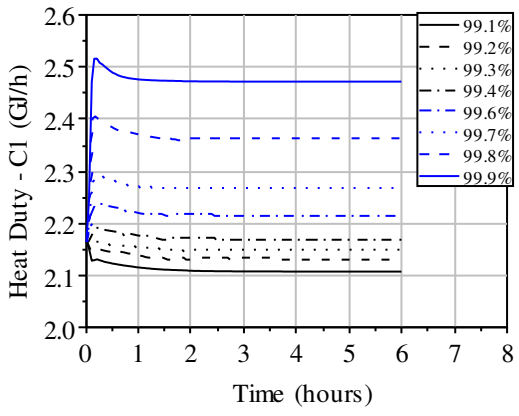

(b) Heat Duty (C2)

To ensure the proper operation of the intelligent control system, it is necessary to check the behavior of the reflux vessel and sump levels of each column to assess whether the process in the new desired condition will be stable regarding overflow and emptying. The results presented in Figure 4.10 show that there were no significant variations in the levels, thereby proving that there were no problems related to overflow or emptying. This reaffirms the stability of the process for the new specification.

For a real plant is necessary an *Aspen Plus*™ model validated with industrial data. In this case, the soft-sensor generated from ANN database should be linked to the programmable logical controller (PLC) of the plant, using a OLE (object linking embedding) for process control (OPC) and, whenever necessary, the operator change the value of the desired specification and all set-points of the controllers are updated by the PLC. Another option is to use historical data from the industrial plant to generate the soft-sensor database. In both cases,

at preset time intervals, ANN can be trained with new data so that the soft sensor is updated to maintain high performance of the intelligent control system.

Figure 4.10. Levels of reflux vessels and sumps.

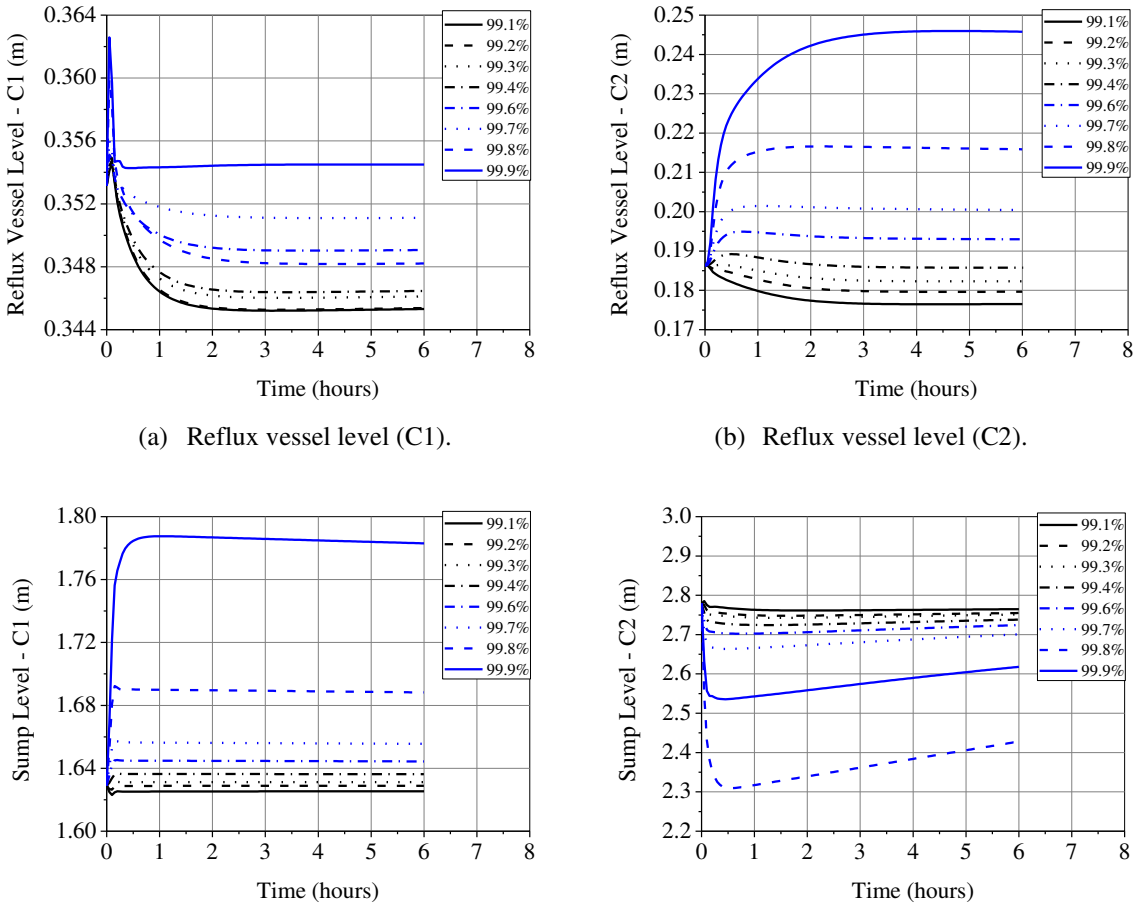

(a) Reflux vessel level (C1).

(b) Reflux vessel level (C2).

(c) Sump level (C1).

(d) Sump level (C2).

4. 6 Concluding remarks

Using a soft-sensor based on ANNs, this work proposed an intelligent control system to contemplate the changes in the specifications of anhydrous ethanol, considering the extractive distillation process (extractive and recovery columns) and keeping the process operating at an optimal point.

Contrary to conventional control systems, using the developed intelligent control system dispenses the need to manually change the set-points of controllers and the only necessary modification is the new specification because all set-points values of the temperature controllers and the solvent to azeotropic feed ratio controller are updated automatically. In this work, the new set-point values of the temperature of the sensitive trays and S/F ratio controllers are

changed in the extractive distillation plant implemented in *Aspen Plus Dynamics*™, via MATLAB®/Simulink.

To ensure the accuracy and generalization capacity of the developed soft-sensor, a mathematical model validate (in this work, an *Aspen Plus*™ model) or an historical data from an industrial plant is necessary. An ANN for each temperature and S/F ratio, totaling five SISO ANNs, were enough to guarantee the success of the soft-sensor.

A good performance of the intelligent control system resulted in reaching the new specification value of ethanol purity in a short period of time. However, it should be noted that the time to reach the new steady-state is longer for specification values greater than the nominal value. The results obtained show that there were no problems related to overflow or emptying, thus reaffirming the stability of the process for the new specification.

In addition to the easy implementation of the intelligent control system, the existing control structure remains unchanged, not requiring the investment for new instrumentation. The next step of the project aims to obtain an intelligent control system that simultaneously considers the feed disturbances (temperature, flowrate, and composition) and change specification.

CAPÍTULO 5

ANN-BASED INTELLIGENT CONTROL SYSTEM FOR SIMULTANEOUS FEED DISTURBANCES REJECTION AND PRODUCT SPECIFICATION CHANGES IN EXTRACTIVE DISTILLATION PROCESS[i]

[i] Paper published in Separation and Purification Technology. DOI: https://doi.org/10.1016/j.seppur.2020.118104

CAPÍTULO 5 – ANN-BASED INTELLIGENT CONTROL SYSTEM FOR SIMULTANEOUS FEED DISTURBANCES REJECTION AND PRODUCT SPECIFICATION CHANGES IN EXTRACTIVE DISTILLATION PROCESS

T. G. Neves[1], A. P, de Araújo Neto[2], F. A. Sales[2], L. G. S. Vasconcelos[2] and R. P. Brito[2i]

[1]Federal Institute of Education, Science and Technology of Rio Grande do Norte, Chemistry Department, Pau dos Ferros, RN, Brazil, 59900-000

[2]Federal University of Campina Grande, Chemical Engineering Department, Campus Universitario, Campina Grande, PB, Brazil, 58109-970

Abstract - Distillation is one of the most studied processes in the control literature because of its importance as a separation process. However, little attention has been paid to the dynamics and control of the simultaneous changes in the feed and product specifications. In this study, it is proposed an intelligent control system based on artificial neural network using the extractive process to obtain anhydrous ethanol using ethylene glycol as a solvent. The study considered the changes in the azeotropic feed and the specification of anhydrous ethanol simultaneously, taking both the extractive and recovery columns into account, and keeping the process operating at minimum energy consumption condition. The performance of the intelligent control system was evaluated using *Aspen Plus Dynamics*^{TM}, and the results showed that it is is able to efficiently determine the new setpoints of controllers when facing changes in anhydrous ethanol specification and/or disturbances in the azeotrope feed. The new steady-state is reached in a short time interval (2−4 h, depending on the disturbance type). Based on the integral squared error, integral absolute error, and steady-state error, the results showed that the intelligent control system presented superior performance when compared to conventional control systems. The implementation of the developed control is simple and the existing control structure remains unchanged.

Keywords: Ethanol, Distillation column, Intelligent control system, Artificial neural networks

[i] Corresponding author: Federal University of Campina Grande, Chemical Engineering Department. Tel.: +55 83 2101-1891; Fax +55 83 2101-1114. E-mail: romildo.brito@ufcg.edu.br (Romildo Pereira Brito)

5. 1 Introduction

Distillation remains one of the most important separation processes and, despite the technological advances in the field, the diversity in the mixtures, specifications, and configurations increases its degree of specificity.

Distillation columns, in general, constitute a significant fraction of the capital investment and production cost of chemical/petrochemical plants, which justifies the need for an effective and reliable control system to ensure efficient and safe operation. One of the major issues in distillation processes is maintaining the composition of the product streams (top and bottom), considering the feed disturbances and changes in the product specification.

The distillation process is based on the difference in volatility of the components to be separated. However, in azeotropic mixtures, conventional distillation fails to promote the desired separation. Therefore, extractive or azeotropic distillation techniques are generally employed. In both these processes, a third component, known as a solvent, is added to enable the separation.

Lynn and Hanson (1986) were the first to state that extractive distillation (ED) was competitive with azeotropic distillation regarding energy consumption. Using multiple-effect columns, the authors dehydrated aqueous ethanol mixtures with ethylene glycol as the solvent.

In terms of process control, Gil and Rodríguez (2012) used proportional-integral (PI) controllers for the production of anhydrous ethanol via ED. This study aimed to control the composition of ethanol using the inference of temperature. The authors pointed out that the largest offsets were observed during variations in the azeotropic feed composition.

Gehlen et al. (2015) used thermodynamic models based on temperature values to infer the ethanol composition in the distillate. In the study, the authors used the supervisory control and data acquisition (SCADA) and MATLAB® software.

Ramos et al. (2016) opted for a double PI temperature control in both columns (extractive and recovery) in the extractive ethanol distillation process. The authors found that operating with a high solvent content (ethylene glycol) is difficult to control, especially when there is a thermal integration between the azeotrope feed stream with the recovered solvent feed stream.

Figure 5.1 shows the difficulty in controlling the composition by inference using the conventional tray temperature control, since the setpoints are fixed in PI structure. The analysis,

based on the study of Ramos et al. (2016), shows the values of the temperatures selected as controlled variables (CV) according to the azeotrope feed characteristics (see Table 5.1). This analysis demonstrated that, if the objective is to maintain the products (bottom and top) with fixed specifications during random disturbances in feed temperature (T), flow (F), and ethanol composition (x_{Feed}^{ETOH}), the conventional control is ineffective because there is a specific set of temperature setpoints for each process input.

Figure 5.1. Temperature in the extractive column ((a) stage#10 and (b) stage#20) and in the recovery column ((c) stage#3 and (d) stage#6) to keep the top and bottom specifications at 99.5%mol, and 0.01%mol, respectively

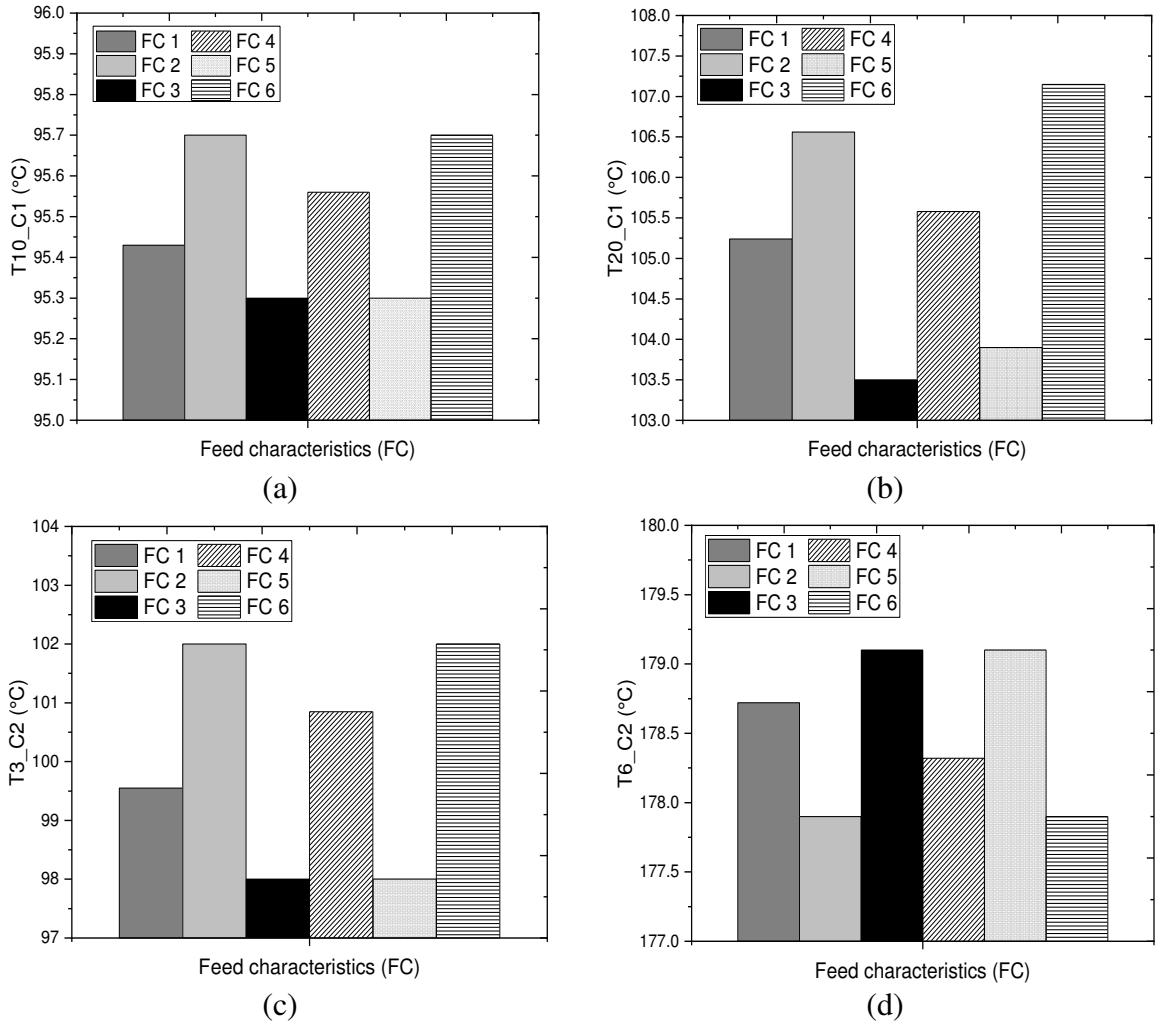

Table 5.1. Azeotrope feed characteristics

	FC 1	**FC 2**	**FC 3**	**FC 4**	**FC 5**	**FC 6**
x_{Feed}^{ETOH}	0.86	0.82	0.88	0.84	0.88	0.82
F (kmol.h^{-1})	96.6	103.3	105.5	92.2	96.6	103.3
T (°C)	40.3	36.6	30.0	36.6	38.8	43.3

Model predictive control (MPC) has emerged as a promising alternative to conventional controllers (Iqbal and Azis, 2012; Qian et al., 2019). However, most of the algorithms are based on a linear model, while the distillation process is strongly nonlinear (Sharma and Singh, 2012). Furthermore, if an MPC is used to reject the feed disturbances, the number of parameters to be tuned increases, and these are often difficult to estimate (Rivera, 2003).

The system linearization step is performed using a steady-state reference. Therefore, the linearized model represents the real process well if the process remains operating at that point. However, it is common for the operating conditions of the process to change over time, resulting in a significant deterioration in the MPC performance (Holtorf et al., 2019). Thus, significant attention is being paid to the development of control strategies that consider the nonlinearities and changes in the operating conditions. To fill the gaps in the MPC, nonlinear MPC (NMPC) is used.

One of the major hindrances in using the NMPC is the solution to the non-convex optimization problem (Aydin et al., 2018; Camacho and Bordons, 2004). For example, Venkateswarlu and Reddy (2008), developed two strategies with NMPC that use genetic algorithms and simulated annealing to control a reactive distillation column. Yousuf *et al.* (2010) proposed a scheme that uses the particle swarm optimization (PSO) paradigm to find the solution to the MPC optimization problem by considering the nonlinearities. These works present significant improvement compared to other control models presented in the literature; however, there is an increase in the computational effort when compared to the linear MPC. Therefore, in processes with fast dynamics, this problem can cause performance loss and extrapolation of the system sampling time, which hinders the control action (Gouta et al., 2017).

NMPCs based on artificial neural networks (ANN) have been developed as an alternative to conventional NMPCs. These controllers have a learning algorithm that receives data from the real process (plant history), making the model close to reality. Furthermore, they are extremely fast in processing the results as most of the calculations are performed in the ANN training step (Li et al., 2015; Kimaev and Ricardez-Sandoval, 2019).

ANN consist of mathematical models with a high capacity to solve complex and nonlinear problems. They provide better interpolation, are computationally simple and, therefore, are fast to process. Also, the ANN predict the desired variable using the secondary variables as the input parameters (Bahar, 2004; Zanata, 2005; Fortuna, et al., 2005; Patil and Ghate, 2015; Bashah et al., 2015; Jana and Banerjee, 2018; Singh et al., 2019).

Neves et al. (2018) studied the dynamic behavior of an ED column – the recovery column was not considered – to obtain anhydrous ethanol (99.5 mol%). Results showed that, amid feed stream disturbances, it is possible to determine new operating conditions to maintain the specification of the product streams (top and bottom) through an ANN-based control. The proposed strategy maintains the original plant's control system by adjusting only the setpoints of the existing controllers. The problem shown in Figure 5.1 was minimized by using this new strategy.

In addition to the difficulty in controlling the compositions to be near the nominal values, there is still an issue with the specification change. International standards imposed by the European Union (EN 15376) and the American Society for Material Testing (ASTM D 4806) state that the alcohol content in anhydrous ethanol should be between 99.0−99.8 wt.% (Kiss and Suszwalak, 2012; Ramírez- Márques et al., 2013), which may vary according to market demand. Araújo Neto et al. (2019) used an ANN in the development of an intelligent control system to make changes to controllers' setpoints in an ED process. This study accounts for both the extractive and recovery columns to change the specifications of the top product but does not consider the disturbances in the azeotrope feed.

Therefore, the objective of this study is to develop an intelligent control system (ICS), based on an ANN, capable of – individually or simultaneously – rejecting disturbances to the azeotrope feed and allowing changes in the specification of the anhydrous ethanol produced in an ED process that uses ethylene glycol as solvent, while maintaining a condition of minimum energy consumption in the extractive and recovery columns. The dehydration of aqueous mixtures of ethanol was chosen as a case study due to its industrial importance. The performance of the developed ICS was compared with that of the conventional control system (CCS). To the best of our knowledge, there are no published studies that have simulated the proposed ICS to simultaneously reject feed disturbances and change specifications in an ED process.

5. 2 Steady-State Process Modelling

According to the process flowsheet shown in Figure 5.2 and implemented on the *Aspen Plus*™ platform, the extractive column (C1) was fed with streams of the azeotropic ethanol-water mixture (ETHANOL-WATER) and, in an upper stage, the ethylene glycol solvent (EG). The solvent changes the relative volatility of the components present in the azeotropic stream

so that ethanol is obtained at the top, while the bottom product is a mixture of water and ethylene glycol. This mixture feeds the recovery column (C2), where the water-rich stream is obtained at the top, while the bottom product consists of pure EG, which then returns to C1.

A solvent make-up stream was used to compensate for the loss of EG across the top of columns C1 and C2. In order to take advantage of the energy potential of the C2 bottom stream (EG-RECYCLE), thermal integration was carried out with the azeotropic stream through the heat exchanger (E). The EG-RECYCLE stream, whose temperature was approximately 186 °C, was split into two parts: 20% was diverted to the extraction column, while the rest was directed towards the thermal integration. The percentage is defined to obtain an EG recycling stream with a temperature close to 80 ºC (Ramos et al., 2016). At the operating pressure, the top temperature of the extractive column is close to 78 °C, while in the recovery column it is 86 oC, therefore, guaranteeing the use of cooling water in both condensers.

Figure 5.2. Flowsheet for the production of anhydrous ethanol using thermal integration

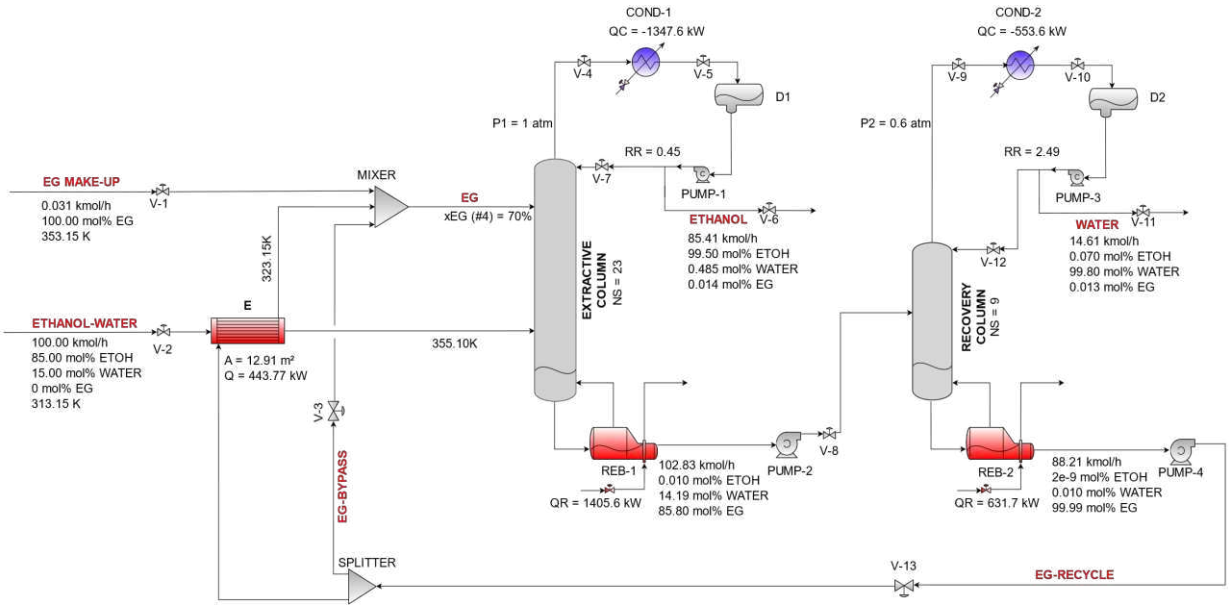

For column simulation, the RadFrac routine was used, which consists of a rigorous model for calculating the operations with multiple stages. The simulation of the heat exchanger used for thermal integration was carried out with the HeatX routine, which uses a rigorous shell and tube type exchanger model. To represent the vapor-liquid equilibrium (VLE), the non-random two-liquid (NRTL) thermodynamic model was chosen. The steam phase was considered ideal because the columns operate at low pressures (Meirelles et al., 1992).

The design and process specifications, which are shown in Table 5.2, are based on the studies by Ramos et al. (2016) and Figueirêdo et al. (2015). The dimensions, height and diameters, of the reflux vessels and sumps were calculated to reach a 50% capacity, considering a 5-minute hold-up (Luyben, 2013; Chen et al., 2017).

The process simulation was subject to the following restrictions:

- Ethanol composition at the top of C1 ($\boldsymbol{x_{Top}^{ETOH}}$): 99.10–99.90 mol% (depending on the production planning);
- Ethanol composition at the bottom of C1 ($\boldsymbol{x_{Bottom}^{ETOH}}$) 0.010 mol%;
- Water composition at the top of C2 ($\boldsymbol{x_{Top}^{H2O}}$): 99.80 mol%;
- Ethylene glycol composition at the bottom of C2 ($\boldsymbol{x_{Bottom}^{EG}}$): 99.99 mol%.

Table 5.2. Design and process information

Variable	**Columns**	
	Extractive Column	**Recovery Column**
Number of stages	23	9
Solvent feed stage	4	-
Azeotropic feed stage	18	-
C2 feed stage	-	5
Solvent content (tray #4)	0.7	-
Top pressure (atm)	1.0	0.6
Column pressure drop (atm)	0.2	0.09
Reflux ratio	0.45	2.29
Reboiler duty (kW)	1,405.60	631.71
Condenser duty (kW)	1,347.58	553.56
Column diameter (m)	0.73	0.61
Column base height (m)	3.39	2.38
Reflux vessel diameter (m)	1.68	1.37
Reflux vessel length (m)	3.37	2.74

Variable	**Streams**			
	ETHANOL-WATER	**EG**	**ETHANOL**	**WATER**
Temperature (°C)	40.0	80.0	78.5	86.4
Molar flow rate (kmol·h^{-1})	100.0	88.2	85.4	14.6
Molar fraction of ethanol (%)	85.0	-	99.50	0.070
Molar fraction of water (%)	15.0	0.010	0.485	99.98
Molar fraction of EG (%)	-	99.99	0.015	0.013

To meet these specifications, the following variables were manipulated: from C1, the solvent flow rate (S), reflux ratio (RR), and distillate flow rate (ETHANOL); and, from C2, the distillate flow rate (WATER) and reflux ratio (RR).

Additionally, the solvent content (molar fraction) in the liquid phase at its feeding stage of the extractive column ($xEG_{\#4}$) was analyzed, as it influences the column composition profile and, consequently, the energy consumption. As different composition profiles meet the process restrictions, the solvent content was chosen considering the reboilers' energy consumption, as shown in Figure 5.3. That was then specified as 70 mol% because, in this condition, regardless of the molar specification of ethanol in the distillate (spec), the other restrictions were met with lower energy consumption.

Figure 5.3. Effect of solvent content on energy consumption

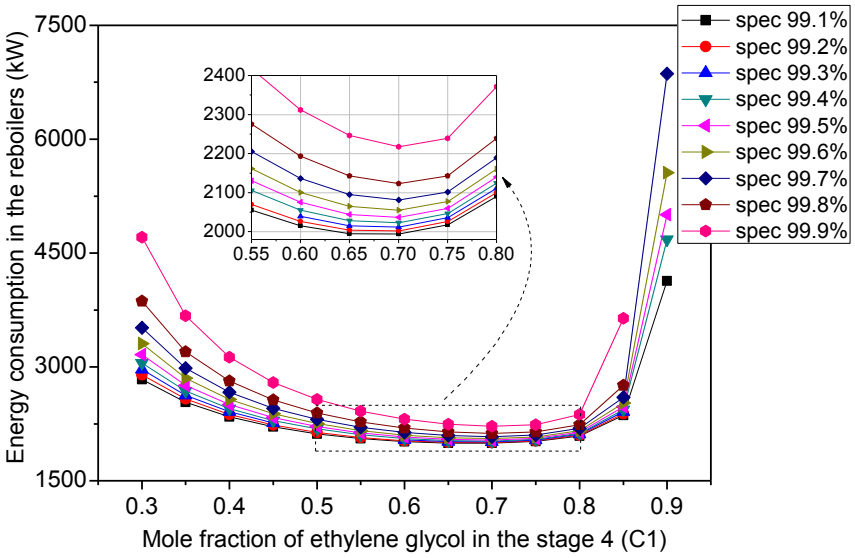

5. 3 Artificial Neural Network and Control System

ANN are made up of processing units, called neurons, whose function is inspired by the biological nervous system. The final solution depends on the connections between these units.

Figure 5.4 shows the schematic of an artificial neuron, where the signals propagate from left to right. The inputs are represented by x and outputs by y (Haykin, 2009). This neuron is composed by a set of synaptic weights (w), which are adjustable and represent the memory and knowledge used to solve the problem, and an activation function (φ) that is applied to an intermediate outlet (u), which is the sum of all products between the inputs and their respective synaptic weights.

ANN training was performed by adjusting the values of the connections (synaptic weights) between the neurons. The network output was compared to the expected value and the weights re-adjusted until, for a given input, the ANN output was approximately equal to that, satisfying the previously established criteria (Haykin, 2009; Beale et al., 2010). The data for ANN training, validation, and testing were obtained from the simulations performed on *Aspen Plus*™, aided by the sensitivity analysis tool, when varying the ethanol specification in the C1 distillate and the characteristics of the azeotropic feed (ethanol molar fraction, temperature, and flow rate). These variables were used as ANN inputs.

Figure 5.4. Schematic of an artificial neuron

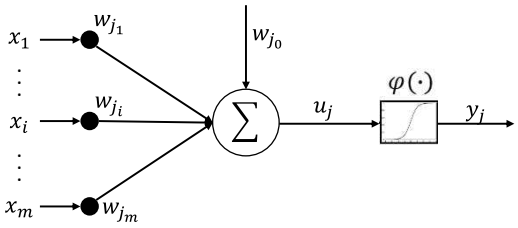

The temperatures of trays #10 (T10_C1) and #20 (T20_C1) in C1, trays #3 (T3_C2) and #6 (T6_C2) in C2, and the feed ratio (S/F) between solvent (S) and azeotrope (F) were used as the outputs of the ANN (Ramos et al., 2016; Neves et al., 2018).

Complying with the operating restrictions mentioned above, more than 1,000 simulations were performed to cover the different operating scenarios. The dataset containing each input vector with its respective output vector was stored. It was later split randomly, with 70% of the input/output pairs to be used for training, 15% to be used for validation, and 15% to be used for the ANN tests.

Figure 5.5 illustrates the procedure used to generate the data to build the ANN-based ICS. Aided by the Design Specification tool from *Aspen Plus*™, the output variables were the setpoints of the controllers, collected when the process met all the restrictions for each disturbance/specification. The input and the output variables were normalized within the range of [-1, 1], according to Equation 5.1. This interval was chosen because it corresponds to the numerical limits of the sigmoidal tangent function (tansig), used as activation function for all neurons in the training stage of the ANN in MATLAB®.

$$x_{norm} = \frac{(x_i - x_{min})(L_{sup} - L_{inf})}{(x_{max} - x_{min})} + L_{inf}, \quad (5.\ 1)$$

where x_{norm} is the normalized value of the variable; x_i are the actual values of the variables; L_{sup} and L_{inf} are the upper and lower limits established by the analyst, respectively; and, x_{max} and x_{min} are the maximum and minimum values of the variables, respectively.

To find an ANN with high generalization capacity, the size of the training data set was fixed, and an attempt was made to determine the best ANN architecture. Two types of architectures were selected as candidates – the feedforward multilayer perceptron network (MLP) and the Elman recurrent network – and evaluated regarding their performance with the problem's data. The training algorithm used in this study was the Levenberg–Marquardt (LM), which is a variation of the standard Backpropagation method that uses the second derivative as a form of optimization. This algorithm can complete the training in less time, as the ANN performance is evaluated using the mean squared error (MSE), and its goal is to minimize functions that are the sums of the square of other nonlinear functions (Singh et al., 2007).

Figure 5.5. Procedure and tools used in data collection for building the ANN-based ICS.

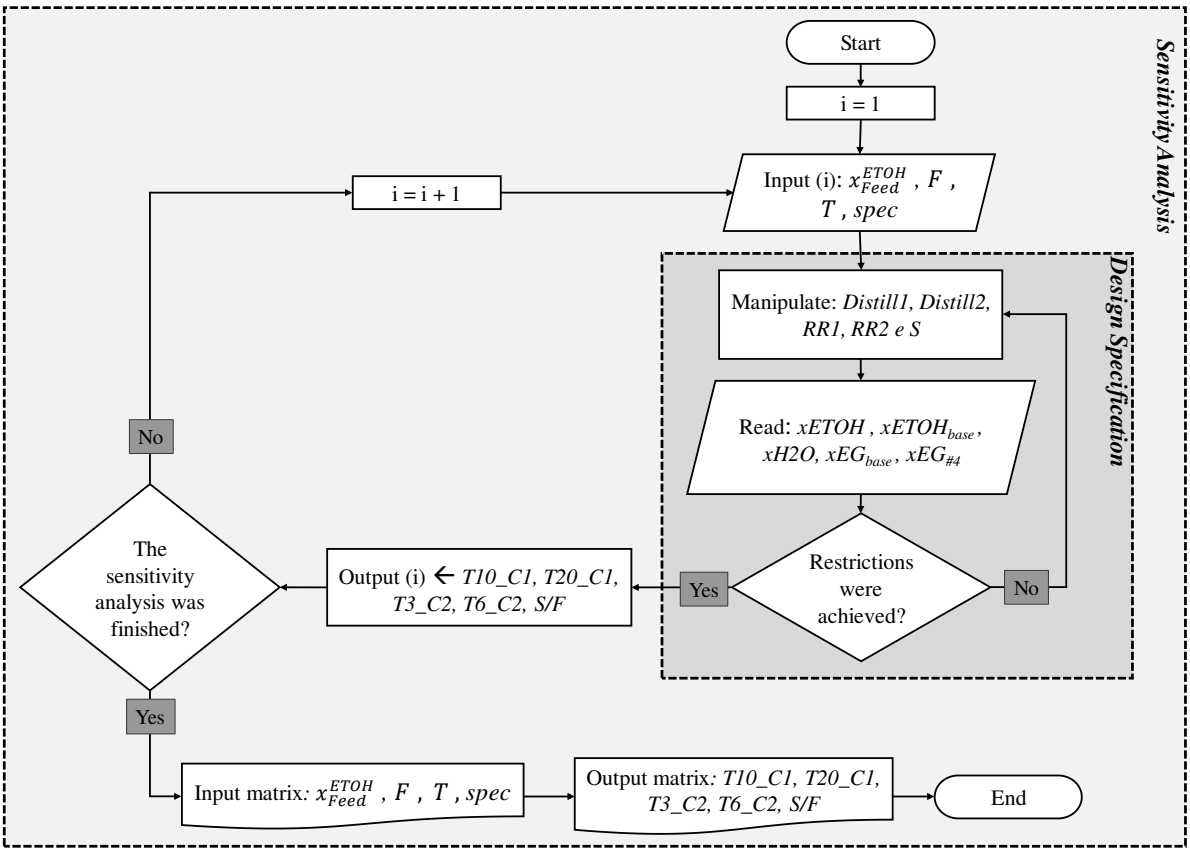

An excessive number of neurons in the hidden layers can cause the network to only memorize the training data (overfitting) and not extract the general characteristics that will allow generalization. In contrast, few neurons can also cause convergence issues during training and, consequently, high errors when predicting the output values. Some stopping criteria have been established for ANN training, such as the number of training epochs, gradient vector magnitude, error progress, and cross-validation. The training was interrupted when any of these criteria was met. The values recommended by MATLAB® were used for both the stopping criteria and the parameters associated with the training method. The type of network chosen was the feedforward MLP with 15 neurons in the hidden layer since, as shown in Table 5.3 by the mean squared error (MSE), there isn't any significant improvement when increasing the number of neurons and hidden layers beyond that.

Table 5.3. Summary of the results from the tested ANN

Hidden layers	Neurons hidden layer	Feedforward ANN			Recurrent Elman ANN		
		MSE			MSE		
		Training	Validation	Testing	Training	Validation	Testing
1	2	6.20×10^{-3}	6.00×10^{-3}	5.70×10^{-3}	5.90×10^{-3}	6.50×10^{-3}	6.30×10^{-3}
1	5	1.00×10^{-3}	1.00×10^{-3}	1.00×10^{-3}	8.90×10^{-4}	8.20×10^{-4}	8.60×10^{-4}
1	7	4.45×10^{-4}	3.85×10^{-4}	4.42×10^{-4}	3.70×10^{-4}	3.60×10^{-4}	3.28×10^{-4}
1	10	6.50×10^{-5}	5.70×10^{-5}	6.00×10^{-5}	7.51×10^{-5}	7.61×10^{-5}	7.3×10^{-5}
1	15	2.18×10^{-6}	2.10×10^{-6}	2.28×10^{-6}	6.72×10^{-6}	7.23×10^{-6}	7.78×10^{-6}
1	20	2.15×10^{-6}	2.09×10^{-6}	2.25×10^{-6}	2.10×10^{-6}	2.09×10^{-6}	2.15×10^{-6}
2	2. 2	5.40×10^{-3}	5.20×10^{-3}	5.10×10^{-3}	4.70×10^{-3}	4.10×10^{-3}	5.20×10^{-3}
2	5. 5	3.40×10^{-4}	3.78×10^{-4}	3.27×10^{-4}	1.18×10^{-4}	1.05×10^{-4}	1.28×10^{-4}
2	10. 10	1.92×10^{-6}	1.92×10^{-6}	1.64×10^{-6}	1.88×10^{-6}	2.25×10^{-6}	1.64×10^{-6}

To avoid overfitting the chosen ANN, another set of test data was used. The verification was performed by applying a different input to the model and comparing the model output to the actual output. To compare the expected results of each variable to the outputs of the ANN, an identity function was assumed. The results are shown in Figure 5.6.

The determination coefficient (R^2) was calculated to assess the quality of the model's fit to the sample data, while the error of each sample or residue was calculated as the difference between the value estimated by the ANN and the data provided by *Aspen Plus*™.

It can be seen from Figure 5.6 that the ANN predicts the data with an accuracy equal to or greater than 99.9% and with a low deviation between the estimated value and the real value. These results indicate that the ANN was able to generalize the predictions through a highly

representative mathematical model. As the ANN inferences are the controlled variables of the process, the expectation is that the control based on this model will be able to provide satisfactory characteristics both from the servo point of view (change in product specifications) and from the regulatory point of view (disturbances rejection).

5. 4 Intelligent Control System

The steady-state model was exported to *Aspen Plus Dynamics*™ using the Pressure Driven option, which considers the influence of pressure between the equipment and currents, which makes the simulation more realistic. In the process flowsheet shown in Figure 5.7, the controllers described in Table 5.4 were added, in addition to the respective control loops of the ICS based on the developed ANN.

Figure 5.6. Relationship between the responses provided by the ANN and the expected setpoints ((a), (c), (e), (g), (i)) and the errors associated with the measurements ((b), (d), (f), (h), (j))

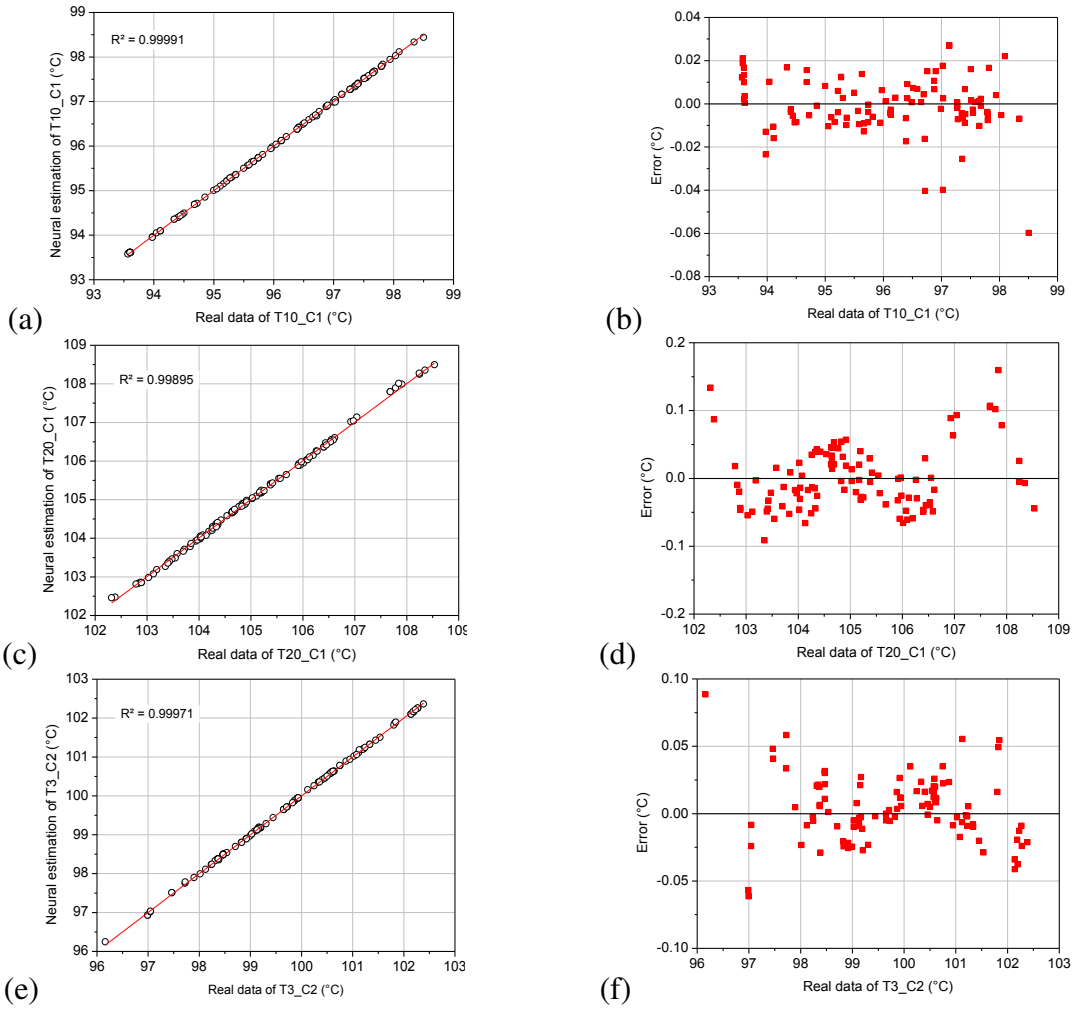

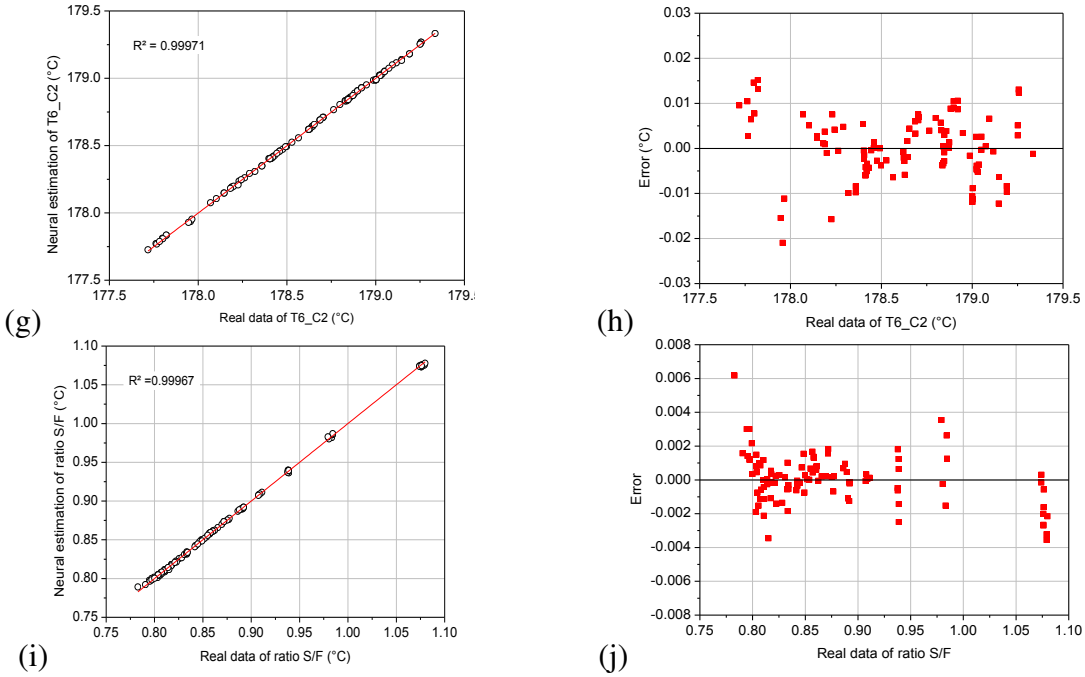

Figure 5.7. ANN-based ICS configuration

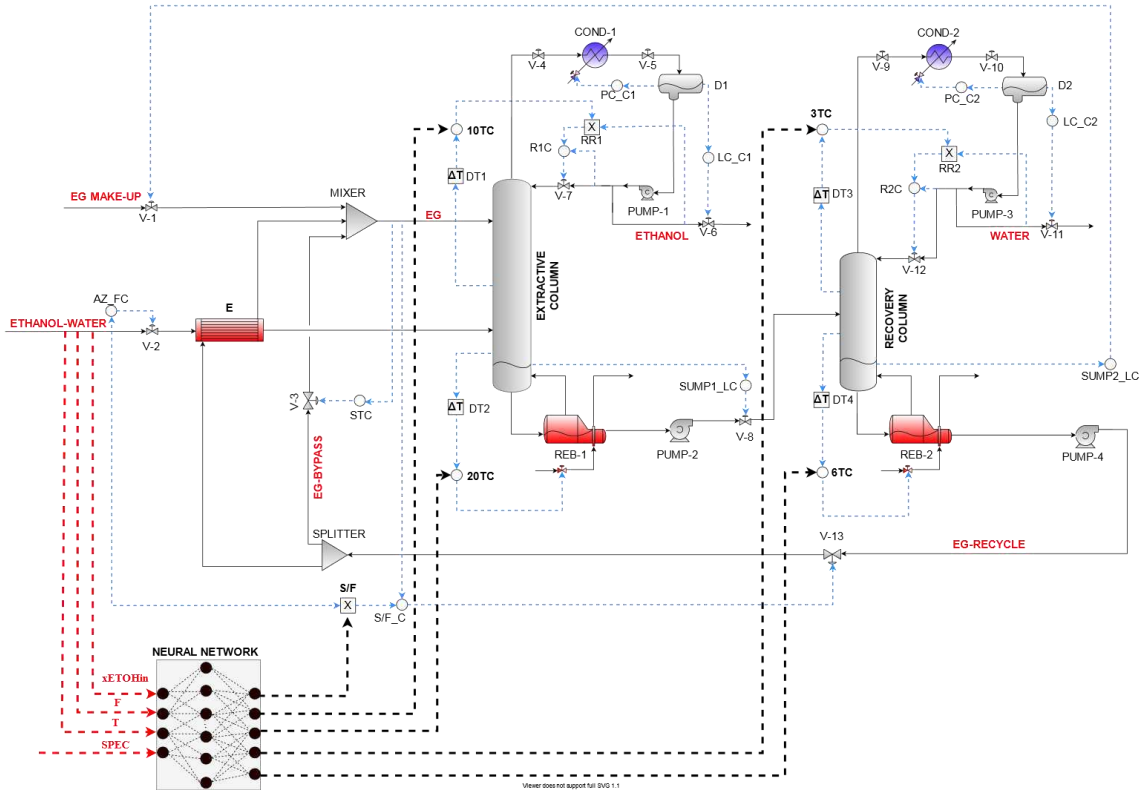

The PID controller translates the idea that the manipulated variable will be changed proportionally (P) to the instantaneous error, to the integral (I) of the error over time, and to the rate of change (D) of the controlled variable error. Its control law is as follows:

$$u(t) = k_c(y_d - y(t)) + \frac{k_c}{\tau_I}\int_0^t (y_d - y(t))dt + k_c.\tau_d.\frac{d(y_d - y(t))}{dt} + u_s \quad (5.\ 2)$$

Table 5.4. Controllers used in the flowsheet shown in Figure 5.7

Controller	Controlled variable	Manipulated variable
AZ_FC	Azeotrope feed flow rate	V-2 valve opening
S/F_C	S/F Ratio	RECYCLE stream flow rate (V-13)
STC	EG stream temperature	EG bypass stream flow rate (V-3)
10TC	Temperature of stage #10 of C1	Reflux ratio RR1
20TC	Temperature of stage #20 of C1	C1 reboiler heat duty (REB-1)
R1C	C1 reflux flow rate	V-7 valve opening
PC_C1	D1 reflux vessel pressure	COND-1 cooling fluid flow rate
LC_C1	D1 reflux vessel level	C1 distillate stream flow rate (V-6)
SUMP1_LC	C1 base level	C1 bottom stream flow rate (V-8)
3TC	Temperature of stage# 3 of C2	Reflux ratio RR2
6TC	Temperature of stage# 6 of C2	C2 reboiler heat duty (REB-2)
R2C	C2 reflux flow rate	V-12 valve opening
PC_C2	D2 reflux vessel pressure	COND-2 cooling fluid flow rate
LC_C2	D2 reflux vessel level	C2 distillate stream flow rate (V-11)
SUMP2_LC	C2 base level	EG MAKE-UP stream flow rate (V-1)

where $u(t)$ is the controller output as a function of time; u_s is the output of the controller in the steady-state; k_c is the gain of the proportional part of the controller; τ_I is the time constant of the controller integral action; τ_d is the time constant of the controller derivative action; and $(y_d - y(t))$ is the error between the setpoint and the controlled variable. The numerical values of the constants must be determined to avoid instability in the process and achieve high control performance.

To tune the column temperature controllers, the Tyreus–Luyben method was used (Tyreus and Luyben, 1992). The flow rate and level controllers used the settings recommended by Luyben (2002) while, for the pressure controllers, the parameters suggested by the *Aspen Plus Dynamics*™ were maintained. For the control loop of the solvent stream temperature (STC), the Internal Model Control (IMC) method was used, as presented in the study by Gil et al. (2012). According to the aforementioned works, it is not recommended to use the derivative action for the control purpose of this study. Besides, as the ICS modifies the setpoints in real-time, the derivative term is disregarded so that it is possible to eliminate the frequent changes in its value, which could cause unnecessary control actions and instability in the process (Stephanopoulos, 1984). Table 5.5 shows the type, action, setpoint, and tuning parameters for each controller used.

Table 5.5. Parameters of the controllers used in the flowsheet shown in Figure 5.7

Controller	Type	Action	Setpoint	k_C	τ_I (min)
AZ_FC	PI	Direct	Variable	0.50	0.30
STC	PI	Reverse	80.0 °C	2.46	1.19
10TC	PI	Direct	Modified by ICS	3.88	14.52
20TC	PI	Reverse	Modified by ICS	54.32	2.64
R1C	PI	Direct	Variable	0.5	0.30
PC_C1	PI	Direct	1.0 atm	20	12.00
LC_C1	P	Direct	2.10 m	2	9,999.00
SUMP1_LC	P	Direct	1.87 m	10	9,999.00
3TC	PI	Direct	Modified by ICS	4.09	6.60
6TC	PI	Reverse	Modified by ICS	4.39	7.92
R2C	PI	Direct	Variable	0.50	0.30
PC_C2	PI	Direct	0.60 atm	20.0	12.00
LC_C2	P	Direct	1.18 m	2.0	9,999.00
SUMP2_LC	P	Reverse	1.34 m	2.0	9,999.00

The S/F block multiplies the flow rate of the ETHANOL-WATER stream by the desired ratio to obtain the setpoint for the EG stream flow rate. In a conventional control, this ratio has a fixed value; however, in the proposed intelligent control, this ratio was variable, just as the setpoints for the temperature controllers of the sensitive trays.

The output signal from controllers 10TC and 3TC establishes the reflux ratio setpoint, represented by the multiplier RR1 for C1 and RR2 for C2, respectively. This value was multiplied by the distillate flow rate to obtain the setpoint for controllers R1C and R2C, and their output signals go to the valve actuators that control the reflux flow rate. This cascade control consists of two conventional controllers and a single control valve, forming two closed-loops.

The input information for the controller is the error between the setpoint value and the measured value of the process output variable. The controller's effort will always be to reduce this error, keeping the process output variable under control. Therefore, it is also called the controlled variable. The dead time blocks (DT1, DT2, DT3, and DT4), with a time interval of 1.0 min, were inserted to account for the delays in the temperature measurement in the column trays.

According to Figure 5.7, the disturbances in the composition (x_{Feed}^{ETOH}), molar flow (F), and temperature (T) of the azeotrope feed are ICS inputs. Besides, the specification of the molar fraction of ethanol in the extractive column distillate is another input defined by the operator (spec). The communication between MATLAB® and *Aspen Plus Dynamics*™ was carried out by employing the Elipse SCADA software, using the Object Linking Embedding for Process

Control (OPC) communication protocol, as shown in Figure 5.8. It has already been implemented by approximately 20 industry sectors (Latif et al., 2019).

Figure 5.8. Communication between the software that constitute the ICS

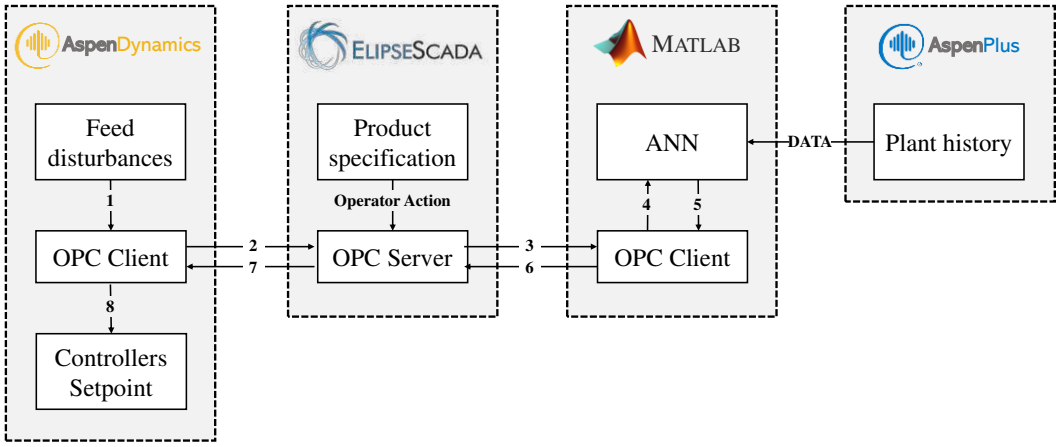

According to Figure 5.8, the mechanism follows these steps:

1. The disturbances simulated by the *Aspen Plus Dynamics*™ are identified as exported variables;
2. The disturbances are sent from the *Aspen Plus Dynamics*™ to the Elipse SCADA supervisory.
3. In the Elipse SCADA supervisory, the operator defines the desired ethanol specification and this value is sent to MATLAB® with the disturbances obtained in Step 2;
4. The new ethanol specification and disturbances are identified as the inputs for the ICS based on ANN trained in offline mode with the results obtained by the *Aspen Plus*™ steady-state;
5. ICS infers the new setpoint values using MATLAB®;
6. The new setpoint values are sent from MATLAB® to Elipse SCADA;
7. Elipse SCADA exports the new setpoint values to the *Aspen Plus Dynamics*™;
8. The controllers implemented in the *Aspen Plus Dynamics*™, with the new setpoints obtained, act on the process by modifying the specifications and/or rejecting the disturbances.

The mechanism occurs dynamically, allowing the change in ethanol specification in real-time. If necessary, the ANN can be retrained offline with a new dataset.

5. 5 Intelligent Control System Performance

The performance of the control system may be assessed through simulation results for changes in setpoints, step disturbances in the process feed stream, and changes in the specification of anhydrous ethanol, according to the consulted literature (Gil et al., 2012; Ramos et al., 2016; Qian et al., 2019; Neves et al., 2018; Araújo Neto et al., 2020).

As previously mentioned, changes in the product specifications may occur due to market demand, which can also influence the changes in the feed flow rate. The temperature and feed composition may change due to upstream processes. Simulations were carried out to evaluate the process control during a 15 h timespan. Initially, the process was in its nominal condition, operating with an ethanol in the distillate specification (spec) of 99.5 mol%.

Figure 5.9 shows the process response for a change in the product specification to 99.9 mol%, considering the step disturbances in the composition, flow rate, and temperature of the azeotrope stream every 5 h.

Figure 5.9. System response to system feed disturbances and change in ethanol specification from 99.5 mol% to 99.9 mol%: (a) xETOH, (b) S / F, (c) T10_C1, (d) T20_C1 and (d) T20_C1; (e) T3_C2 and (f) T6_C2

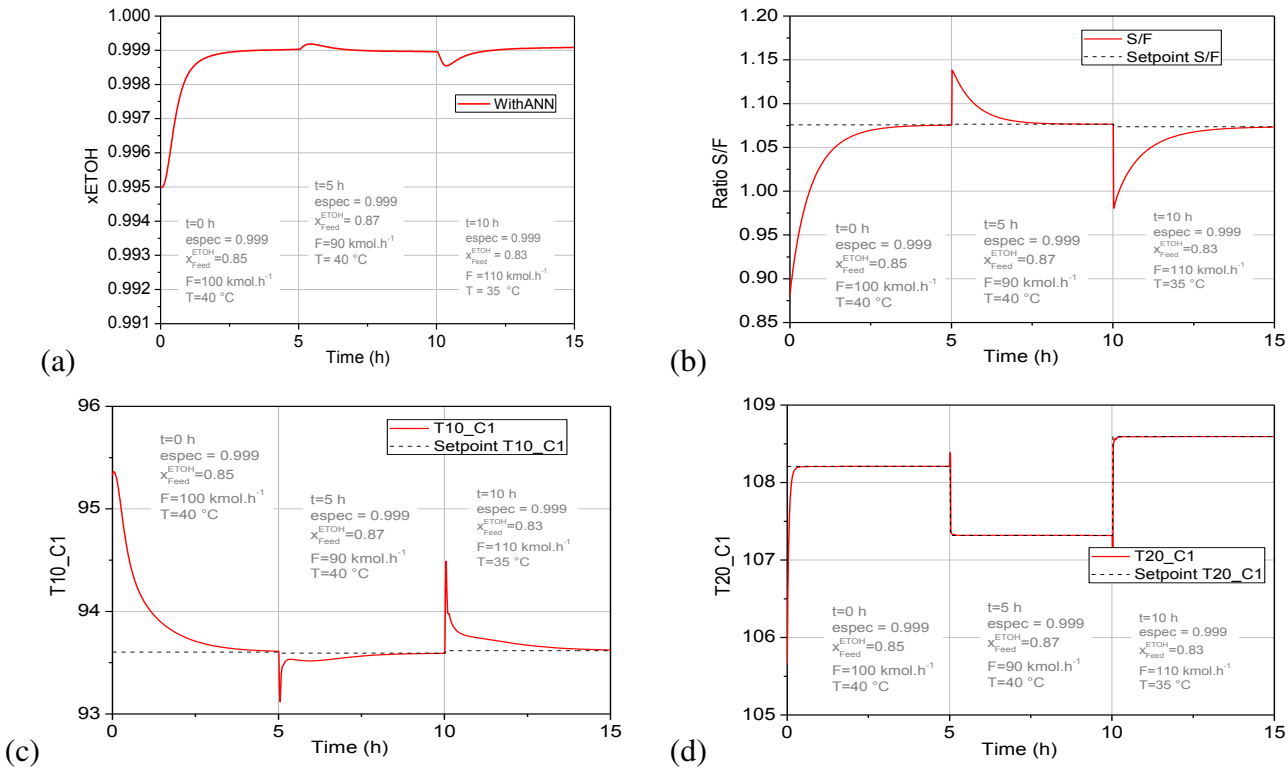

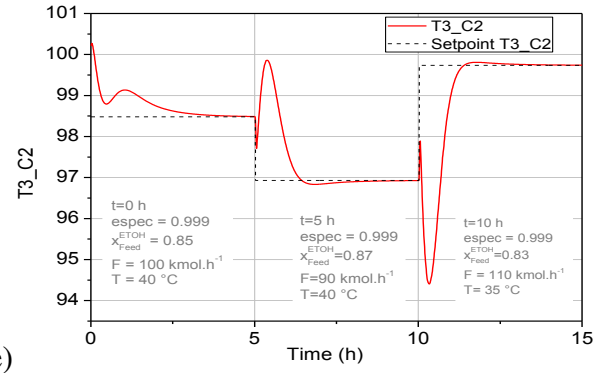

(e)

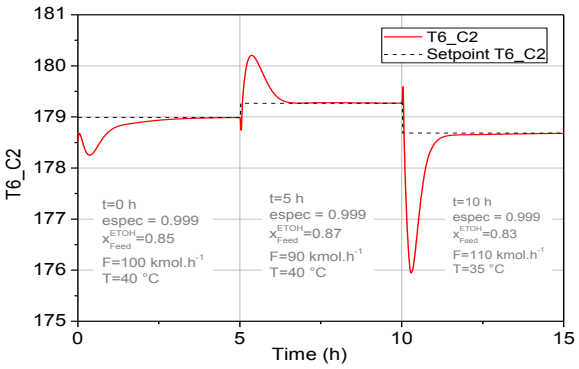

(f)

At time 0 h, the command to change the product specification was performed, and the ICS calculated the new setpoints for the controllers. The new specification (99.9 mol%) was reached in less than 3 h (Figure 5.9a). To achieve this result, an increase in the solvent flow rate was necessary, which led to an increase in the S/F ratio (Figure 5.9b). The changes in the S/F ratio setpoint occurred in order to maintain the solvent content in tray #4 at 70 mol%, ensuring minimum energy consumption, and were more significant at 0 h. Also, to achieve a higher purity level, the ICS acted on the extractive column to reduce the temperature setpoint of tray #10 (T10_C1) to increase the reflux ratio (Figure 5.9c), as they are reversely related. In addition, the temperature setpoint of tray #20 (T20_C1) was increased to increase the reboiler heat duty (Figure 5.9d), as they are directly related.

After a time interval of 5 h, the ethanol composition in the feed was changed to 87 mol% and the azeotrope flow rate to 90 kmol.h^{-1}. In this case, T20_C1 had its setpoint decreased (Figure 5.9d). The S/F ratio was slightly increased; however, it was sufficient to alter the vapor-liquid equilibrium (VLE), causing T10_C1 to reach a new setpoint to maintain the product specifications (Figure 5.9c). The lower feed flow rate in C1 resulted in a lower feed flow rate in C2, initially causing an excess of reboiler heat duty and, consequently, an initial increase in the temperature inside the recovery column (Figure 5.9e and 5.9f). The new feeding condition of C2 was perceived by the ICS, which increased the temperature setpoint of tray #6 (T6_C2); the result is shown in Figure 5.9f. Thus, a part of the solvent vaporized and affected the purity of the distillate. Therefore, increasing the reflux is necessary to compensate for this effect, which is reflected in the decrease in the temperature setpoint of tray #3 (T3_C2) of the same column (Figure 5.9e).

At 10 h, the ethanol composition in the feed changed to 83 mol%, the feed flow rate increased to 110 kmol.h^{-1}, and the temperature was reduced to 35 °C. This indicates that higher energy consumption is required in C1 to maintain the ethanol composition at the top at 99.9

mol%. In this case, the ICS acts in a way that the temperature of the bottom controller has its setpoint increased (Figure 5.9d). The S/F ratio slightly decreased, followed by an increase in the reflux ratio. To achieve the specifications in this new condition, the T3_C2 setpoint increased (Figure 5.9e) and, given their inverse relationship, it reduced the reflux ratio. It is noteworthy that the new reflux ratio value decreased the amount of liquid inside the column because, in that 10 h timespan, the C2 had received more liquid due to the disturbance in the feed flow rate.

Another evaluated scenario was the reduction in the ethanol specification from 99.5 mol% to 99.1 mol%, considering the step disturbances in composition, flow rate, and temperature of the azeotrope stream every 5 h. The results are shown in Figure 5.10.

Figure 5.10. System response to system feeding disturbances and change in ethanol specification from 99.5 mol% to 99.1 mol%: (a) xETOH, (b) S/F, (c) T10_C1, (d) T20_C1 and (d) T20_C1; (e) T3_C2 and (f) T6_C2

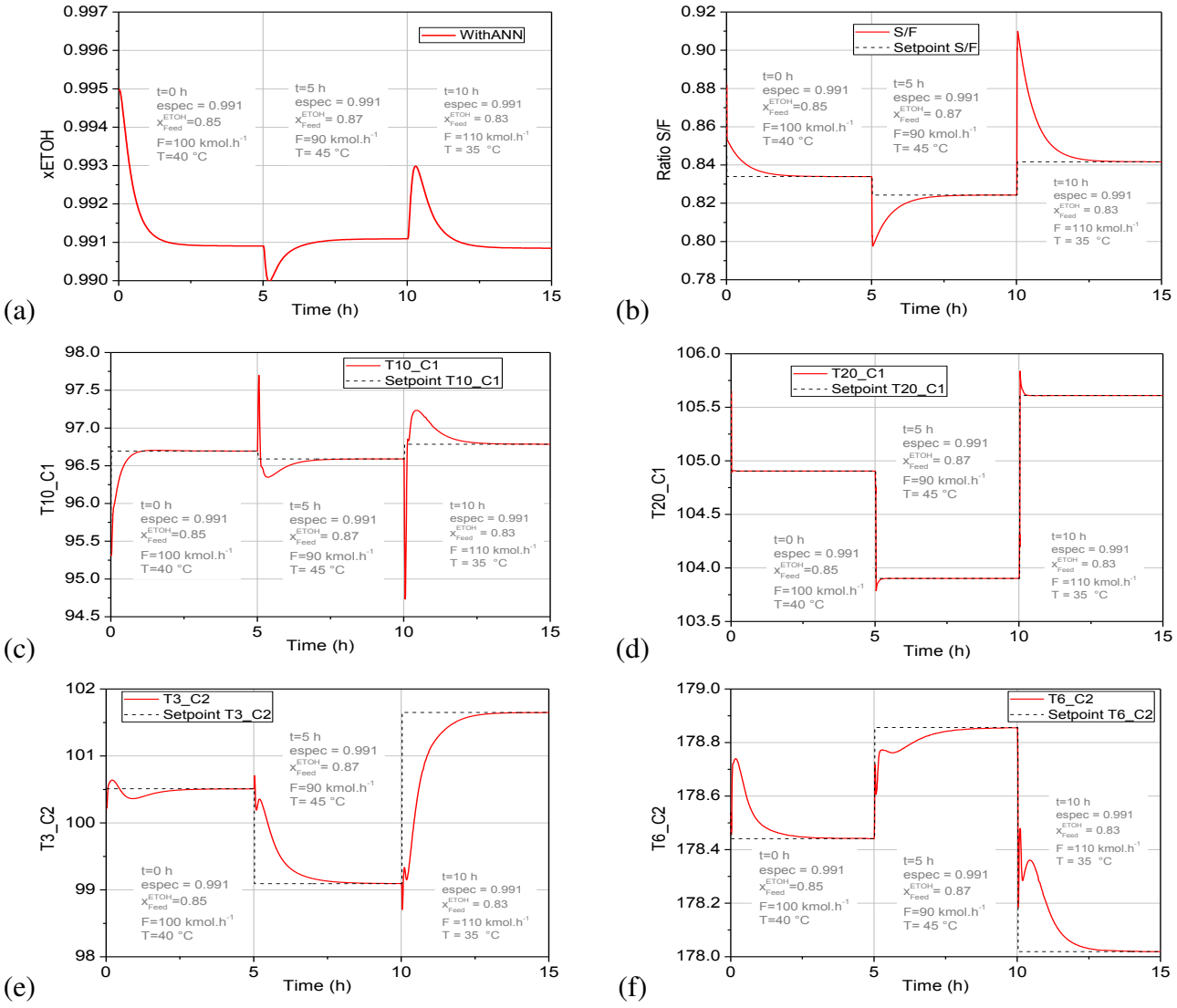

Unlike the previous scenario, at time 0 h, the goal was to reduce the purity of ethanol in the distillate. In this case, there was a reduction in the S/F ratio setpoint (Figure 5.10b), an increase in the T10_C1 setpoint (Figure 5.10c), a reduction in the reflux ratio, and the heat duty of the C1 reboiler was less required. This led to a decrease in the T20_C1 setpoint (Figure 5.10d). New setpoints for the C2 sensitive trays, considering the disturbances in the C1, were also estimated so that the process always remained within the restrictions (Figure 5.10e and 5.10f). The process reached a new steady-state and remained within the ± 0.01% offset range in less than 2 h. Additionally, disturbances rejection also occurred in less than 2 h (Figure 5.10a). The analysis of the controllers' setpoints for disturbances at 5 h and 10 h are analogous to those previously detailed.

The process was also evaluated by simultaneously modifying the specification of anhydrous ethanol and the characteristics of the azeotropic feed every 3 h. The results are shown in Figure 5.11.

Figure 5.11. System response to system power disturbances and change in product specifications every 3 h: (a) xETOH, (b) S/F, (c) T10_C1, (d) T20_C1, (d) T20_C1; (e) T3_C2, (f) T6_C2 and (g) energy consumption and solvent content

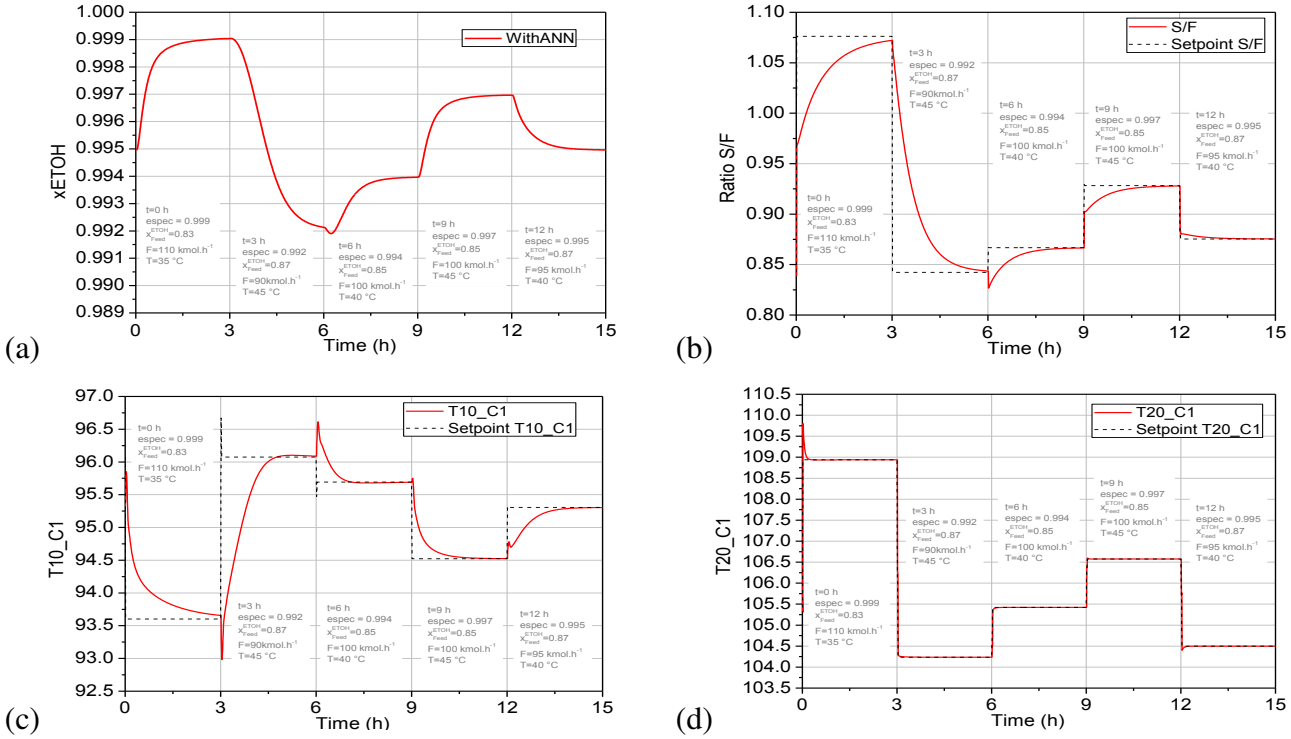

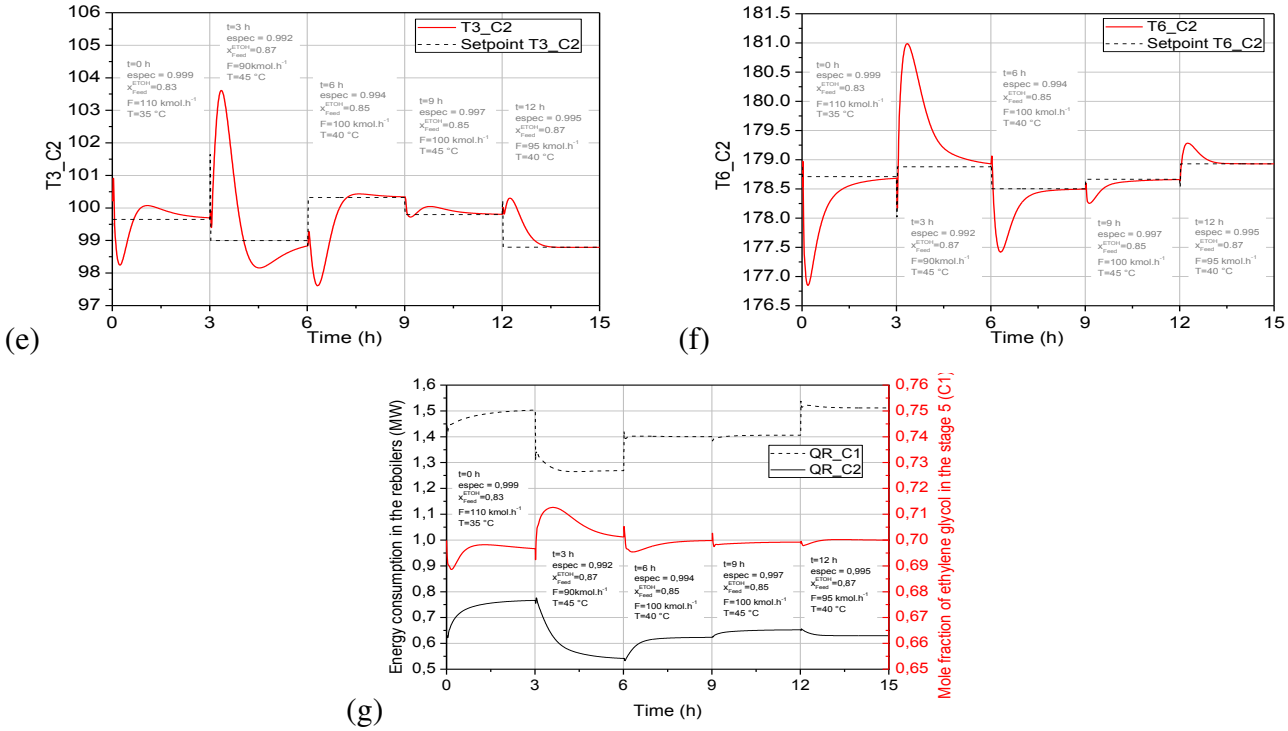

At 0 h, there were disturbances in the feed stream, which represented the change in flow rate, temperature, and ethanol composition values to 110 kmol.h^{-1}, 35 °C, and 83 mol%, respectively, in addition to the change in the ethanol specification to 99.9 mol%. It was noticed that the system achieved the new condition and rejected the disturbances in approximately 3 h.

At 3 h, the ethanol specification was changed from 99.9 mol% to 99.2 mol%. This modification, along with the feed disturbances, held the process from reaching the new steady-state completely in a short time, as shown in Figure 5.11a. However, the results indicate that the process was leaning towards the new operating condition. For all the following disturbances (at 6 h, 9 h, and 12 h), the ICS was able to control the process to the desired specifications in a short time (less than 3 h for all these cases).

As shown in Figure 5.11g, the ICS made the necessary changes to the setpoints so that the solvent content was kept at approximately 70 mol% (red curve), regardless of the specification or disturbances applied to the system.

In general, the controllers responded quickly to the changes in the setpoints, with relatively low times – rising time, descending time, and settling time for an interval of ± 2% of the setpoint value – and percentage of overshoot and undershoot. Thus, the new specifications for ethanol were reached in a short period (less than 3 h), and this value was controlled in the face of disturbances. Also, oscillations were not observed, indicating that the control did not

perform excessive actions, which in practice initiate a process of internal wear of the valves caused by the friction between the parts (Hägglund, 2011; Mishra et al., 2015).

The water composition in the recovery column distillate was less sensitive to the assessed disturbances, so its results were suppressed; this composition remained virtually at 99.8 mol% for any specification of ethanol in the distillate of the extractive column.

To compare the performance of the conventional control and intelligent control, positive and negative disturbances were applied to the initial values of the following variables: composition, flow rate, and temperature of the azeotrope, with amplitudes of 3%, 10%, and 25%, respectively. The magnitude of the disturbances was based on the values found in the literature (Gil et al., 2012; Ramos et al., 2016; Qian et al., 2019; Neves et al., 2018; Araújo Neto et al., 2020) . The response of the ethanol composition at the top of C1 to these disturbances is shown in Figure 5.12.

Figure 5.12. Behavior of the ethanol specification in face of disturbances of (a) + 3% in x_{Feed}^{ETOH}; (b) – 3% in x_{Feed}^{ETOH}; (c) + 10% in F; (d) -10% in F; (e) + 25% in T; (f) –25% in T

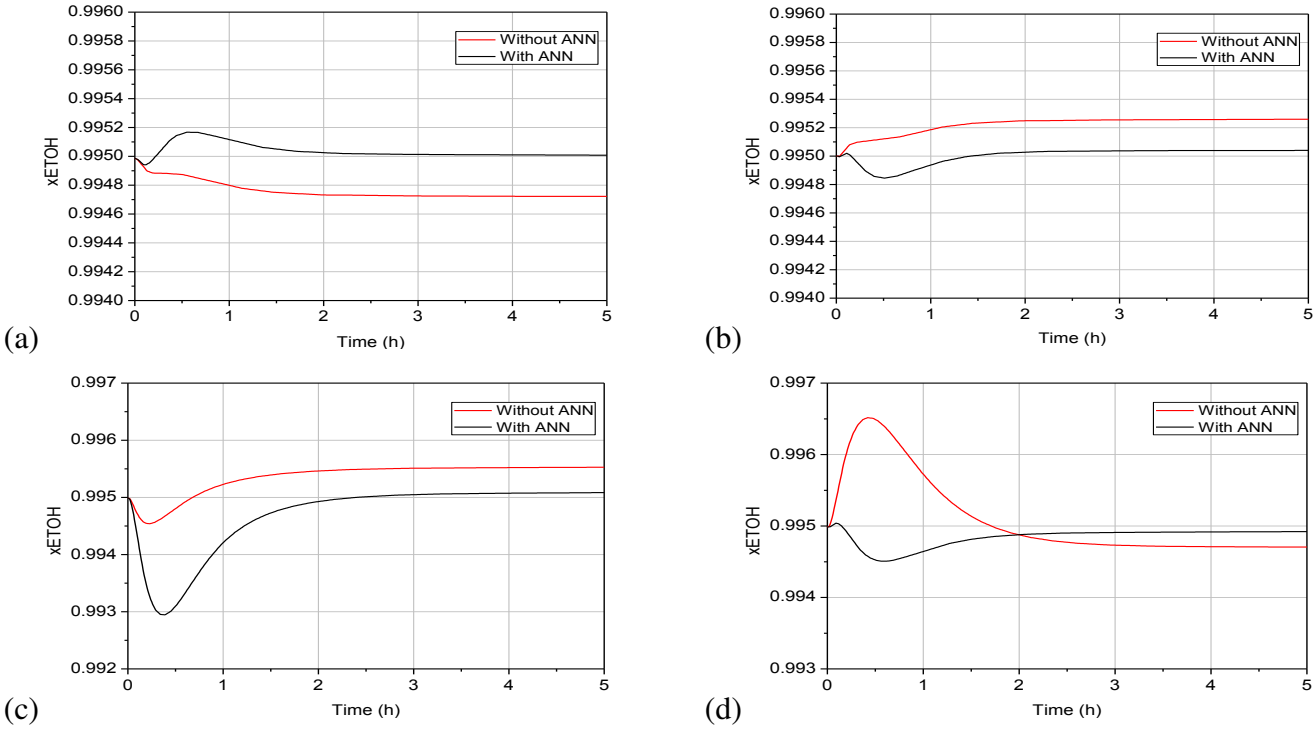

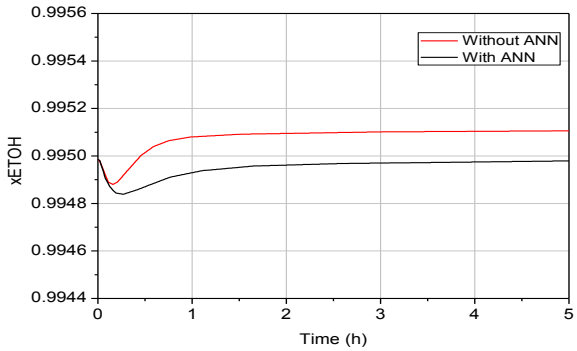

(e)

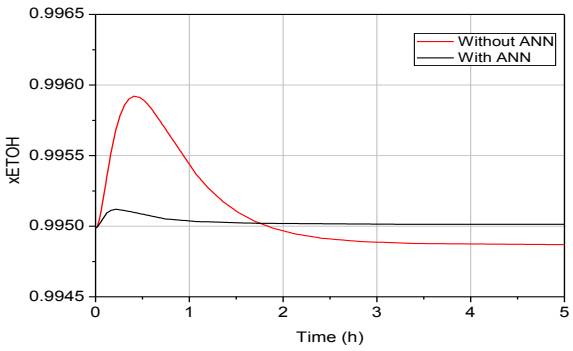

(f)

As a way of quantifying the error (e) accumulated over time (t) between the ethanol composition and the specification, the integral squared error (ISE), calculated using Equation 5.3, and the integral absolute error (IAE), calculated using Equation 5.4, were computed.

$$ISE = \int_0^\infty \left[e(t)\right]^2 dt \tag{5. 3}$$

$$IAE = \int_0^\infty \left|e(t)\right| dt \tag{5. 4}$$

In addition to ISE and IAE, the steady-state error, which is the difference in the ethanol composition when the process reached the new steady-state and the nominal specification, was also evaluated. Table 5.6 presents a summary of these indices and provides a comparison between the conventional control system (CCS) and the intelligent control system (ICS).

For the evaluated time (5 h), the ICS showed an ISE higher than the CCS only for the positive disturbance to the azeotrope flow rate. This metric sums the squares of the errors, making the weight higher for large errors and lower for small errors. This result reflects the behavior observed in Figure 5.12c, as the ICS presented a higher overshoot than the CCS. However, as the evaluation time increases, the ISE for the CCS tends to become higher than for the ICS because the steady-state error for the CCS is higher than that of the ICS. As the IAE treats all the errors equally, since it does not add any weight to the error, the ICS presented the best values for this index, considering all the analyzed disturbances.

Table 5.6. Performance indices for CCS and ICS

Disturbance	ISE		IAE		Steady-state error	
	CCS	ICS	CCS	ICS	CCS	ICS
Composition (+)	2.76×10^{-7}	2.52×10^{-8}	1.21×10^{-3}	2.18×10^{-4}	2.78×10^{-4}	8.00×10^{-6}
Composition (-)	2.96×10^{-7}	1.78×10^{-8}	1.11×10^{-3}	2.28×10^{-4}	2.59×10^{-4}	4.00×10^{-5}
Flow rate (+)	1.06×10^{-6}	2.31×10^{-6}	1.28×10^{-3}	7.87×10^{-4}	5.28×10^{-4}	8.40×10^{-5}
Flow rate (-)	1.64×10^{-6}	1.85×10^{-7}	1.82×10^{-3}	8.60×10^{-4}	2.95×10^{-4}	7.80×10^{-5}
Temperature (+)	5.60×10^{-8}	1.26×10^{-8}	4.59×10^{-4}	2.41×10^{-4}	1.06×10^{-4}	2.10×10^{-5}
Temperature (-)	5.60×10^{-7}	1.18×10^{-8}	1.17×10^{-3}	3.91×10^{-4}	1.30×10^{-4}	1.30×10^{-5}

The high performance of the ICS is ultimately demonstrated by the analysis of the steady-state error. In all of the cases, the ICS was able to stabilize the ethanol composition close to its nominal value of 99.5% mol, which resulted in deviations 5 to 35 times smaller than that of the CCS.

5. 6 Concluding remarks

The developed ANN-based ICS was able to reject the azeotrope feed disturbances and/or change the specification of the anhydrous ethanol produced (top product of the extractive column) while maintaining a condition of minimum energy consumption in the reboilers of the columns. This new control approach is conceptually simple and can be easily implemented. Also, due to its feedforward characteristics, it shows an improved performance when compared that of the conventional control system.

The development of the ICS considered the ANN architecture. The training dataset was composed of 1,000 data points and the chosen network was a feedforward MLP with 15 neurons in the hidden layer. It was verified that increasing the number of hidden layers and neurons beyond that did not result in any significant performance improvement.

To ensure the accuracy and generalization capacity of the developed ICS, a representative dataset is necessary The chosen ANN may be trained with data generated by a mathematical model validated with industrial data or with data from the plant itself. It is important emphasize, before a training stage using plant data, the use of statistical techniques to eliminate outliers is necessary. In this study, an Aspen Plus™ simulation model was used for data generation and, later on, as plant to evaluate the ICS performance.

The performance of the intelligent control system was evaluated for variations in the anhydrous ethanol specification (99.1 mol% to 99.9 mol%), considering step disturbances in the composition, flow rate, and temperature of the azeotrope stream. The process reached a new steady-state and remained within the range of ± 0.01% in the time interval of 2–4 h. According to metrics such as ISE, IAE, and the steady-state error, the performance of the intelligent control system was superior to that of the conventional control system. Another advantage of the ICS is that it minimizes human intervention in the process since, in the event of disturbances, the controllers' setpoints are automatically modified.

The communication between MATLAB® and Aspen Plus Dynamics™, carried out with the help of the Elipse SCADA software, is simple, and the intelligent control proposed maintains the original structure of the plant's control system, adjusting only the setpoints of the existing controllers.

The ICS may present low performance when it is used outside of its training range. Therefore, whenever new process data is available, the ANN should be submitted to a new training stage. As the ANN-based ICS (feedforward control) must act in conjunction with the conventional control (feedback control), in case of unsatisfactory responses by the model, the operator can turn off the ICS and return to the conventional control system. After retraining the ANN, the ICS can be switched on again.

CAPÍTULO 6

CONCLUSÕES E SUGESTÕES PARA TRABALHOS FUTUROS

CAPÍTULO 6 – CONCLUSÃO GERAL E SUGESTÕES PARA TRABALHOS FUTUROS

6. 1 Conclusões

Devido à complexidade das operações envolvidas no processo de destilação extrativa, em uma planta real, os dados coletados experimentalmente podem ser amplificados pelo uso da técnica de modelagem e simulação, justificando o uso do *Aspen Plus*™ e do *Aspen Plus Dinamics*™ que permitiram prever o desempenho do processo em condições difíceis de serem realizadas experimentalmente.

A utilização de redes neurais artificias para melhorar o desempenho do controle de um processo implicou em ganho de tempo e simplicidade na elaboração de modelos, os quais são mais fáceis de serem obtidos do que os modelos baseados nos fenômenos físicos e químicos. O modelo foi alimentado em modo online, sendo extremamente rápido no processamento dos resultados dos novos *set-points*, já que a maior parte dos cálculos foi efetuada na fase de treinamento da RNA.

A tentativa de utilizar controle inteligente fora da faixa de treinamento (extrapolação) pode resultar em erros. Diante disso, sempre que novos dados experimentais do processo estejam disponíveis, a RNA precisa ser submetida a um reaprendizado. Destaca-se que para a aplicação em uma planta real, o modelo do *Aspen Plus*™ deve ser validado por testes estatístico mediante a análise de um conjunto de dados gerados pelo modelo e os dados reais do processo. Só assim, é possível estabelecer um nível de confiabilidade que se requer para que esse modelo seja aceitável na aplicação prevista.

Para a aplicação do controle proposto nesse trabalho, foi necessário um protocolo padrão de comunicação entre diferentes dispositivos, pois sem essa padronização, programar uma comunicação confiável, entre diferentes equipamentos para fins de controle, seria uma tarefa complexa, obrigando a utilização de funções de baixo nível e entendimento de características cada vez mais próximas do hardware. Portanto, uma das vantagens da comunicação OPC utilizada nesse trabalho foi a redução do tempo de desenvolvimento. O OPC está se tornando rapidamente o padrão de comunicação adotado pelo mercado de automação industrial e pela indústria. Então, de acordo com a proposta de controle apresentada, o operador pode definir qualquer especificação do produto, desde que esteja dentro do intervalo dos dados utilizados no treinamento da RNA e a comunicação é feita para que o sistema de controle leve a planta para

o novo regime estacionário, sendo capaz de rejeitar simultaneamente possíveis distúrbios na alimentação. Com auxílio de um sistema SCADA é possível determinar valores ótimos de trabalho monitorando algumas variáveis do processo, tais como: temperatura, pressão, vazão, nível, etc. Além disso, pode-se operar o processo localmente ou remotamente, tarefa que pode ser centralizada em poucos funcionários especializados. Essa praticidade possibilita detecção de falhas e intervenções mais rápidas, aumentando o desempenho da produção e consequentemente reduzindo os custos operacionais.

Apesar das malhas de controle terem características *feedback*, o controle inteligente adicionou características *feedfoward*, já que mediu a perturbação e tomou ações antecipadas na planta. As características do controle *feedback* continuam sendo de igual importância, pois distúrbios imensuráveis podem ser corrigidos.

De forma geral, o controle inteligente apresentou o melhor desempenho para o problema, com baixa oscilação e respostas rápidas. De acordo com os resultados, conclui-se que a rede captou toda a dinâmica envolvida no processo e minimizou o tempo para a coluna entrar em um novo regime estacionário.

6. 2 Sugestões para trabalhos futuros

Sugere-se para trabalhos futuros:

- Substituir o controle dual de temperatura, utilizado nos capítulos 4 e 5, pelo controle singular nas colunas de destilação. As saídas da rede neural referentes aos *set-points* de temperatura dos controladores de topo podem ser substituídas por *set-points* de razão de refluxo, conforme foi feito no capítulo 3. O controle dual apresenta interação entre as malhas, dificultando a sintonia dos controladores; pode não ser economicamente viável, já que mais malhas de controle são introduzidas;
- Implementar o controle inteligente em outros processos químicos para comprovar a generalidade da metodologia aplicada;
- Avaliar a implementação do controle inteligente com outras classes de redes neurais artificiais;
- Utilizar RNA com algoritmos que possibilitam o treinamento em tempo real. Nesses casos, a rede fornece os valores das variáveis de saída dependendo dos estímulos de entrada, ao mesmo tempo em que essa resposta é comparada aos dados do processo.

Dessa forma é possível que o algoritmo de aprendizado recalcule os pesos e vieses dos neurônios para que o modelo não perca a eficiência caso o processo mude de comportamento;

- Inferir os melhores parâmetros de sintonia dos controladores para os diferentes estados estacionários.

REFERÊNCIAS BIBLIOGRÁFICAS

REFERÊNCIAS BIBLIOGRÁFICAS

Aguirre, L. A. **Introdução à identificação de sistemas: técnicas lineares e não lineares aplicadas a sistemas reais**. 4ª ed. Belo Horizonte: Ed. UFMG, 2015.

Ahmed, M. R.; Doyle, N.; Connolly, C.; McSweeney, S.; Krüse, J.; Morrissey, J.; Prentice, M. B.; Fitzpatrick, D. Tracking Yeast Metabolism and the Crabtree Effect in Real Time via CO2 Production using Broadband Acoustic Resonance Dissolution Spectroscopy (BARDS). **Journal of Biotechnology**, v. 308, p. 63–73, 2020.

Alvarez, V. H.; Maciel Filho, R.; Aznar, M.; Mattedi, S. An evaluation and industrial application of ionic liquid as separation agent for separation of diluted ethanol-water mixtures. **Fenómenos de Transferencia**, v. 4, p. 8-12, 2009.

An, Y.; Li, W.; Li, Y.; Huang, S.; Ma, J.; Shen, C.; Xu, C. Design/optimization of energy-saving extractive distillation process by combining preconcentration column and extractive distillation column. **Chemical Engineering Science**, v. 135, p.166–178, 2015.

Anokhina, E.; Timoshenko, A. Criterion of the Energy Effectiveness of Extractive Distillation in the Partially Thermally Coupled Columns. **Chemical Engineering Research and Design**, v. 99, p. 165-175, 2015.

Araújo Neto, A. P.; Farias Neto, G. W.; Neves, T. G.; Ramos, W. B.; Brito, K. D.; Brito, R. P. Changing product specification in extractive distillation process using intelligent control system. **Neural Comput and Applic.**, 2019.

Arifin, S., Chien, I. L. Design and control of an isopropyl alcohol dehydration process via extractive distillation using dimethyl sulfoxide as an entrainer. **Industrial and Engineering Chemistry Research**, v. 47, p. 790–803, 2008.

Aspen Technology Inc., **Aspen User Guide**, 2017.

Aspentech. **Aspen Plus: Getting started building and running a process model**. Version 11.1. Aspen Tecnology, Inc. Cambridge, 2001.

Atkins, P. W.; de Paula, J. **Physical Chemistry**. 10 ed. Oxford University Press, 2014.

Aydin, E.; Bonvin, D.; Sundmacher, K. Computationally efficient NMPC for batch and semi-batch processes using parsimonious input parameterization. **Journal of Process Control**, v. 66, p. 12–22, 2018.

Bahar, A.; Özgen, C.; Leblebicioğlu, K.; Halıcı, U. Artificial Neural Network Estimator Design for the Inferential Model Predictive Control of an Industrial Distillation Column. **Industrial & Engineering Chemistry Research**, v. 43n. 19, p. 6102–6111, 2004.

Bakhtadze N.N. Virtual analyzers: Identification approach. **Automation and Remote Control**, v. 65, n. 11, p. 1691-1709, 2004.

Bashah, N. A. A.; Othman, M. R.; Aziz, N. Feed Forward Neural Network Model for Isopropyl Myristate Production in Industrial-scale Semi-batch Reactive Distillation Columns. **Journal of Engineering Science**, v. 11, p. 59–65, 2015.

Bastidas, P.A.; Gil, I.D.; Rodriguez, G. Comparison of the Main Ethanol Dehydration Technologies through Process Simulations. **In 20th European Symposium on Computer Aided Process Engineering–ESCAPE-20**. Ischia, Italy, 2010.

Beale, M. H.; Hagan, M. T.; Demuth, H. B. **Neural Network Toolbox 7 User Guide. Mathworks**, 2010.

Boyer, S. A. ***SCADA:*** **Supervisory Control and Data Acquisition**. 4 Ed. International Society of Automation, 2010

Brasil. Agência Nacional do Petróleo, Gás natural e Biocombustíveis. **Resolução ANP Nº 764, de 20.12.2018 - DOU 21.12.2018**. Disponível em: < http://legislacao.anp.gov.br/?path=legislacao-anp/resol-anp/2018/dezembro&item=ranp-764-2018>. Acesso em: 20/05/2019.

Brito, K. D.; Cordeiro, G. M.; Figueirêdo, M. F.; Vasconcelos, L. G. S.; Brito, R. P. Economic Evaluation of Energy Saving Alternatives in Extractive Distillation Process. **Computers & Chemical Engineering**, v. 93, p. 185-196, 2016.

Brito, R. P. **Processo de Destilação Extrativa: Modelagem Dinâmica, Simulação e Avaliação de Nova Configuração**. 202 f. Tese (Doutorado) - Universidade Estadual de Campinas, Campinas-SP, 1997.

Brosilow, C. B.; Tong, M. The structure and dynamic of inferential control system. **AIChE Journal**, v. 24, p. 492-499, 1978.

Camacho, E. F.; Bordons, C. **Model Predictive Control**. Springer-Verlag, London, United Kingdom, 2004.

Chen, M.; Yu, N.; Cong, L.; Wang, X.; Zhu, M.; Sun, L. Design and control of a heat pump assisted azeotropic dividing wall column for EDA/Water separation. **Ind. Eng. Chem. Res.**, v. 56, p.9770–9777, 2017.

Chinprasit, J.; Panjapornpon, C. Model predictive control of vinyl chloride monomer process by Aspen Plus Dynamics and MATLAB/Simulink co-simulation approach. **IOP Conference Series: Materials Science and Engineering**, 778, 2020.

Ciannella, S.; Damasceno, A. S.; Nunes, Í. C.; de Farias Neto, G. W.; Ramos, W. B.; Brito, R. P. Using hot-vapor bypass for pressure control in distillation columns. **Chinese Journal of Chemical Engineering**, v. 26, p. 144–151, 2018.

Confalonieri, G.; Quartieri, S.; Vezzalini, G.; Tabacchi, G.; Fois, E.; Daou, T. J.; Arletti, R. Differential penetration of ethanol and water in Si-chabazite: High pressure dehydration of azeotrope solution. **Microporous and Mesoporous Materials**, 2019.

Dahlqvist, S. A. Application of Self-Tuning Regulators to the Control of Distillation Columns. **IFAC Proceedings Volumes**, v. 13, n. 9, 167–174, 1980

Daneels, A.; Salter W. ***What is SCADA? International conference on accelerator and large experimental physics control systems***. Trieste, Italy, 1999.

De Lima, M. L.; Camponogara, E.; de Campos, M. C. M. M.; Miyatake, L. K. Automatic control of flow gathering networks: A mixed-integer receding horizon control applied to an onshore oilfield. **Control Engineering Practice**, v. 86, p. 48–55, 2019.

Dias, M.; Ensinas, A.; Nebra, S.; Maciel Filho, R.; Rossell, C.; Wolf, M. Production of bioethanol and other bio-based materials from sugarcane bagasse: Integration to conventional bioethanol production process. **Chemical Engineering Research and Desing**, v. 87, p. 1206-1216, 2009.

Doherty, M.D.; Malone, M. D. **Conceptual Design of Distillation Systems**. McGraw-Hill, 2001.

Dong, K.; Liu, X.; Dong, H.; Zhang, X.; Zhang, S. Multiscale studies on ionic liquids. **Chem. Rev**. v. 117, p. 6636–6695, 2017.

Dong, Y.; Dai, C., Lei; Z. Extractive distillation of methylal/methanol mixture using ethylene glycol as entrainer. **Fluid Phase Equilibria**, v. 462, p. 172-180, 2018.

Elman, J. L. Finding structure in time. **Cognitive Science**, v. 14, p. 179-211, 1990.

Fausset, L. **Fundamentals of neural networks: Architectures, algorithms, and applications**. New Jersey: Prentice Hall, 1994.

Figueirêdo, M. F.; Ramos, W. B.; Brito, K. D.; Brito, R. P. Effect of Solvent Content on Controllability of Extractive Distillation Columns. **Computer Aided Chemical Engineering**. v. 202, p. 1607-1612, 2015.

Figueroa, J. E. J. **Análise e otimização do processo de obtenção de etanol anidro, empregando líquidos iônicos**. 199 f. Dissertação (Mestrado em Engenharia Química), Universidade Estadual de Campinas, Campinas-SP, 2011.

Fonseca, R. R., Thompson, Jr., J. P., Franco, I. C., da Silva, F. V. Automation and Control of a Dissolved Air Flotation Pilot Plant. **IFAC-PapersOnLine**, v. 50, n. 1, p. 3911–3916, 2017.

Fortuna, L.; Graziani, S.; & Xibilia, M. G. Soft sensors for product quality monitoring in debutanizer distillation columns. **Control Engineering Practice**, v. 13, n. 4, 499–508, 2005.

Fruhwirth, T.; Pauker, F.; Fernbach, A.; Ayatollah, I.; Kastner, W.; Kittl, B. Guarded state machines in OPC UA. **In Industrial Electronics Society, IECON 2015-41st Annual Conference of the IEEE**, p. 4187-4192, 2015.

Gehlen, C. O.; Apio, A.; Koch, G. G.; Franchi, C. M.; Hoffmann, R.; Salau, N. P. G Implementation of an indirect control structure for composition in a hybrid distillation column. **Separation Science and Technology,** v. 50, n. 16, p. 2532-2544, 2015.

Gil, I. D.; Gomez, J. M.; Rodríguez, G. Control of an extractive distillation process to dehydrate ethanol using glycerol as entrainer. **Computers and Chemical Engineering**, v. 39, p. 129-142. 2012.

Gnansounou, E.; Dauriat, A. Ethanol fuel from biomass: a review. **J Sci Ind Res**, v. 64, p. 809–82, 2005.

Golob, M.; Bratina, B. Web-Based Monitoring and Control of Industrial Processes Used for Control Education. **IFAC Proceedings Volumes**, v. 46, n. 17, p. 162–167, 2013.

Goodfellow, I.; Bengio, Y.; Courville, A. **Deep Learning**. 2016.

Gouta, H., Saïd, S. H., Barhoumi, N., M'Sahli, F. Generalized predictive control for a coupled four tank MIMO system using a continuous-discrete time observer. **ISA Transactions**, v. 67, p. 280–292, 2017.

Guan, J.; Graham, J.; Hieb, J. A digraph model for risk identification and management in SCADA systems. 2011 IEEE international conference on intelligence and security informatics (ISI), **IEEE CP**, p. 150–5, 2011.

Guang, C.; Shi, X.; Zhang, Z.; Wang, C.; Wang, C.; Gao, J. Comparison of heterogeneous azeotropic and pressure-swing distillations for separating the diisopropylether/isopropanol/water mixtures. **Chem. Eng. Res. Des.**, v. 143, p. 249-260, 2019.

Hagan, M.T.; Demuth, H. B. Neural Networks for Control. **Proceedings of the 1999 American Control Conference**. San Diego, CA, p. 1642–1656, 1999.

Hägglund, T. A shape-analysis approach for diagnosis of stiction in control valves. **Control Engineering Practice**, v. 19, n. 8, p. 782–789, 2011.

Haykin, S. **Neural networks and learning machines**, third ed. Pearson, Upper Saddle River, NJ, 2009.

Hecht-Nielsen, R. Theory of the backpropagation neural network. **International Joint Conference on Neural Networks (IJCNN)**, v. 1, p. 593-605, 1989.

Hernandez, L.; Baladron, C.; Aguiar, J. M.; Calavia, L.; Carro, B.; SanchezEsguevillas, A.; Gomez, J. A study of the relationship between weather variables and electric power demand inside a smart grid/smart world framework. **Sensors**, v. 12, n. 9, p. 11571-11591, 2012.

Holtorf, F., Mitsos, A.; Biegler, L. T. Multistage NMPC with on-line generated scenario trees: Application to a semi-batch polymerization process. **Journal of Process Control**, v. 80, p. 167–179, 2019.

Hoskins, J. C.; Himmelblau, D. M. Artificial Neural Network Models of Knowledge Representation in Chemical Engineering. **Computers & Chemical Engineering**, v. 12, n. 9-10, p. 881-890, 1988.

Hu, Y.; Su, Y.; Jin, S.; Chien, I.L.; Shen. Systematic approach for screening organic and ionic liquid solvents in homogeneous extractive distillation exemplified by the tert-butanol dehydration. **Sep. Purif. Technol.**, v. 211, p. 723-737, 2019.

Huang, W.; Nakamori, Y.; Wang, S.-Y. Forecasting stock market movement direction with support vector machine. **Computers and Operations Research**, v.32, n. 10, p. 2513 - 2522, 2005

Hussain, M.A. Review of the applications of neural networks in chemical process control. Simulation and on-line implementations. **Artificial Intelligence in Engineering**, v. 13, p. 55–68, 1999.

Iqbal, S.I.; Aziz, M. N. Comparison of MIMO MPC and PI decoupling in controlling methyl tert-butyl ether process. **Comput Aided Chem Eng.**, v. 31, p. 345–9, 2012.

Jana, A. K.; Banerjee, S. Neuro estimator-based inferential extended generic model control of a reactive distillation column. **Chemical Engineering Research and Design**, v. 130, p. 284–294, 2018.

Jelinski, T.; Cysewski, P. Screening of ionic liquids for efficient extraction of methylxanthines using COSMO-RS methodology. **Chem. Eng. Res**. *Des*. V. 122, p. 176–183, 2017.

Junqueira, T. L., Dias, M. O. S., Wolf-Maciel, M., Maciel Filho, R., Rossell, C. E.V. Simulation of anhydrous bioethanol production process using efficiency correlations for conventional and extractive distillation. **9th Distillation & Absorption Conference**, p. 521-526, 2010.

Kalbani, F. A., Zhang, J. Inferential active disturbance rejection control of a distillation column. **9th IFCH Symposium on Advanced Control of Chemical Processes**, v. 48, p. 403-408, 2015.

Kano, M., Showchaiya, N., Hasebe, S. Hashimoto, I. Inferential control of distillation compositions: selection of model and control configuration. **Control Engineering Practice**, v. 11, p. 927-933, 2003.

Kerton, F.M.; Marriott, R. Alternative Solvents for Green Chemistry. **Royal Society of Chemistry**, 2013.

Kimaev, G.; Ricardez-Sandoval, L. A. Nonlinear Model Predictive Control of a Multiscale Thin Film Deposition Process Using Artificial Neural Networks. **Chemical Engineering Science**, v. 207, p. 1230-1245, 2019.

Kiss, A.A.; Suszwalak, P.C. Enhanced bioethanol dehydration by extractive and azeotropic distillation in dividing-wall columns. **Separation and Purification Technology**, v. 86, p. 70-78, 2012.

Kiss, A.A.; Suszwalak, P.C. Enhanced bioethanol dehydration by extractive and azeotropic distillation in dividing-wall columns. **Separation and Purification Technology**, v. 86, p. 70-L78, 2012.

Kister, H. Z.; Hanson, D. W. Control Column Pressure via Hot-Vapor Bypass. **Chemical Engineering Progress**, 2015.

Kittisupakorn, P., Charoenniyom. T., Daosud, W. Hybrid neural network controller design for a batch reactor to produce methyl methacrylate. **Engineering Journal**, v. 18, p. 145-162, 2014

Konakom, K., Kittisupakorn, P., Mujtaba, I. M. Neural network-based controller design of a batch reactive distillation column under uncertainty**. Asia-Pacific Journal of Chemical Engineering**, v. 7, p. 361–377, 2012.

Kummer, A.; Varga, T. Process simulator assisted framework to support process safety analysis. **Journal of Loss Prevention in the Process Industries**, v. 58, p. 22-29. 2019.

Latif, H.; Shao, G.; Starly, B. Integrating A Dynamic Simulator and Advanced Process Control using the OPC-UA Standard. **Procedia Manufacturing**, v. 34, p. 813–819, 2019.

Lee, F.M.; Pahl, R.H. Solvent screening and conceptual extractive distillation process to produce anhydrous ethanol rom fermentation broth. **Industrial Engineering Chemical Process Design & Development,** v. 24, p. 168–172, 1985.

Lei, Z., Li, C. and Chen, B. **Extractive distillation: A review**. Separation and Purification Reviews, v.32, n.2, p.121-213, 2003.

Lei, Z.; Chen, B.; Zhu, J. Extractive distillation with ionic liquids: a review. **AIChE J.**, v. 60, p. 3312–3329, 2014.

Leung, D. Y. C.; Wu, X.; Leung, M. K. H. A review on biodiesel production using catalyzed transesterification. **Applied Energy***,* 2010.

Li, S.; Li, Y.-Y. Neural network based nonlinear model predictive control for an intensified continuous reactor. **Chemical Engineering and Processing: Process Intensification**, v. 96, p. 14–27, 2015.

Lu, C. H., Tsai, C. C., Liu, C. M., Charng, Y. H. Neural-network-based predictive controller design: An application to temperature control of a plastic injection molding process. **Asia-Pacific Journal of Chemical Engineering**, v. 12, p. 680–691, 2010.

Luo, N.; Wang, X.; Van, F.; Ye, Z.-C.; Qian, F. Integrated Simulation Platform of Chemical Processes Based on Virtual Reality and Dynamic Model. **Computer Aided Chemical Engineering**, p. 581–586, 2015.

Luyben, W. L. **Distillation Design and Control Using Aspen Simulation**, second ed. John Wiley & Sons, New Jersey, 2013.

Luyben, W. L. Improved design of an extractive distillation system with an intermediate-boiling solvent. **Separation and Purification Technology**, v. 156, p. 336–347, 2015.

Luyben, W. L. **Plantwide dynamic simulators in chemical processing and control**, New York: Marcel Dekker, 2002.

Luyben, W. L. **Process Modeling, Simulation and Control for Chemical Engineers**, second ed. McGraw Hill: New York, 1990.

Luyben, W. L. Quantitative Comparison of Alternative Control Schemes for Air-Cooled Condensers. **AIChE Journal**, v. 52, p. 611-622, 2006.

Lynn, S.; Hanson, D. N. Multieffect extractive distillation for separating aqueous azeotropes. **Industrial & Engineering Chemistry Process Design and Development**, v. 25, n. 4, p. 936–94, 1986.

Maciejowski, J. M. **Predictive Control with Constraints**, London: Prentice Hall, 2002.

Manochio, C.; Andrade, B. R.; Rodriguez, R. P.; Moraes, B. S. Ethanol from biomass:A comparative overview. **Renewable and Sustainable Energy Reviews,** v. 80, p. 743-755, 2017.

Mansouri, S. S., Sales-Cruz, M., Huusom, J. K., Woodley, J. M., Gani. R. Integrated process design and control of reactive distillation processes**. In S. Skogestad (Ed.), Proceedings of the 19th Nordic Process Control Workshop**. Norwegian University of Science and Technology, v. 48, p. 1120-1125, 2015

Marquardt, D. W. An algorithm for least-squares estimation of nonlinear parameters. **SIAM J. Appl. Math***,* v. 11, p 431-441, 1963.

MathWorks. **Neural Network Toolbox**, User's Guide. 2018.

Mcculloch, W.S.; Pitts, W. A logical calculus of the ideas immanent innervous activity. **Bulletin of Mathematical Biophysics**, v. 5, n. 4, p.115-133, 1943.

Meirelles, A.; Weiss, S.; Herfurth, H. Ethanol dehydration by extractive distillation. **Journal of Chemical Technology and Biotechnology**, v.56, p.181-188, 1992.

Mejdell, T., Skogestad, S. Composition estimator in a pilot-plant distillation column using multiple temperatures. **Industrial & Engineering Chemistry Research**, v. 30, p. 2555-2564, 1991.

Meyer, C.; Seborg, D. E.; Wood, R. K. An experimental application of time delay compensation techniques to distillation column control. **IFAC Proceedings**, v. 10, n. 16, p. 439-446, 1977.

Mishra, P.; Kumar, V.; Rana, K. P. S. An online tuned novel nonlinear PI controller for stiction compensation in pneumatic control valves. **ISA Transactions**, v. 58, p. 434–445, 2015.

Mondal, S.K.; Saha, P. Separation of hexavalent chromium from industrial effluent through liquid membrane using environmentally benign solvent: a study of experimental optimization through response surface methodology. **Chem. Eng. Res. Des**., v. 132, p. 564–583, 2018.

Morsi, I.; El-Din, L. M. SCADA system for oil refinery control. **Measurement**, v. 47, p. 5–13, 2014.

Nagy, Z. K. Model based control of a yeast fermentation bioreactors using optimally designed artificial neural networks. **Chemical Engineering Journal**, v. 127, n. 1–3, p. 95–109, 2007.

Nerrand, O., Roussel-Ragot, P., Personnaz, L., Dreyfus, G. Neural networks and nonlinear adaptive filtering: unifying concepts and new algorithms. **Neural Computation**, v. 5, p. 165-199, 1993.

Neves, T. G**. Redes neurais artificiais aplicadas ao controle inteligente de colunas extrativas**. 78f. Dissertação de Mestrado – Universidade Federal de Campina Grande, 2016.

Neves, T. G., Ramos, W. B., de Farias Neto, G. W.; Brito, R. P. Intelligent control system for extractive distillation columns. **Korean J. Chem. Eng**., v. 35, p. 826–834, 2018.

Niamsuwan, S., Kittisupakorn, P., I. Mujtaba, M. Control of milk pasteurization process using model predictive approach, **Computers & Chemical Engineering**, v. 66, p. 2–11, 2014.

Osuolale, F. N.; Zhang, J. Energy efficiency optimisation for distillation column using artificial neural network models. **Energy**, v. 106, p. 562–578, 2016.

Patil, S. R.; Ghate, V. N. A Generalized Regression Neural Network Based on Soft Sensor for Multicomponent Distillation Column. **International Journal of Computer and Communication Engineering**, v. 4, n. 6, 2015.

Pla-Franco, J.; Lladosa, E.; Loras, S.; Montón, J.B. Azeotropic distillation for 1-propanol dehydration with diisopropyl ether as entrainer: equilibrium data and process simulation. **Sep. Purif. Technol**., v. 212, p. 692-698, 2019.

Qian, X., Huang, K., Jia, S., Chen, H., Yuan, Y., Zhang, L., & Wang, S. Composition/temperature cascade control for a Kaibel dividing-wall distillation column by combining PI controllers and model predictive control integrated with soft sensor. **Computers & Chemical Engineering**, v. 126, p. 292-303, 2019.

Qin, S.J., Badgwell, T. A. A survey of industrial model predictive control technology. **Control Engineering Practice**, v. 11, p. 733-764, 2003.

Ramaswamy, S.; Cutright, T. J.; Qammar, H. K. Control of a continuous bioreactor using model predictive control. **Process Biochemistry**, v. 40, n. 8, p. 2763-2770, 2005.

Ramírez-Márquez, C.; Segovia-Hernández, J.G.S.; Hernádez, S.; Errico, M.; Rong, B.G. Dynamic behavior of alternative separation processes for ethanol dehydration by extractive distillation. **Industrial & Engineering Chemistry Research**, v. 52, n. 49, p. 17554-17561, 2013.

Ramos, W. B.; Figueirêdo, M. F.; Brito, K. D.; Ciannella, S.; Vasconcelos, L. G. S.; Brito, R. P. Effect of Solvent Content and Heat Integration on the Controllability of Extractive Distillation Process for Anhydrous Ethanol Production. **Industrial & Engineering Chemistry Research**, v. 55, n. 43, p. 11315–11328, 2016.

Rao, S. S. **Engineering Optimization Theory and Practice**. John Wiley & Sons, Inc., Hoboken, New Jersey, 4th edition, 2009.

Ravagnani, M. A. S. S.; Reis. M. H. M.; Marciel Filho, R.; WOLF-MACIEL, M. R. Anhydrous ethanol production by extractive distillation: A solvent case study. **Process Safety and Environmental Protection**, v. 88, n. 1, p. 67-73, 2010.

Reid, R. C.; Prausnitz, J. M.; Poling, B. E. **The properties of gases and liquids**. 4.ed. New York: McGraw-Hill, 1988.

Reis, M. H. M. **Desenvolvimento de um Programa para Geração de Mapas de Curvas Residuais e Aplicação a Processos de Destilação Azeotrópica e Extrativa**. Dissertação de mestrado. Universidade Estadual de Campinas, Faculdade de Engenharia Química. Departamento de Processos Químicos, 2002.

Rivera, D. E.; lee, H.; Braun, M.W.; Mittelmann, H. D. Plant-friendly system identification: a challenge for the process industries. **Preprints 13th IFAC Symposium on System Identification**. Rotterdam, p.917-922, 2003.

Rohjans, S.; Piech, K.; Lehnhoff, S. UML-based modeling of OPC UA address spaces for power systems. **In Intelligent Energy Systems (IWIES), IEEE International Workshop**, p 209- 214, 2013.

Schwab, A. W.; Bagby, M. O.; Freedman, B. Preparation and properties of diesel fuels from vegetable oils. **Fuel**, v. 66, n. 10, p. 1372-1378, 1987

Seader, J. D.; Henley, E.J. and Roper, D. K., **Separation Process Principles**, 3rd Ed. John Wiley Andamp; Sons, New York, 2011.

Sharma, N.; Singh, K. Model predictive control and neural network predictive control of TAME reactive distillation column. **Chem Eng Process.**, v. 59, p. 9–21, 2012.

Shealy, G. S.; Hagewiesche, D.; Sandler, S. I. Vapor-Liquid Equilibrium of Ethanol/Water/N,N-Dimethylformamide. **J. Chem. Eng. Data**, v.32, n. 3, p. 366-969, 1987.

Sholl, D.S.; Lively, R.P. Seven chemical separations to change the world. *Nature*, v. 532, p. 435–437, 2016.

Singh, H.; Pani, A. K.; Mohanta, H. K. Quality monitoring in petroleum refinery with regression neural network: Improving prediction accuracy with appropriate design of training set. **Measurement**, v. 134, p. 698–709, 2019.

Singh, V.; Gupta, I.; Gupta, H.O. ANN-based estimator for distillation using Levenberg–Marquardt approach. **Engineering Applications of Artificial Intelligence**, v. 20 p. 249–259, 2007.

Skogestad, S. The do's and don'ts of distillation column control. **Transactions on IChemE**, v. 85, p. 13–23, 2007.

Sloley, A. W. Effectively Control Column Pressure. **Chem. Eng. Prog**., v. 97, p. 38-48, 2001.

Sossa, H.; Garro B. A.; Villegas, J.; Avilés, C.; Olague, G. Automatic Design of Artificial Neural Networks and Associative Memories for Pattern Classification and Pattern Restoration. In: Carrasco-Ochoa J.A., Martínez-Trinidad J.F., Olvera López J.A., Boyer K.L. (eds) Pattern Recognition. MCPR 2012. **Lecture Notes in Computer Science**, v. 7329. Springer, Berlin, Heidelberg, 2012.

Stephanopoulos, G. **Chemical Process Control: An Introduction to Theory and Practice**. 1st ed. New Jersey: Prentice-Hall International Inc, 1984.

Tabatabaei, M.; Aghbashlo, M.; Dehhaghi, M.; Panahi, H. K. S.; Mollahosseini, A.; Soufiyanc, M. H. M. M. Reactor technologies for biodiesel production and processing: A review. **Progress in Energy and Combustion Science**, v. 74, p. 239–303, 2019.

Tolliver, T.L.; McCune, L.C. Finding the optimum temperature control trays for distillation columns. **InTech**, v. 27, n. 9, p. 75-80, 1980.

Tripodi, A.; Compagnoni, M.; Ramis, G.; Rossetti, I. Pressure-swing or extraction-distillation for the recovery of pure acetonitrile from ethanol ammoxidation process: a comparison of efficiency and cost. ***Chem. Eng. Res. Des***., v. 127, p. 92-102, 2017.

Tututi-Avila, S.; Jiménez-Gutiérrez, A.; Hahn, J. Control analysis of an extractive dividing-wall column used for ethanol dehydration. **Chemical Engineering and Processing: Process Intensification**, v. 82, p. 88–100, 2014.

Tyreus, B. D., Luyben, W. L. Dynamics and control of recycle systems. ternary systems with one or two recycle streams**. Industrial Engineering and Chemical Research**, v. 32, p. 1154-1163, 1993.

Tyreus, B. D.; Luyben, W. L. Tuning of PI controllers for integrator dead time processes. **Industrial and Engineering Chemistry Research**, v. 31, p. 2625–2628, 1992.

Udugama, I. A., Munir, T., Kirkpatrick, R., Young, B. R., Yu, W. High purity, high recovery, multi-component methanol distillation control. **Computer Aided Chemical Engineering**, v. 37, p. 1613-1618, 2015.

Van Ness, H. C.; Smith, J. M.; Abbott, M. M. **Intrduction to Chemical Engineering Thermodynamics**. 7 ed. Singapura: MacGraw-Hill International Editions, 2005.

Venkateswarlu, C.; Reddy, a. D. Nonlinear model predictive control of reactive distillation based on stochastic optimization**. Industrial & Engineering Chemistry Research**, v. 47, p. 6949–6960, 2008.

Vijayaraghavan, V., Lau, E.V., Goyal, Ankit, Niu, Xiaodong, Liang Gao, A. G. Design of explicit models for predicting the efficiency of heavy oil-sand detachment process by floatation technology. **Measurement**, v. 137, p. 122-129, 2019.

Vorayos, N.; Kiatsiriroat, T.; Vorayos, N. Performance analysis of solar ethanol distillation. **Renewable Energy**, v. 31, n. 15, p. 2543–2554, 2006.

Wang, C.; Guang, C.; Cui, Y.; Zhang, Z.; Zhang, X. Separation of a ternary mixture with multiple azeotropes via pressure- swing distillation. **J. Chem. Technol. Biotechnol**., v. 94, p. 2023- 2033, 2019.

Wu, Y. C.; Hsu, P. H. C.; Chien, I. L. Critical Assessment of the Energy-Saving Potential of an Extractive Dividing-Wall Column. **Industrial & Engineering Chemistry Research**, v. 52, p. 5384, 2013.

Xiong, Q.; Jutan, A. Grey-box modeling and control of chemical processes. **Chemical Engineering Science**, v. 57, p. 1027–1039, 2002.

Yang, A.; Su, Y.; Chien, I. L.; Jin, S.; Yan, C.; Wei, S. A.; Shen, W. Investigation of an energysaving double-thermally coupled extractive distillation for separating ternary system benzene/toluene/cyclohexane. **Energy**, v. 186, 2019.

Yousuf, M. S.; Al-Duwaish, H. N.; Al-Harmouz, Z. M. PSO based single and two interconnected area predictive automatic generation control. WSEAS Transactions on Systems and Control, v. 5, p. 677–690, 2010.

Zamprogna, E; Barolo, M.; Seborg, D. Optimal selection of soft sensor inputs for batch distillation columns using principal component analysis. **J. Process Control**., v. 15, p 39-52, 2005.

Zanata, D. R. P. and Garcia, C. Soft sensor as composition estimator in multicomponent distillation column. **Anais do XXI Congreso Interamericano de Ingeniería Química, Lima-Peru**, 2005.

Zhang, L.; Ge, Y.; Ji, D.; Ji, J. Experimental measurement and modeling of vapor – liquid equilibrium for ternary systems containing ionic liquids: A case study for the system

water + ethanol + 1-hexyl-3-methylimidazolium chloride. **Journal of Chemical & Engineering Data**, v. 54, p. 2322-2329, 2009.

Zhongzhou, C., Henson, M. A., Belanger, P., Megan, L. Nonlinear model predictive control of high purity distillation columns for cryogenic air separation. **IEEE Transactions: Control Systems Technology,** v. 18, p. 811-821, 2010.

APÊNDICE A

RESULTADOS COMPLEMENTARES DO CAPÍTULO 5

APÊNDICE A – Resultados complementares do capítulo 5

Figura A.1. Resposta do sistema diante distúrbios na alimentação e mudança na especificação de etanol de 99,5 mol% a 99,8 mol%: (a) xETOH, (b) S / F, (c) T10_C1, (d) T20_C1 e (d) T20_C1; (e) T3_C2 e (f) T6_C2

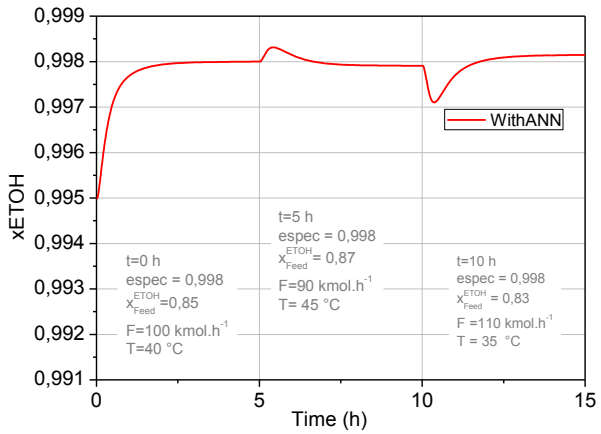

a)

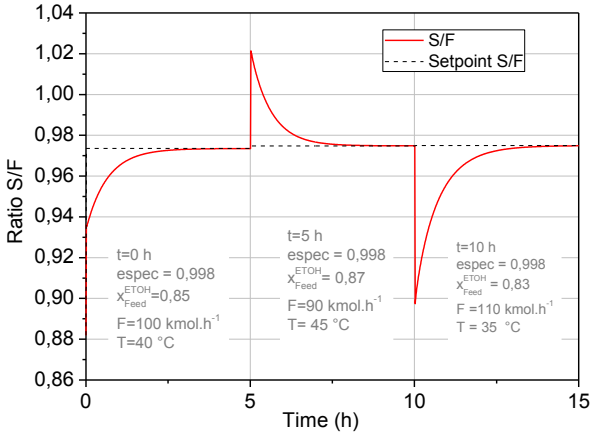

b)

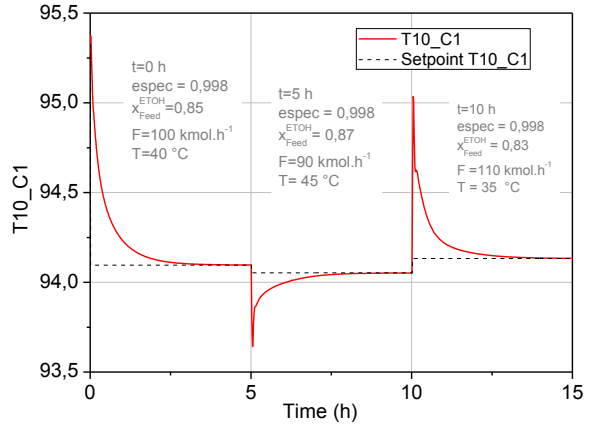

c)

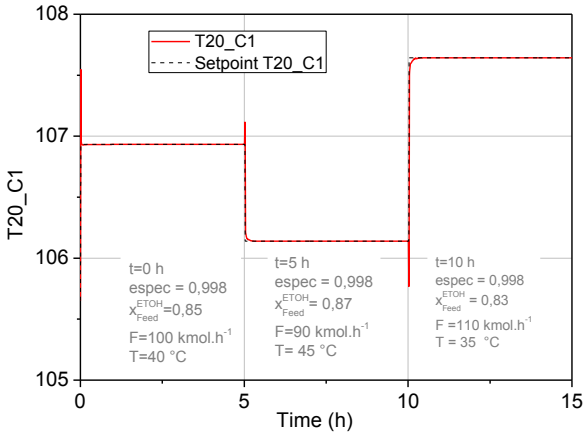

d)

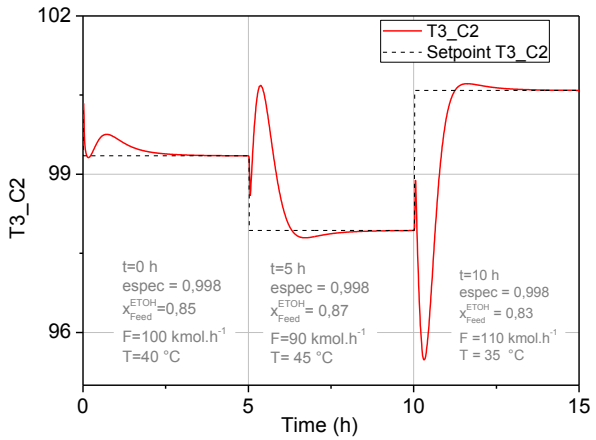

e)

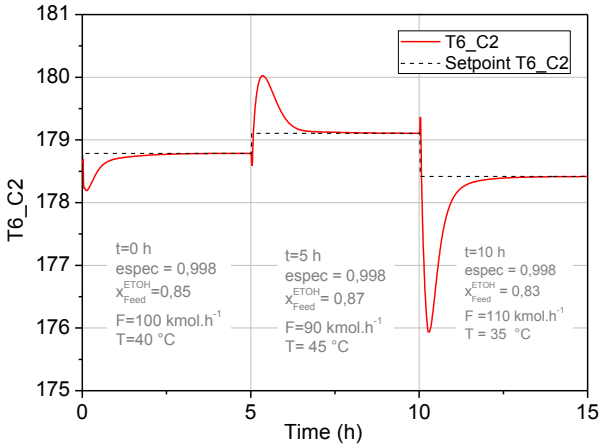

f)

Figura A.2. Resposta do sistema diante distúrbios na alimentação e mudança na especificação de etanol de 99,5 mol% a 99,7 mol%: (a) xETOH, (b) S / F, (c) T10_C1, (d) T20_C1 e (d) T20_C1; (e) T3_C2 e (f) T6_C2

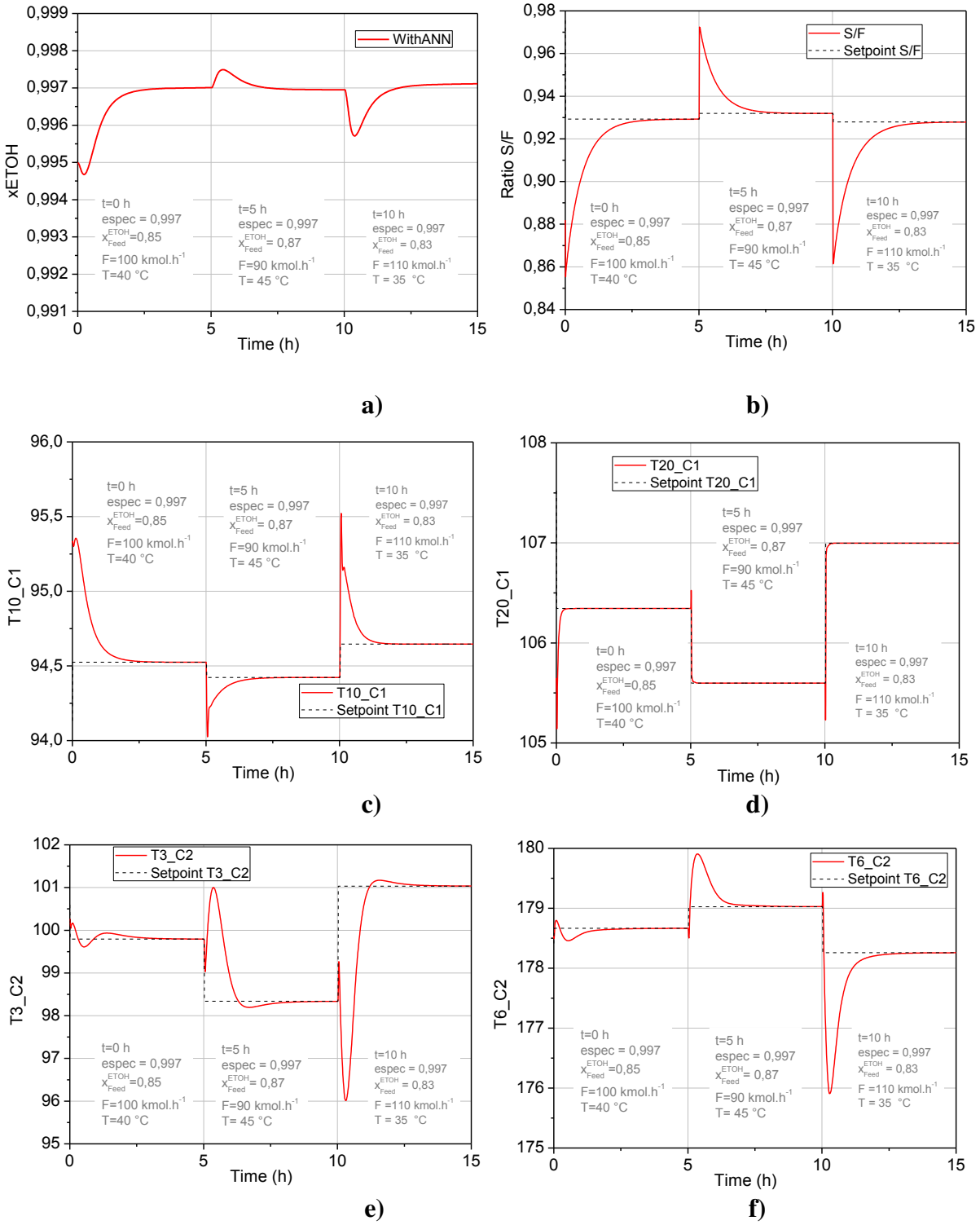

Figura A.3. Resposta do sistema diante distúrbios na alimentação e mudança na especificação de etanol de 99,5 mol% a 99,6 mol%: (a) xETOH, (b) S / F, (c) T10_C1, (d) T20_C1 e (d) T20_C1; (e) T3_C2 e (f) T6_C2

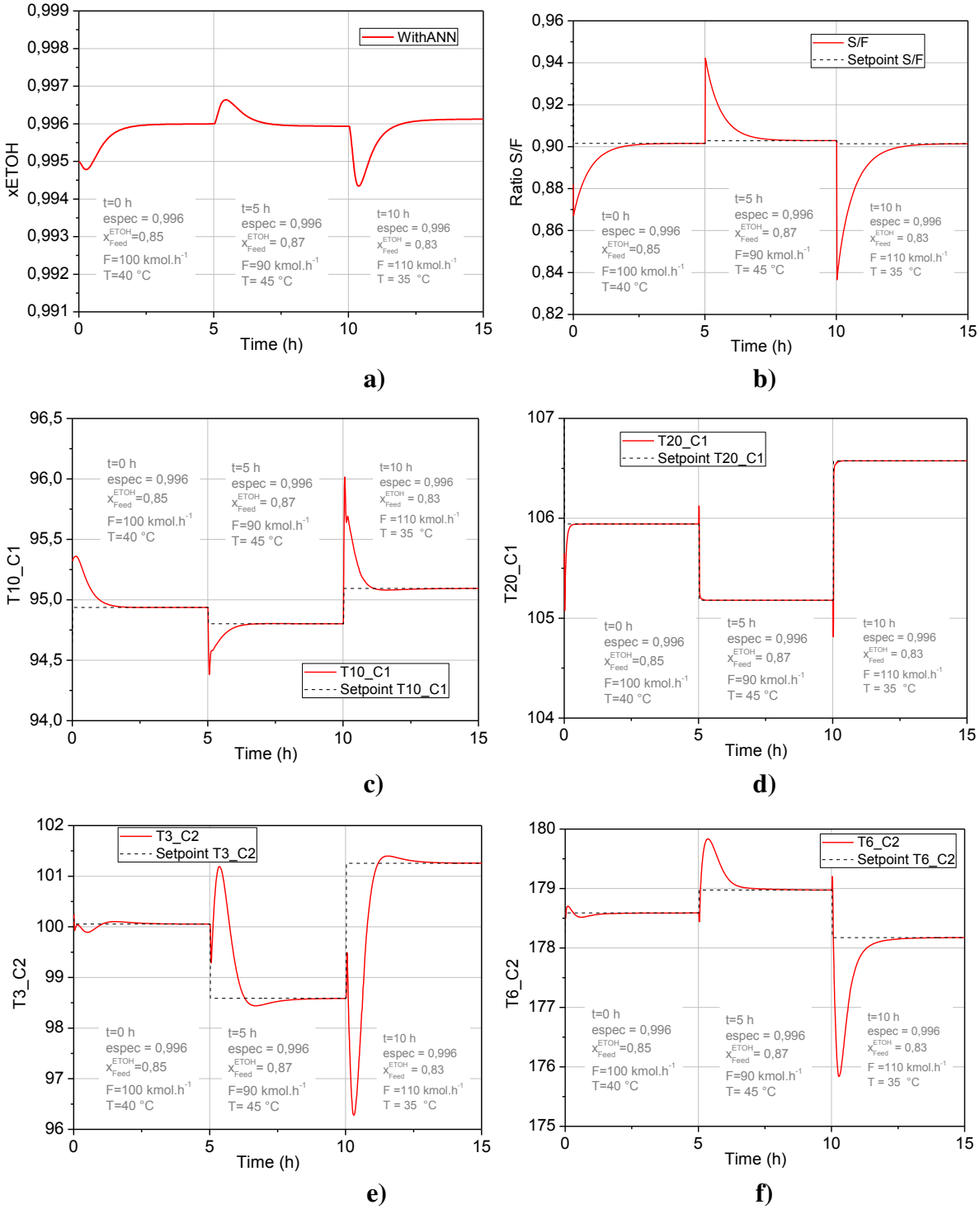

Figura A.4. Resposta do sistema diante distúrbios na alimentação para a especificação de etanol de 99,5 mol%: (a) xETOH, (b) S / F, (c) T10_C1, (d) T20_C1 e (d) T20_C1; (e) T3_C2 e (f) T6_C2

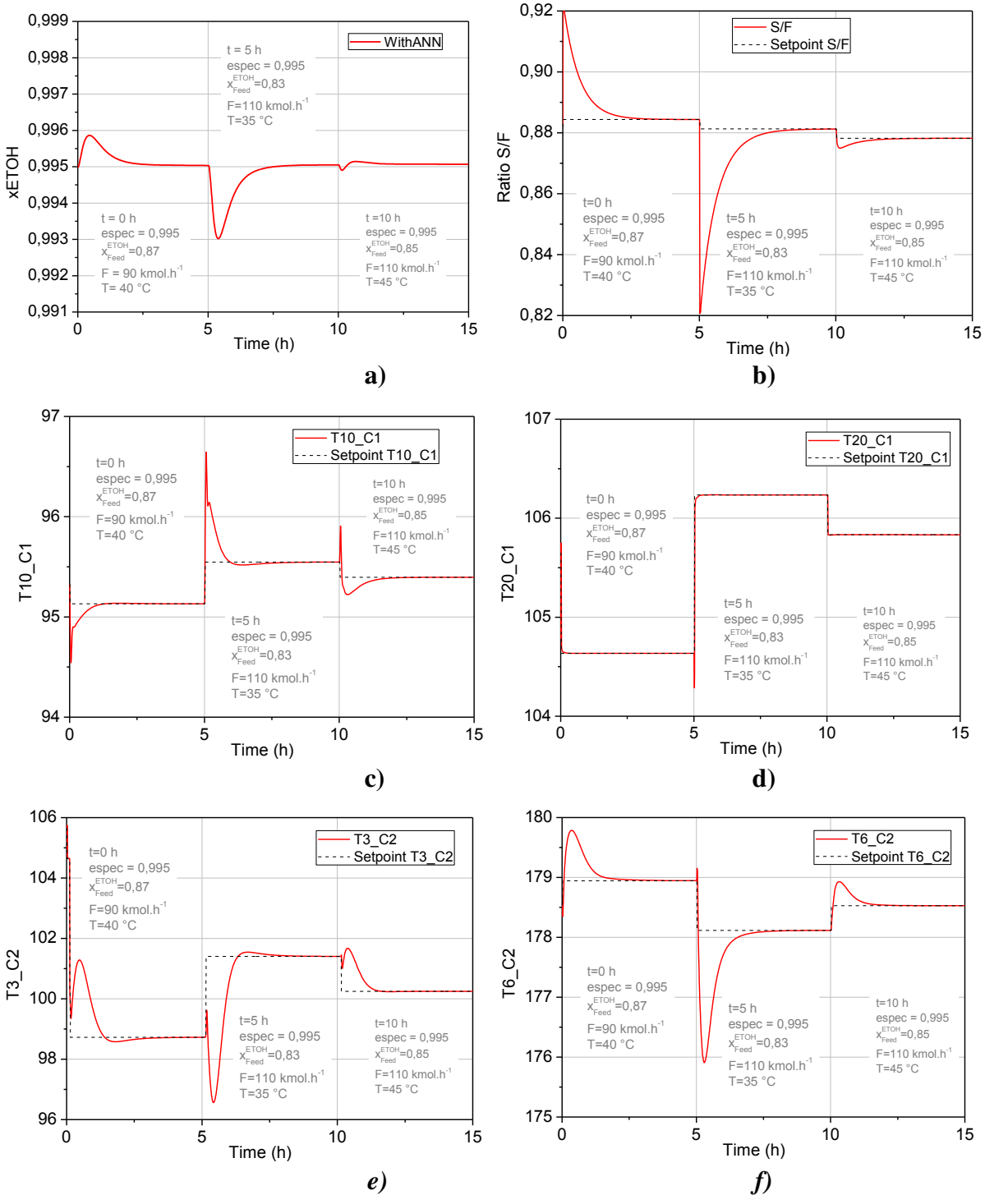

Figura A.5. Resposta do sistema diante distúrbios na alimentação e mudança na especificação de etanol de 99,5 mol% a 99,4 mol%: (a) xETOH, (b) S / F, (c) T10_C1, (d) T20_C1 e (d) T20_C1; (e) T3_C2 e (f) T6_C2

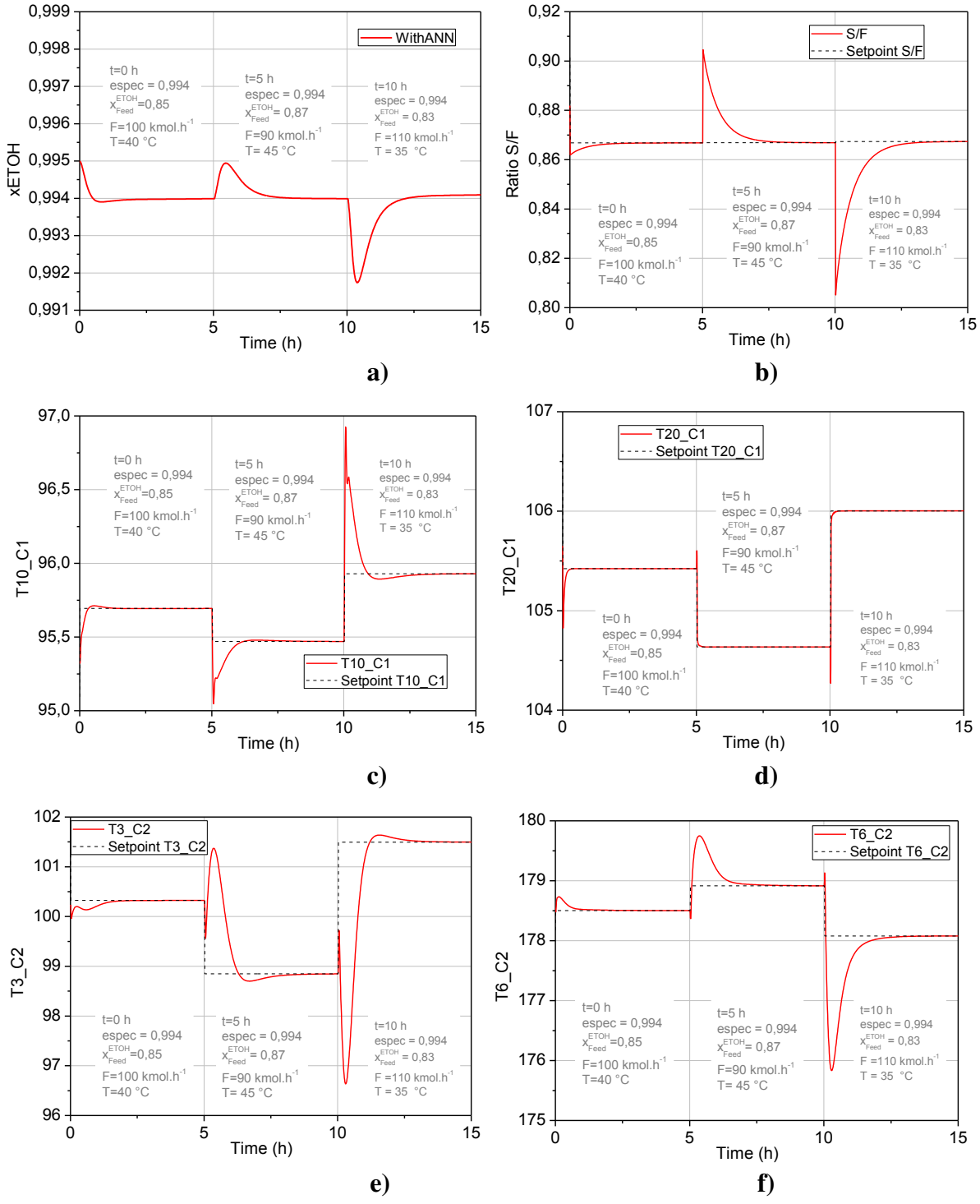

Figura A.6. Resposta do sistema diante distúrbios na alimentação e mudança na especificação de etanol de 99,5 mol% a 99,3 mol%: (a) xETOH, (b) S / F, (c) T10_C1, (d) T20_C1 e (d) T20_C1; (e) T3_C2 e (f) T6_C2

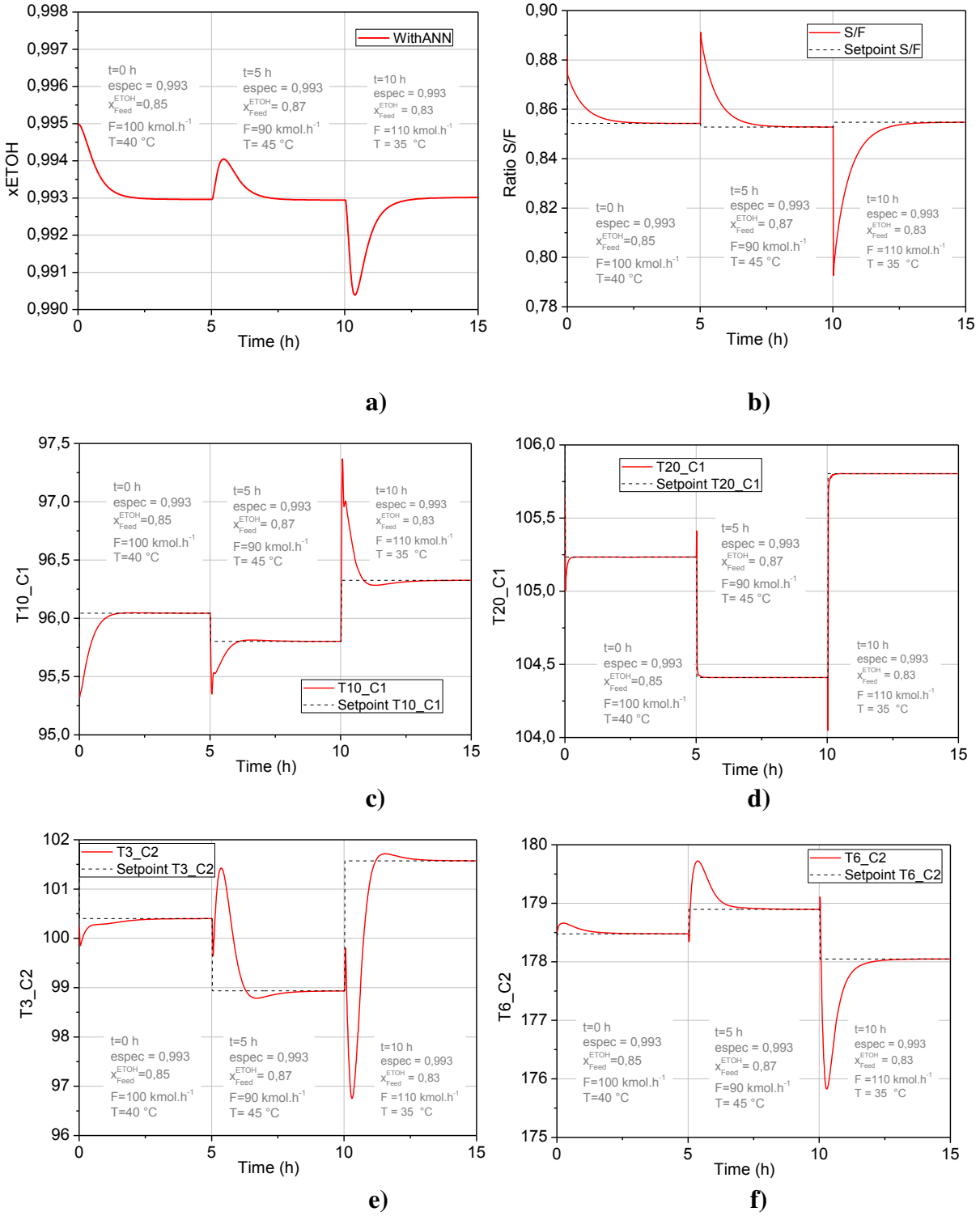

Figura A.7. Resposta do sistema diante distúrbios na alimentação e mudança na especificação de etanol de 99,5 mol% a 99,2 mol%: (a) xETOH, (b) S / F, (c) T10_C1, (d) T20_C1 e (d) T20_C1; (e) T3_C2 e (f) T6_C2

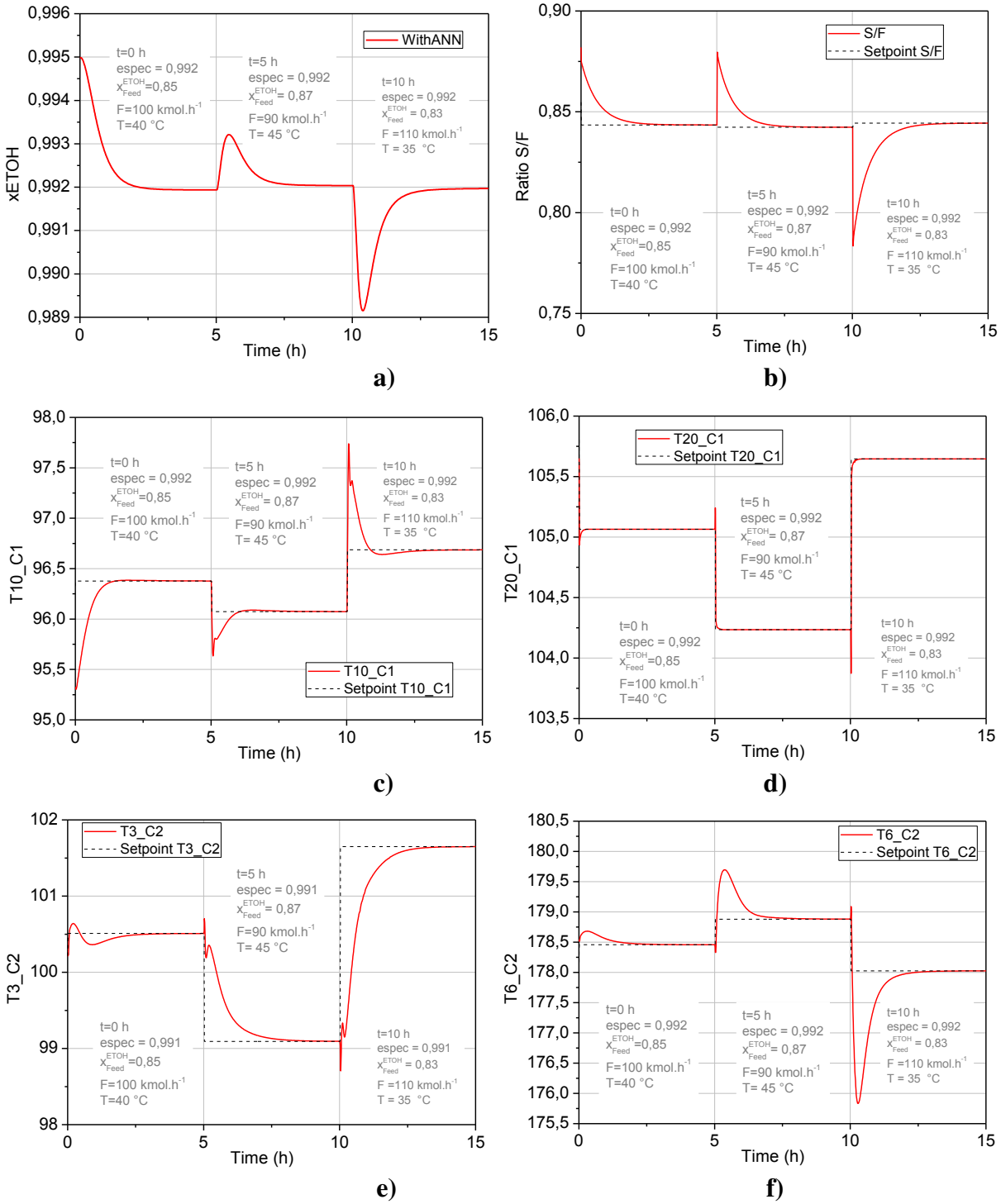

Figura A.8. Resposta do sistema diante distúrbios na alimentação e mudança na especificação de etanol a cada 5 h: (a) xETOH, (b) S / F, (c) T10_C1, (d) T20_C1 e (d) T20_C1; (e) T3_C2 e (f) T6_C2

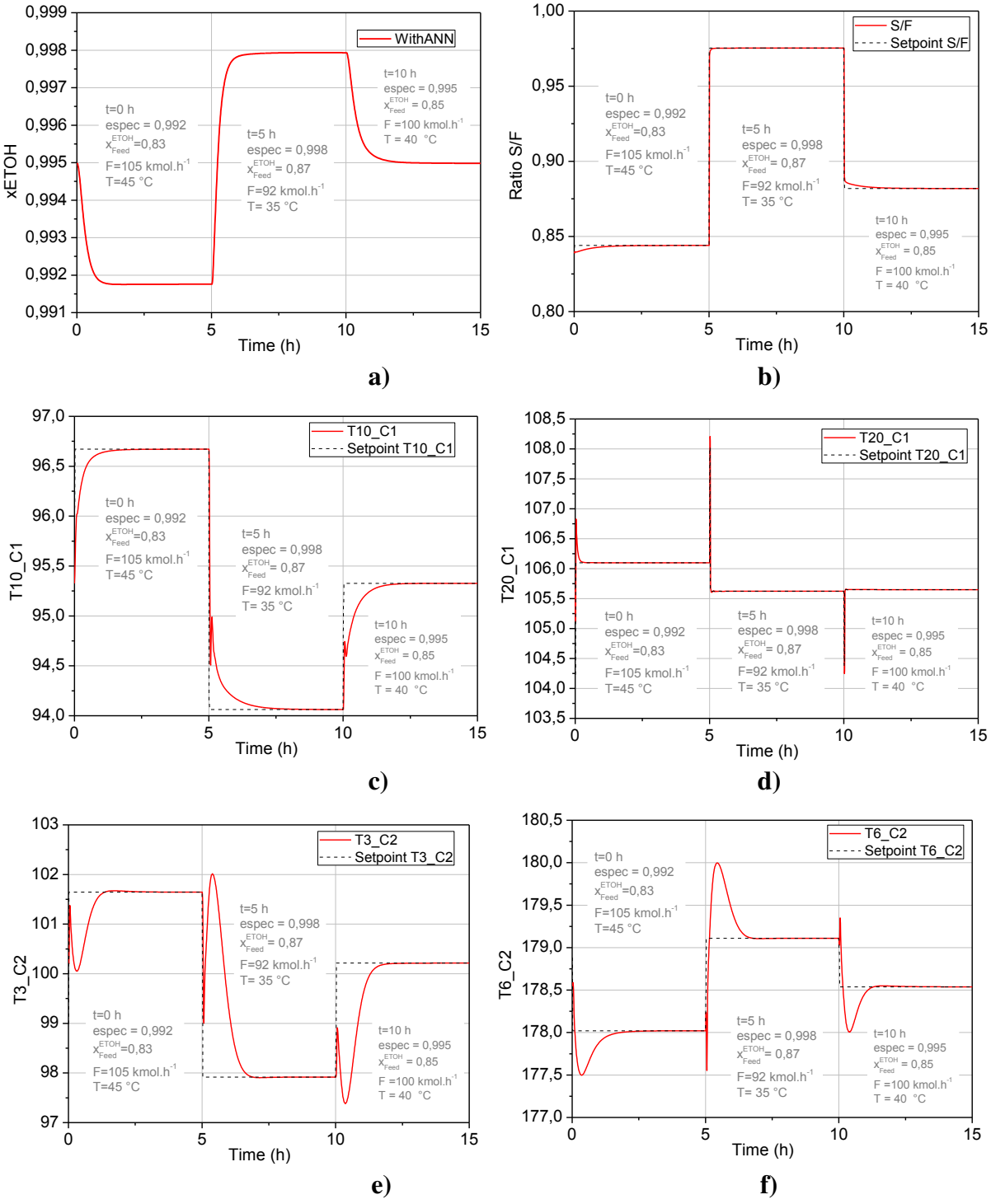

Figura A.9. Resposta da composição de água no destilado da coluna de recuperação diante distúrbios na alimentação e mudança na especificação de etanol.